SEASONAL EFFECTS OF FROZEN SOIL ON THE STIFFNESS OF BRIDGE PILES

By

Jacob E. Horazdovsky

RECOMMENDED: _____

_____

_____
Advisory Committee Chair

_____
Chair, Department of Civil and Environmental Engineering

APPROVED: _____
Dean, College of Engineering and Mines

_____
Dean of the Graduate School

_____
Date

SEASONAL EFFECTS OF FROZEN SOIL ON THE STIFFNESS OF BRIDGE PILES

A

Thesis

Presented to the Faculty

of the University of Alaska Fairbanks

in Partial Fulfillment of the Requirements

for the Degree for

MASTER OF SCIENCE

By

Jacob E. Horazdovsky

Fairbanks, Alaska

August 2010

ProQuest LLC
789 East Eisenhower Parkway
P.O. Box 1346
Ann Arbor, MI 48106-1346

Abstract

In the northern regions, the upper layer of soil is frozen throughout winter months. Soil stiffness can be expected to increase several orders of magnitude as it changes from thawed to frozen. Thus, pile foundation systems embedded in frozen soils are considerably stiffer during winter months when subjected to lateral loads. This thesis explores and quantifies stiffness change for 16 inch diameter steel jacketed, reinforced concrete pilings in seasonally frozen silt. Two test piles were driven 20 feet into silty soil at a site approximately 1.5 miles from Fairbanks, Alaska. Three quasi-static lateral load cyclic tests were conducted on the piles throughout the year; one in September when the soil was thawed, the other two in January and March with frost depths of 4.5 and 7.5 feet respectively. Soil temperatures ranged from thawed to -18 degrees C. The shear demand on the piles increased by over 400 percent. Depth to fixity changed from approximately 6 pile diameters (thawed) to less then 0.75 pile diameters (frozen).

Table of Contents

Page

Signature Page..... i

Title Page..... ii

Abstract..... iii

Table of Contents..... iv

Acknowledgements..... xi

1 Introduction..... 1

2 Literature Review..... 7

2.1 Analytical Modeling of Piles Embedded in Seasonally Frozen Soils..... 7

2.2 Full Scale Field Testing of Piles Embedded in Seasonally Frozen Soils..... 9

2.3 Fairbanks Silt..... 12

2.3.1 Soil Exploration at the Farmers Loop Test Site..... 12

2.3.2 Properties of Frozen Fairbanks Silt..... 17

3 Pile Instrumentation..... 19

3.1 Deflection Above Ground Surface and Measurement of Applied Load..... 20

3.2 Instrumentation of the Rebar Cage 20

3.2.1 Strain Gages..... 21

3.2.2 Inclinometer..... 23

3.2.3 Soil and Pile Temperatures..... 25

3.3 Data Acquisition System..... 26

4 Site Selection and Pile Installation..... 29

4.1 Site Selection and Soil investigation 29

4.2 Pile Installation..... 31

5 Testing..... 34

5.1 Pile Testing Procedure..... 34

5.2 Test Frame Design Construction and Testing..... 37

5.3 Pile Testing..... 40

5.3.1 September Testing..... 40

Page

5.3.2 Pile Rehabilitation 44
5.3.3 Snow Conditions at the Test Site..... 45
5.3.4 January Testing..... 45
5.4 Test Frame Redesign..... 50
5.5 March Testing..... 51
5.6 Formation of Soil Gap..... 56
6 Soil Properties..... 59
6.1 Classifying the Soil..... 59
6.2 Shear Wave Velocity Testing..... 61
7 Pile Flexural Behavior and Experimental Results 64
7.1 Material Properties..... 65
7.1.1 Concrete Strength..... 65
7.1.2 Steel Strength..... 68
7.2 Flexural Stiffness of the Pile..... ... 69
7.3 Pull Over Analysis..... 73
7.3.1 Experiment Results..... 73
7.4 Depth to Fixity Analysis..... 76
7.4.1 Depth to Fixity Flexural Analysis..... 76
7.4.2 Depth to Fixity Maximum Moment Analysis..... 79
7.5 Soil Spring Model..... 84
7.5.1 Thawed Soil Springs..... 85
7.5.2 Frozen Soil Springs..... 91
8 Findings..... 96
8.1 Depth to Fixity..... 98
8.2 Soil Springs..... 99
8.3 Quantify Stiffness Increase and Moment of Maximum Moment 100
9 Conclusions..... 102
9.1 Suggestions for further research..... 103

Page

References……104

Appendices ……..…….....109

List of Figures

Page

Figure 2.1 Soil Profile (Yang et al. 2008)..... 9
Figure 2.2 Suleiman Pile Test Setup (Suleiman et al. 2006)..... 11
Figure 2.3 Tri-axial Test Results Unconsolidated Undrained, Natural Water Content..... 16
Figure 2.4 Tri-axial Test Results Unconsolidated Undrained 16
Figure 2.5 The Effect of Temperature on Strength of Fairbanks Silt (Haynes and Karaluis 1977) 18
Figure 3.1 Instrumented Rebar Cages..... 21
Figure 3.2 Strain Gage Installed on Rebar..... 23
Figure 3.3 Strain Gage Installed on Rebar Cage and Protected with Silicone..... 23
Figure 3.4 Inclinometer as Installed in the Test Pile..... 24
Figure 3.5 Inclinometer setup (Geodaq) 25
Figure 3.6 Pile Instrumentation Cross Section..... 26
Figure 4.1 Site Map..... 30
Figure 4.2 Pile Installation..... 31
Figure 4.3 Small Soil Removal Apparatus 32
Figure 5.1 Flow Chart for Hydraulic Pump..... 36
Figure 5.2 Test Frame Overview..... 38
Figure 5.3 Test Pile Connection Detail..... 39
Figure 5.4 Pile As Built..... 40
Figure 5.5 September Target Displacement Increments..... 41
Figure 5.6 September Cyclic Load vs Deformation at Point of Load..... 42
Figure 5.7 Test Pile at Final September Load Increment..... 42
Figure 5.8 Reaction Pile at Final September Load Increment..... 43
Figure 5.9 Plastically Deformed Soil in Front of Test..... 43
Figure 5.10 January Target Load Increments..... 46
Figure 5.11 Temperatures with Depth January 18, 2010..... 48

Page

Figure 5.12 Bearing Failure of Test Frame at Reaction Pile..... ... 49
Figure 5.13 Soil Crack at 150 Kips January Test..... 49
Figure 5.14 January Cyclic Load vs Deformation at Point of Load..... 50
Figure 5.15 March Target Load Increments..... ... 51
Figure 5.16 Temperatures with Depth March 24, 2010..... 53
Figure 5.17 March Cyclic Load vs. Deformation at Point of Load 0 to 207 kips..... 54
Figure 5.18 March Cyclic Load vs. Deformation at Point of Load 0-150 Kips..... 55
Figure 5.19 207 Kips Final Loading of the South Pile..... 55
Figure 5.20 207 Kips Unloaded Plastically Deformed Soil Gap..... 56
Figure 5.21 Plastically Deformed Soil Gap in Front of Pile September Test..... 57
Figure 5.22 Plastically Deformed Soil Gap in Front of Pile March Test..... 57
Figure 5.23 Soil Gap Location..... 58
Figure 5.24 March Soil Cracking Summarized..... 58
Figure 6.1 Moisture Contents 7/24/2010 Soil Borings..... 60
Figure 6.2 Uncorrected SPT Values 7/24/2008 Soil Borings..... ... 60
Figure 6.3 Soil Profile.....61
Figure 6.4 Shear Wave Velocity Testing at the Site Winter 2010..... 62
Figure 6.5 Preliminary Shear Wave Velocity Profile..... 63
Figure 7.1 Concrete Stress Strain Behavior Experimental and Theoretical 67
Figure 7.2 Concrete Strain vs. Modulus of Elasticity..... ... 68
Figure 7.3 Flexural Stiffness vs. Moment.....71
Figure 7.4 Flexural Stiffness vs. Strain in Reinforcing Bars..... ... 72
Figure 7.5 Location of Deflection Measurement..... 73
Figure 7.6 September Pile Test Pull Over Analysis.....74
Figure 7.7 January Pile Test Pull Over Analysis..... 74
Figure 7.8 March Pile Test Pull Over Analysis..... 75
Figure 7.9 September, January, and March Pile Test Pull Over Analysis..... 75

Page

Figure 7.10 Load vs. Depth of Fixity..... 78
Figure 7.11 Pile Short and Long Foundation Behavior and Depth to Fixity..... 79
Figure 7.12 September Pile Test Strain vs. Depth..... ... 80
Figure 7.13 January Pile Test Strain vs. Depth..... ... 81
Figure 7.14 March Pile Test Strain vs. Depth..... 82
Figure 7.15 Bending Stiffness vs. Bending Moment 85
Figure 7.16 Soil Springs Used to Model September Test..... 89
Figure 7.17 Pullover Analysis Model Predicted, and Experimental..... 89
Figure 7.18 Deflected Shape Model Predicted, and Experimental..... 90
Figure 7.19 Deflected Shape Model Predicted, and Experimental..... 90
Figure 7.20 Soil Spring Used to Model March Pile Test..... .. 93
Figure 7.21 Experimental Tensile Rebar Strain vs. Moment in Test Pile..... 94
Figure 7.22 Strain, Model Predicted and Experimental..... 95
Figure 7.23 Strain, Model Predicted and Experimental..... 95
Figure 8.1 Short Pile Embedment vs Deep Pile Embedment..... 96
Figure 8.2 Excavation of South Pile Tested March 2010..... 97
Appendix A Example LPile Output file.....109
Appendix B Campbell CR9000X Code.....143
Appendix C Soil Bore Logs.....154
Appendix D Experimental Data 159

List of Tables

Page

Table 2.1 Test Setup (Suleiman 2006)..... 10
Table 2.2 Summary of 1940s Soil Investigation (USACE 1950)..... 13
Table 2.3 Soils Report (Linell 1973)..... 14
Table 2.4 CRREL Farmers Loop Test Site Summarized (Nidowicz 1981)..... 14
Table 2.5 Cripple Creek Site Summarized (Nidowicz 1981)..... 15
Table 2.6 Cripple Creek Soil Sample Used for Tri-axial Testing (Nidowicz1981)..... 15
Table 3.1 Gage Location / Elevations as Tested..... 27-28
Table 6.1 Shear Wave Velocity Preliminary Results..... 63
Table 7.1 Concrete Compressive Strength and Modulus of Elasticity..... 65
Table 7.2 Concrete Tensile Strength 65
Table 7.3 Pipe Jacket Tensile Strength..... 68
Table 7.4 Reinforcing Bars Tensile Strength..... 69
Table 7.5 Properties of Frozen Fairbanks Silt..... 91
Table 7.6 Properties of Frozen Fairbanks Silt..... 91
Table 7.7 Modulus of Subgrade Reaction from Haynes Silt Properties 92
Table 8.1 Depth to Fixity 16 inch Diameter Steel Jacketed Reinforce Concrete Pipe Pile, Embedded in 19.5 feet of Fairbanks Silt..... 99

List of Other Materials

Research Data ....Pocket

Acknowledgements

This thesis would not have been possible without the support, advice, encouragement and time investment of many people. I would like to thank my advisors, Dr. Leroy Hulsey, Dr. Yuri Shur, Dr. Kenan Hazirbaba, and Dr. Andrew Metzger. To my advisor Leroy Hulsey, I would like to thank him for getting me involved as an undergraduate in this project. Without all of his encouragement, advice, and guidance I would have never went on to get my masters degree.

I would like to thank my friends, Ricky Pitts, George Churchill, Rodney Collins and many others who have helped me throughout the research project.

I am grateful to the Alaska Department to Transportation (AKDOT), the Alaska University Transportation Center, the Institute of Northern Engineering, and the University of Alaska Fairbanks for funding this project and funding me throughout graduate school. I would like to thank Duane Davis for his technical support on the project and the CE office staff for all of the coffee and logistic support.

Finally I would like to thank my fiancée for the love, support and understanding she has given me over that last two years and for her help in putting this thesis together.

1 Introduction

Earthquake engineering has changed over the course of the last century. The field of structural engineering is still based on a force control approach (ASCE 2005). ASCE - 7, published by the American Society of Civil Engineers (ASCE) uses a design base shear to simulate the effects of earthquake loading on a structure. There has been a recent shift in the field of earthquake engineering to move away from a force-based design and toward a serviceability design approach. While the design is still a force-based approach, there is now a "response modification factor," which allows engineers to reduce the amount of base shear that the structure is loaded with based on the flexibility of the structure (ASCE 2005).

Engineers learn from failure. Many of the advancements in earthquake engineering in recent years can be attributed to earthquakes. Many of these earthquakes were in areas that do not have seasonally frozen soil. Based largely on these earthquakes in unfrozen soils, the field of bridge engineering has progressed. While the seismic design of bridges is still based largely on a force-controlled analysis, there has been a shift toward requiring a displacement-based analysis to be performed alongside force-based analysis (AKDOT pers. comm.). One area that has received a lot of attention is the design of bridge foundations. The flexibility of the soil foundation system is an important parameter when designing a bridge to a required displacement. Extensive testing has been conducted in the past to quantify stiffness of piles driven in different types of unfrozen soils.

In cold regions, winter temperatures can cause soil to freeze anywhere from several inches to several feet below the ground surface. As water freezes, ice crystals form, transforming water from a liquid into a solid. As soil freezes, water within the soils is transformed into ice and the soil matrix is reinforced by the formation of ice.

As the unfrozen granular soil is loaded, the load is carried by the soil structure and any water pressure that develops in the soils is dissipated into the surrounding soils. As cohesive soils are loaded, pore water pressure builds. If the loading occurs more rapidly then pore water pressure can be dissipated and loading and unloaded is repeated, the excess water pressure liquefies the soil and most of the strength is lost. As frozen soil is loaded, both the soil structure and the ice are able to carry load. This increases the strength and stiffness of the soil. Stevens in 1973, found that the stiffness soil can increase as much as two orders of magnitude as it freezes (Stevens 1973).

When foundations penetrate a seasonally frozen layer, the stiffness of the foundation will increase with the stiffness of the layer of frozen soil. In the past, rule of thumb practices have been used to account for the increased stiffness of this frozen layer (AKDOT pers. Comm..). As earthquake engineering design changes to a displacement-based model the actual behavior of the pilings in frozen soil becomes more important so that the structure can handle the required displacements. If parts of a structural system have different flexibilities the elements of the structure that are of stiffer will be over loaded before elements that are more flexible are over loaded. It is important that all elements of the structure are flexible enough and have similar flexibility.

In the recent past several researchers have tried to address this problem through both analytical modeling and field testing (Sritharan et al. 2004, Suleiman et al. 2006 and Yang et al. 2008).

In 2004, Sritharan et. al used soil springs to model frozen soils. It was found in clay that a frozen soil layer of approximately 40 inches reduced lateral displacement capacity by 78 percent and increased shear demand by 40 percent (Sritharan et al. 2004). This study was continued in 2005, with full scale pile testing (Suleiman et al. 2006). The pile test was conducted in Iowa in a clay soil with a frost depth of 30 inches. Suleiman et al. (2006) found that seasonal frozen soils increased the effective elastic stiffness by 170 percent, increased shear demand by 44 percent, reduced length of the plastic region by 64 percent and shifted the location of maximum moment upward by 0.84 m (2.75ft).

Throughout the state of Alaska, bridge pile designer's have been using a steel jacketed, reinforced concrete pile (AKDOT pers. comm.). Piles embedded in soils that freeze annually will experience frost depths ranging from a few inches in Southeast Alaska to more then 10 feet in northern regions of Alaska (Andersland and Anderson 1978). Winter soil temperatures may range from 0 to -30 degrees Celsius. Silty soils with moisture contents of more than 40 percent are common. There isn't any record in the literature of any previous full scale pile testing for these unique conditions. For example, if interested in the influence of seasonal frost on a laterally loaded pile embedded in silt, several elements are missing from previous pile tests. These include: strength of frozen silt; this strength is highly dependent on temperature (Haynes and Karalius 1977). A report by Haynes and Karalius (1977) found that compressive strength

of frozen silt can increase by an order of magnitude over a temperature range of 0 to -55 degree Celsius. Steel jacketed, reinforced concrete piles have never been laterally loaded to failure in frozen soils. Further, displacement capacity of this type of pile, embedded in frozen soils, has not been well studied. While assumptions used for current designs are based on past failures, more information is needed to accurately predict lateral displacement capacity of this type of foundation system.

In 2008, Yang et. al. presented an analytical study using a finite element model. The analysis showed that the frozen soil layer reduces the lateral displacement capacity at yielding by 70 percent and a lateral yield force increase of 31 percent. Details of this model are provided in the Literature Review Chapter of this document. These models are based on limited soil properties and assumed soil-pile interface behavior. A full scale pile test was needed to experimentally determine the effect that the seasonally frozen soil has on this system.

AKDOT funded this study to find the upper limit of stiffness for a typical AKDOT bridge pile foundation in a seasonally frozen soil. In this study, full scale lateral load tests were done on steel jacketed, steel reinforced concrete piles embedded in frozen and unfrozen silts. The design of the pile was based on Alaska Department of Transportation's typical pile design. Piles have a longitudinal reinforcement ratio of two percent over the entire length of the member; this percentage neglects the steel jacket. The test site was located in Fairbanks Alaska at the U.S. Army Corps of Engineers Cold Regions Research and Engineering Laboratory (CRREL) Farmers Loop Test Site. The site is an ASCE dedicated research site. In Fairbanks, typical seasonal frost depths in

saturated silts can extend to eight feet below the ground surface and without the cover of snow, soil temperatures can typically be as low as -20 degrees Celsius during the coldest winter months.

The soil at the Fairbanks test site is a very loose, unconsolidated silt with an approximate moisture content of 30 percent. The site is wet year-round with the water table located at or near the ground surface. During the summer, the soil is very soft; heavy trucks and equipment will sink several inches as they are driven over the test site. In the winter, when the soil freezes, the frozen silt becomes extremely strong. The site was chosen because it provides a large stiffness increase for the foundation system.

A pile testing procedure was implemented. This procedure was designed to be in near compliance with the guidelines illustrated in a draft report entitled "Recommendation for Seismic Performance Testing of Bridge Piers." This is a Federal Highway Administration (FHWA 2004) document. Testing was classified as "Quasi Static" (FHWA 2004). In quasi static testing, the dynamic effects of inertia are ignored. Displacement control was used for summer testing in accordance with FHWA (2004) guidelines. However, displacement control is inappropriate for frozen soil conditions. Therefore, force control was used for winter testing. Pile testing was conducted on two test piles. Piles were embedded into the non-plastic silt to a depth of 20 feet. The piles were instrumented to measure strain, temperature, and displacement with depth. The loading apparatus was equipped with a load cell for measuring applied force, and displacement was measured above the ground surface using linear motion transducers. Testing was originally planned to consist of two full scale lateral load tests, one test in

thawed soils and a second test at the maximum anticipated depth of seasonal frost. During summer testing, the soil failed. The pile was returned to a vertical position and soil around the pile was rehabilitated so that an additional test could be conducted when frost was at half of the expected seasonal depth of frost.

Two analysis methods for evaluating test results were requested by AKDOT based on experimental testing. The first method is a simplistic method that is well established. The method simplifies the problem by using a depth to equivalent fixity to approximate a complicated problem. In this method, the soil above the depth of equivalent fixity is neglected and the soil below the depth of equivalent fixity is considered infinitely rigid (Coduto 2001). The second method is a more complicated method that uses soil springs to approximate the behavior of the pile. This method is essentially a beam on elastic or inelastic foundation; the soil resistance is approximated by discretely spaced springs. For this analysis, LPile, a finite difference software (Reese et al. 2004), was used to develop a set of soil springs that would accurately predict the experimental results of the pile. The results of this pile test are also being used to calibrate an OpenSees finite element model that was presented by Yang et. al. (2008).

2 Literature Review

The flexibility of foundation systems in seasonally frozen soils is a problem that until recently has been unexplored. While quasi static lateral load testing in thawed soil has been extensively explored; during the literature review, only one full-scale quasi static lateral load test in seasonally frozen soil was found. Several researchers have addressed the problem using analytical models but there is a lack of full-scale pile testing to calibrate these models.

2.1 Analytical Modeling of Piles Embedded in Seasonally Frozen Soils

In the recent past, several researchers have tried to address this problem through analytical modeling. In 2004, Sritharan et. al. used soil springs to model short term loading in frozen soils. The model was a cast-in-place steel-reinforced concrete pile. LPile, a finite difference software, was used for the analysis (Sritharan et al. 2004). The pile diameter (D) was 24 inches; embedment length was 17.5D and the lateral load was applied 4.4D above ground surface. The pile had a longitudinal steel reinforcement ratio of 2 percent and a transverse reinforcement ratio of 0.8 percent. The pile was modeled for clay conditions. Thawed soil springs for the clay were obtained from LPile's data base (Sritharan et al. 2004). Frozen springs were obtained by using normal stress-strain data obtained from triaxial testing of frozen clay. Depth of the frozen soil was taken as 0, 24, 32, 38, and 48 inches of depth. The result of the model concluded that frozen soil reduces the lateral displacement capacity by 78 percent and increases shear demand by 40 percent. The stiffness of clay can increase by two orders of magnitude as temperatures

drop below freezing. The stiffness increase of the steel and concrete at -20 degrees Celsius has little effect on the lateral response of the column-foundation system.

In 2008, Yang et. al. presented an analytical study using the finite element model to model short-term lateral loading of piles in frozen soils. The pile that was modeled was a steel jacketed, reinforced concrete filled pile. The software that was used was the Open System for Earthquake Engineering Simulation (OpenSees) (Yang et al. 2008). The pile diameter was 16 inches, embedment length was 19.7 feet and the load was applied at 7.9 feet above the ground surface. The pile was embedded into a layered soil; see Figure 2.1 for the soil profile. The pile had a longitudinal steel reinforcement ratio of 2 percent and the wall thickness of the pipe jacket was 0.375 inches. The analysis showed that the frozen soil layer reduces the lateral displacement capacity at yielding by 70 percent and a lateral yield force increase of 31 percent. The maximum bending moment and plastic hinge location moved up considerably with seasonal frost. The analytical results also indicated that the plastic hinge length was considerably reduced.

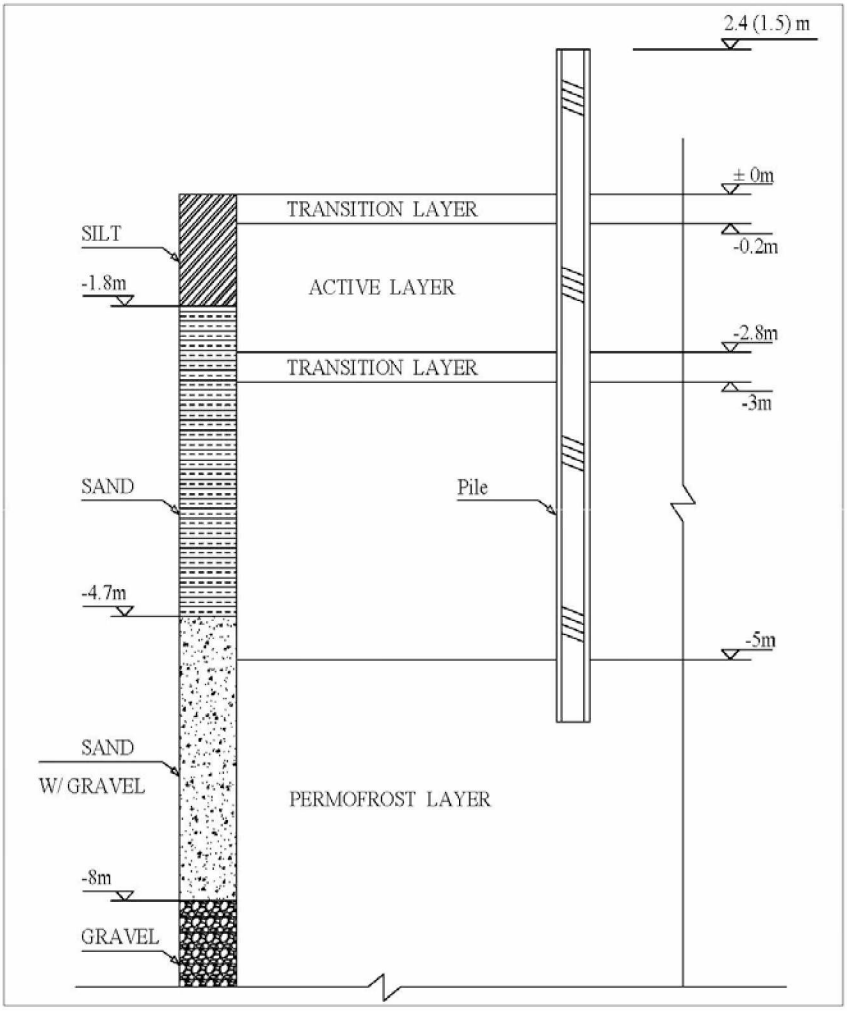

Figure 2.1 Soil Profile (Yang et al. 2008)

2.2 Full Scale Field Testing of Piles Embedded in Seasonally Frozen Soils

While there has been some testing of piles for creep behavior (Rowley 1973, Crowther 1990, Foriero et al. 2005), and some dynamic vibratory testing of piles in frozen soils (Vaziri and Han 1991), there has been very little full-scale lateral short-term load testing on piles in seasonally frozen soil.

In a recent study by Suleiman et. al. (2006), full scale pile tests were conducted in a seasonally frozen soil. This study was conducted in the state of Iowa. The piles were embedded in low plasticity clay. Test piles were cast-in-place steel reinforced concrete piles. The longitudinal steel to concrete reinforcement ratio was two percent over the entire length of the column. Pile as-built schematics documented by Suleiman et al. (2006) are shown in Table 2.1 and Figure 2.2.

Table 2.1 Test Setup (Suleiman 2006)

Test unit ID	Ambient temperature and frost depth	Column diameter (cm)	Column length (m)	Column reinforcement	Shaft diameter (cm)	Shaft length (m)	Shaft reinforcement in the critical region
SS1	23 °C and 0 cm	61	2.69	20, 19 mm long bars 9.5 mm spirals at 63 mm	61	10.36	20, 19 mm long bars; 9.5 mm spirals at 63 mm
SS2	−10 °C and 76 cm	61	2.69	20, 19 mm bars 9.5 mm spirals at 63 mm	61	10.36	20, 19 mm long bars; 9.5 mm spirals at 63 mm
SS3	−6 °C and 76 cm	61	2.44	20, 19 mm bars 9.5 mm spirals at 63 mm	91	10.67	20, 29 mm long bars 9.5 mm inner spirals at 63 mm; 12.7 mm outer spirals at 76 mm

The Iowa test piles were instrumented with 32 strain gages, eight displacement transducers and one rotation device. While testing, lateral load was applied to the pile using force control during the first part of the test. Once a specified displacement was reached, load was applied using displacement control until the pile-soil system failed. The lateral applied test loads were applied with using a computer to control the rate of load (force control) or the rate of deflection (displacement control) Three test piles were laterally loaded: one during summer and two during winter. The depth of seasonal frost was approximately 30 inches during winter testing. Temperatures of the frozen layer ranged from 0 to -5 degrees Celsius. The test results showed that seasonally frozen soils

increased the effective elastic stiffness by 170 percent, increased shear demand by 44 percent, reduced length of the plastic region by 64 percent and shifted the location of maximum moment upward by 0.84 m.

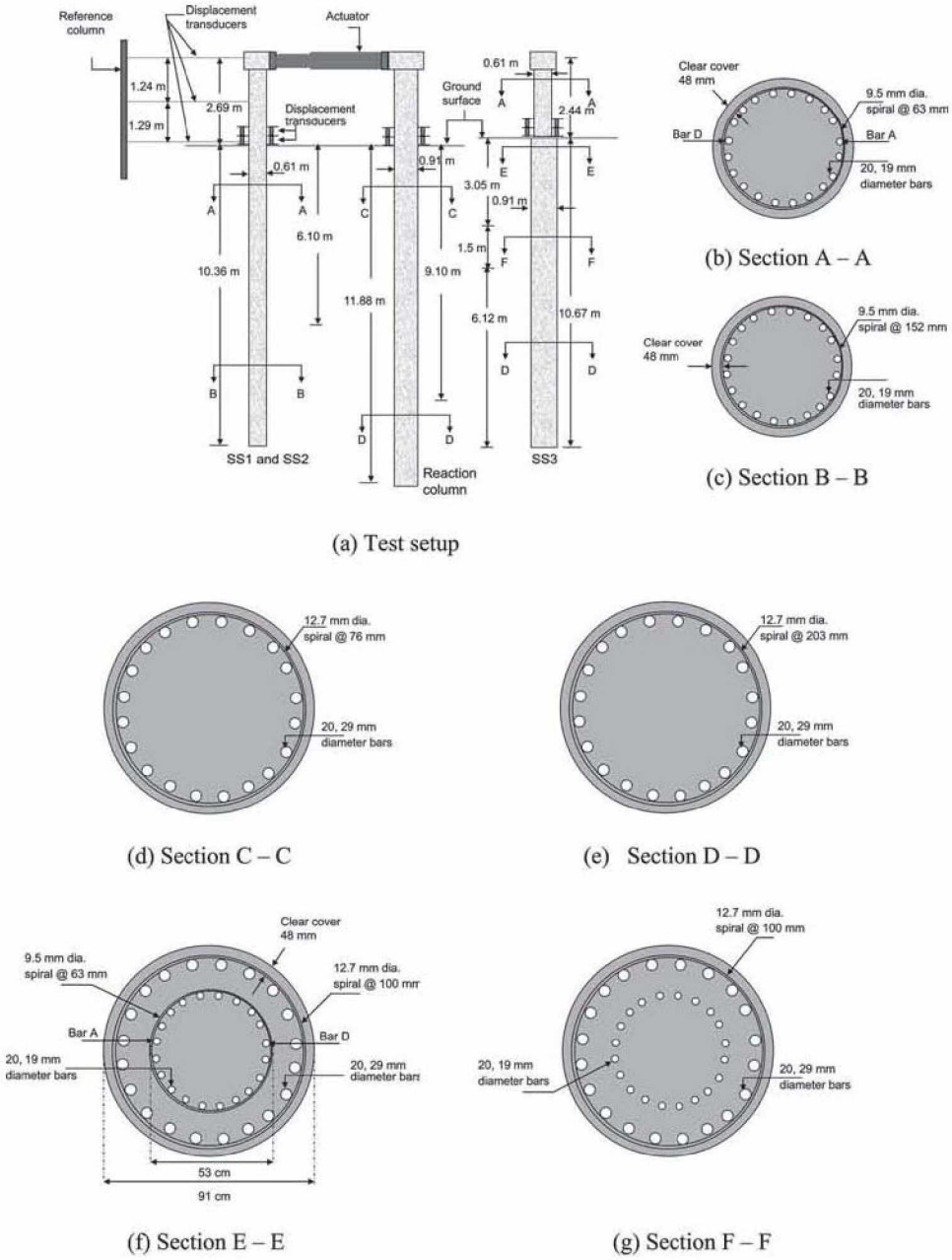

Figure 2.2 Suleiman Pile Test Setup (Suleiman et al. 2006)

2.3 Fairbanks Silt

The testing program discussed in this study was conducted at the ASCE dedicated research site on Farmer's Loop approximately 8 miles from the University of Alaska Fairbanks campus. This site was made available by the U.S. Army Cold Regions Research and Engineering Laboratory (CRREL) for the purpose of testing pile behavior vs seasonal frost depth. The test piles were subjected to quasi static lateral loads. The soils at this site are primarily Fairbanks silt. Fairbanks silt has been studied in the past by many researchers (USACE 1950, Linell 1973, Haynes et al. 1975, Haynes and Karalius 1977, Nidowicz 1981, and others). The relevant results are summarized in the following pages.

2.3.1 Soil Exploration at the Farmers Loop Test Site

The history of the site dates back to the early 1940s when the United States Army Corps of Engineers (USACE) did early work studying building methods in ice rich permafrost. In the 1940s the elevation of the top of the permafrost ranged from a few inches to few feet below ground surface, and in most cases the top of the permafrost was at the bottom of the active layer (USACE 1950). The soils report from early testing is summarized in Table 2.2.

A permafrost degradation study was started by USACE in the 1940s and is summarized by Linell in a 1973 report entitled "Long Term Effects of Vegetative Cover on Permafrost Stability in an Area of Discontinuous Permafrost" (Linell 1973). In the report, the degradation of the permafrost was tracked and quantified. By 1973 the permafrost beneath the ground that was stripped to mineral soil had degraded to a depth

of 6.7 meters. See Table 2.3 for bore logs from the Linell plots. The bore hole was drilled in March 1946. At that time, the surface elevation of the bore hole was 155m, and all soil in the bore hole was frozen (Linell 1973).

Table 2.2 Summary of 1940s Soil Investigation (USACE 1950)

Corps of Engineers U.S. Army (1950).			
Sample #	699	671	677
Depth below ground surface, ft	2.0	6.0	30.0
Physical Constants			
1. All fraction of sample			
Moisture -- field condition, (%)	74	28	35
Natural density, (lb/ft^2)	56	91	81
Speciftic Gravity	2.72	2.76	2.70
Natural Porosity, (%)	67	47	52
Natural Void Ratio	2.03	0.89	1.08
2. Fraction passing no. 40 sieve			
Plastic index	Non-plastic	Non-plastic	Non-plastic
Mechanical Analysis			
Percent of total sample grain size in in or US standard sieve #.			
Gravel: #10 to 3 in	0	0	0
Sand: #200 to #10	4	10	4
Coarse, #40 to #10	0	0	0
Fine, #200 to #40	4	10	4
Silt or clay: Less then no. 200	96	90	96
Effective size in mm	0.0067	0.023	0.0058
Uniformity coefficient	3.4	1.9	5.0
Class (textural)	Silt	Silt	Silt
USED soil group	ML	ML	ML

Table 2.3 Soils Report (Linell 1973)

Depth Below Surface (m)	*Description of soil*	*Moisture Content (%)*	*Dry Density (kg/m^3)*
0.0 - 0.25	Pt, Peat	258	320
0.25 - 0.55	ML, V_s-silt with peat (stratified)	26	1520
0.55-1.2		26	1420
1.2 -2.5		29	1455
2.5 -3.9	ML, $V_{r,s}$-silt with peat (stratified)	37	1310
3.9 -4.8		37	1280
4.8 -6.1		38	1280
6.1 -6.5		41	1215
6.5 -7.3	ML, Vr,s-silt	37	1280
7.3 -8.6		32	1375
8.6 -9.5		33	1375

In the early 1980s, Bernard Nidowicz wrote his thesis, "Consolidation and Shear Strength Characteristics of Fairbanks Silt." In his work, two sites in Fairbanks were studied: the CRREL Site on Farmers Loop Road and a site located at the base of Chena Ridge. Nidowicz classified both sites and the soil properties at each site, see Tables 2.4-2.6.

Table 2.4 CRREL Farmers Loop Test Site Summarized (Nidowicz 1981)

Initial Soil Index Properties-CRREL Site									
Test Number	*Depth (Ft)*	*Density Dry (lb/ft^3)*	*W (%)*	*S (%)*	*LL (%)*	*PI (%)*	*SG*	*e_0*	*Organics (%)*
C-8	2.0	78	37.7	99.7	45.0	NP	2.5	0.85	8
C-22	2.5	64	49.3	87.0	48.0	NP	2.5	1.40	12
C-9	9.0	86	34.5	98.7	33.0	NP	2.7	0.93	6
C-5	10.5	81	38.0	95.0	37.0	NP	2.7	1.06	7
C-10	11.5	73	48.3	100.0	45.0	NP	2.6	1.18	14

Table 2.5 Cripple Creek Site Summarized (Nidowicz 1981)

Initial Soil Index Cripple Creek Site									
Test Number	***Depth (Ft)***	***Density Dry (lb/ft^3)***	***W (%)***	***S (%)***	***LL (%)***	***PI (%)***	***SG***	***e_0***	***Organics (%)***
C-21	6.5	88	25.5	75.5	35.0	NP	2.7	0.91	7
C-19	10.5	88	32.2	93.1	31.0	NP	2.7	0.94	6
C-20	11.0	87	30.5	96.1	31.0	NP	2.7	0.86	6
C-17	13.5	88	33.1	98.6	37.0	NP	2.7	0.90	6
C-16	14.0	88	32.8	97.7	36.0	NP	2.7	0.90	4
C-4	24.0	85	34.0	94.6	34.0	NP	2.7	0.96	5
C-11	26.0	84	37.4	100.0	34.0	NP	2.7	0.99	5

Table 2.6 Cripple Creek Soil Sample Used for Tri-axial Testing (Nidowicz 1981)

Cripple Creek Site											
Test Number	***Depth (Ft)***	***Density Dry (lb/ft^3)***	***W (%)***	***S (%)***	***LL (%)***	***PI (%)***	***SG***	***σ_3 (PSI)***	***Organics (%)***	***Peak Deviator Stress (PSI)***	***Strain at Peak Stress (%)***
T-6	11.0	81	34.8	98.0	40.0	NP	2.65	5	6	17.9	8.0
T-7	11.5	80	39.3	100.0	45.0	NP	2.65	15	6	31.5	12.0
T-4	23.3	81	36.5	100.0	29.0	NP	2.74	5	4	14.9	7.5
T-5	23.9	78	36.5	100.0	30.0	NP	2.74	10	4	20.1	11.0

Nidowicz did tri-axial testing on undisturbed samples from both the CRREL site on Fairbanks Loop and the Cripple Creek Site. Unfortunately there was a problem with his tri-axial apparatus and a large number of the results for the tested samples were unusable. Unfortunately, the only usable results were for tri-axial tests conducted on samples taken from the Cripple Creek Test Site. Figure 2.3 shows the tri-axial test results from an unconsolidated, undrained sample at natural water content. Figure 2.4 shows the tri-axial test results from an unconsolidated, undrained sample that was saturated with back pressure.

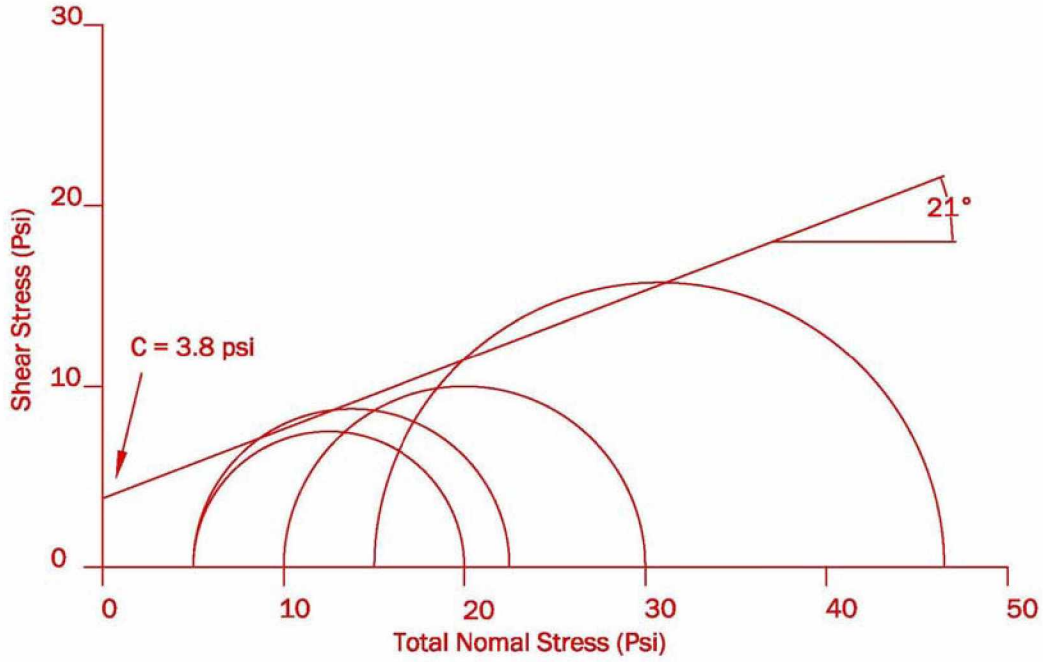

Figure 2.3 Tri-axial Test Results Unconsolidated Undrained, Natural Water Content

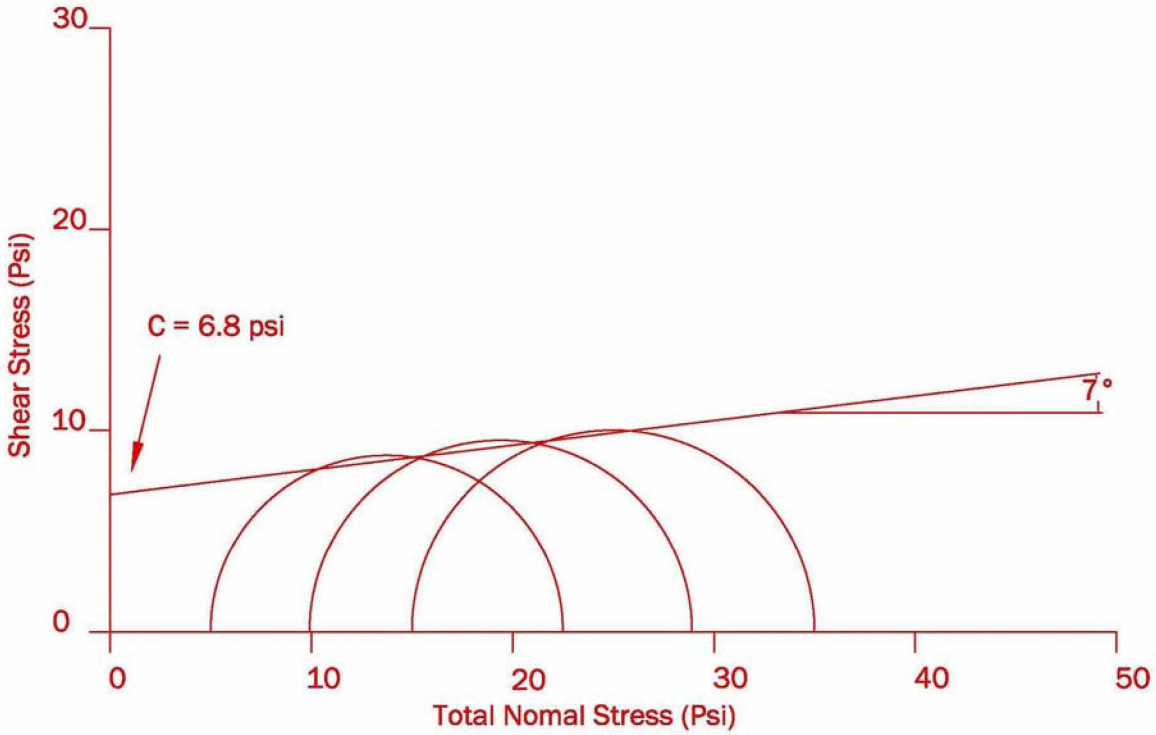

Figure 2.4 Tri-axial Test Results Unconsolidated Undrained, Samples Saturated with Back Pressure

2.3.2 Properties of Frozen Fairbanks Silt

Several studies have been conducted by USACE to evaluate properties of frozen silt (Haynes et al. 1975, Haynes and Karaluis 1977, Yuanlin and Carbeee 1984, 1987). The reports provide frozen soil strength properties for Fairbanks silt. These results are based on uniaxial compression tests. In the 1975 report "Strain Rate Effect on the Strength of Frozen Silt" remolded silt samples were tested at varying strain rates (0.00017 to 3 cm/sec) and a constant temperature of 9.4 degrees Celsius. In the 1977 report, "Effect of temperature on the strength of frozen silt," remolded silt samples were tested at temperatures varying from 0 to -55 degrees Celsius. Two load rates, 4.23 and 0.0423 cm/sec were used throughout testing. In a 1983 paper the researchers conducted uniaxial compression testing on frozen silt using constant deformation rates in an attempt to quantify the compressive strength of frozen silt as a function of applied strain rate, temperature, and water content (Haynes and Karaluis 1977). Figure 2.5 shows the effect of temperature on the strength of Fairbanks silt.

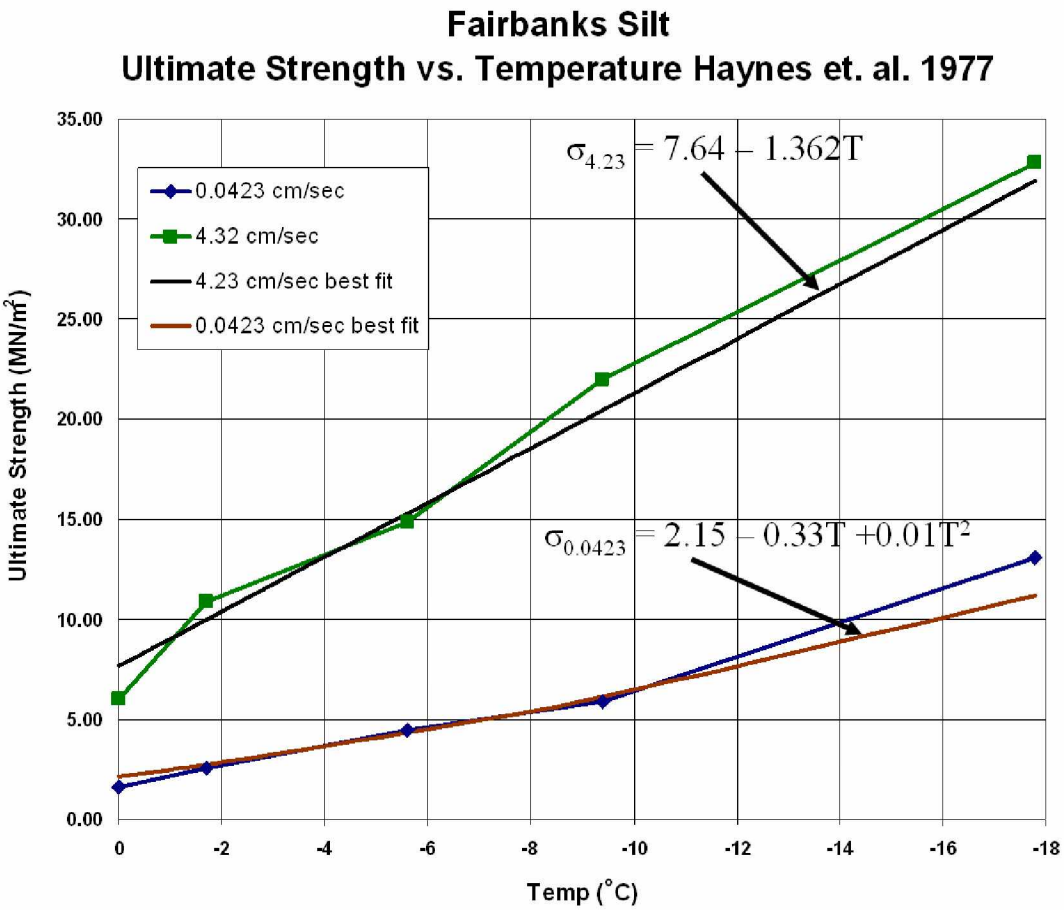

Figure 2.5 The Effect of Temperature on the Ultimate Strength of Fairbanks Silt (Haynes and Karaluis 1977)

3 Pile Instrumentation

Consider that it is important to develop an understanding of how a laterally loaded pile behaves when embedded in a soil. It may be argued that this system (soil-structure) will response is a function of the soil type, soil moisture , the surrounding ground temperature, the stiffness of the pile, the rate of loading, the number of load cycles and conditions prior to the load application.

Thus, an instrumentation plan was developed to assist in understanding how a pile may respond to laterally cyclic quasi-static applied loads for different seasonal exposures (summer versus winter). In order to evaluate the influence of lateral loading of piles in seasonally frozen soils or thawed soils, several parameters were measured.
These included:

1. Deflection at both the ground line and below the ground line;
2. Temperature of the soil with depth;
3. Deflection above ground;
4. Load applied to the pile

For testing the two test piles were instrumented with 30 strain gages, one inclinometer, 22 thermistors and 6 linear motion transducers. See Table 3.1 for instrumentation elevations. All instrumentation except the inclinometer was read and powered by a Campbell Scientific CR9000x data acquisition system. The load frame was equipped with a load cell and the reaction pile was not instrumented.

3.1 Deflection above Ground Surface and Measurement of Applied Load

Deflection above ground surface was measured using linear motion transducers (LMT) manufactured by Ametek. This measurement conformed to ASTM D 3966-07 Standard Test Methods for Deep Foundations under Lateral Load. During testing, 6 LMT sensors were used to monitor the above ground lateral movement of the pile. The elevation of each sensor is presented in Table 3.1.

Loads applied to the pile were measured with a 200 kip load cell. The load cell used for this study was a Honeywell model 41 precision load cell with a 200,000 lb capacity and 150 percent overload capacity. The accuracy of the load cell is ± 0.1 percent of full scale (Honeywell).

During testing, the LMT sensors and load cell were read every 0.1 sec using a Campbell 9000x data acquisition system, see section 3.3.

3.2 Instrumentation of the Rebar Cage

For lateral loaded pile tests it is important to measure load, time, and the corresponding deflection as a function of depth. The above ground surface deflections of the pile were measured using linear motion transducers. Deflection of the pile below ground surface is more difficult to measure and has to be measured indirectly. To accomplish this, two separate systems were employed. The first system consisted of 30 strain gages; the second system was an inclinometer. All of the strain gages located inside the test pile were mounted to the reinforcing bar (rebar) cage in the laboratory and then transported to the test site and lowered into the pile. The rebar cage was built using

metal jigs to ensure that the gages would be placed accurately inside the pile. See Figure 3.1

Figure 3.1 Instrumented Rebar Cages

Placement of the gages in the completed test piles was accurate to approximately 1/8 inch in any direction. After installation, the sensors in both test piles had the same elevation with respect to ground surface. During the winter of 2008-2009 the piles underwent frost jacking with each pile being raised out of the ground to a different elevation. The corrected elevation of each gage is given in Table 3.1.

3.2.1 Strain Gages

In the past, strain gages have been used to measure strains throughout the pile length. Once the strain profile was obtained at a give point during the test, a curve would be fit to the data. The equation of the curve could then be integrated twice to get a deflected shape. Theoretically this works well, but experimentally, errors are

compounded and results can be difficult to interpret. In many cases the pile being tested would be calibrated in the laboratory before being installed in the ground (Foriero et al. 2005, Cox et al. 1974, and Reese and Welch 1975). The pile would be calibrated by subjecting it to bending in the laboratory so that a correlation between strain and the deflected shape of the pile could be made. The calibrated test pile would then be placed in the ground and tested. After testing, the test pile would be removed from the soil and taken back into the lab and again subjected to bending. Another correlation between the deflected shape of the pile and strain measurements could then be made. For this experiment, not only would this type of calibration be difficult and expensive to do, but the pile tested is also a reinforced concrete filled pipe pile that exhibits non-linear properties under bending, so the stiffness changes as the concrete cracks.

Thirty strain gages were installed in each test pile: 20 on outermost tensile rebar, the A-line, and 10 on the outermost compression rebar, the B- line. Table 3.1 shows the elevations for each gage. The strain gages used in this study were full bridge, weld-able strain gages with two active elements per gage. They were manufactured by Hitec Products, Inc. and the model number is HBWF-35-125-6-30GP - SS. The gages have a gage factor of 4.15.

The strain gages were welded to the rebar cage. After the gages were installed onto the rebar cage they were coated in a thick layer of silicone to protect them during installation and to keep the concrete from bonding to the back of the gages. See Figures 3.2 and 3.3. During testing the strain gages were read every 0.1 sec using the Campbell 9000x data acquisition system, see section 3.3.

Figure 3.2 Strain Gage Installed on Rebar

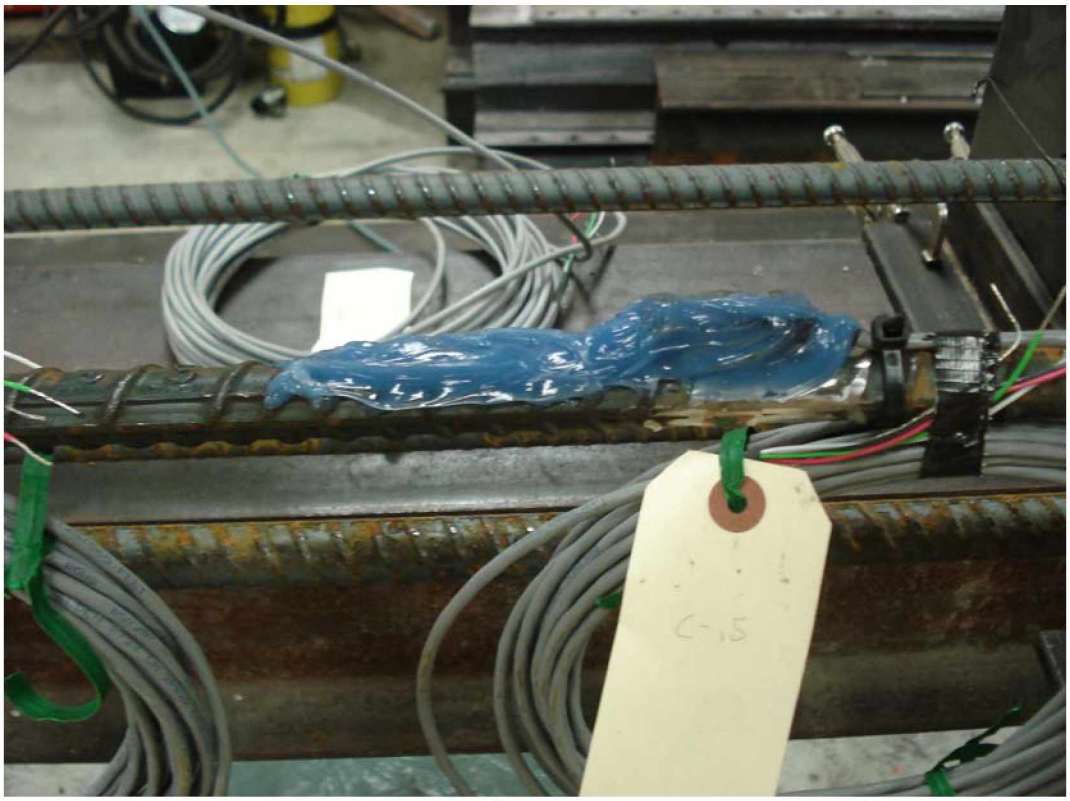

Figure 3.3 Strain Gage Installed on Rebar Cage and Protected with Silicone

3.2.2 Inclinometer

An inclinometer was installed at the center of the rebar cage; the inclinometer uses tilt sensors to measure the angle of the pile at a given point. By knowing the

location of individual inclinometers in space and if spaced sufficiently close together, it is possible to determine the three-dimensional location of the deformed pile at a given point in time. That is, by multiplying the slope by spacing, the deformed shape may be calculated along the length of the pile. The inclinometer used was a model INC300 series inclinometer; it was read using a GCM 1200 control module. Both the inclinometer and the control module were manufactured by Geodaq (Geodaq 2006) . The inclinometer is very accurate for the measurements range used during pile testing; the accuracy of any point is ± 0.03 inches (Geodaq). See Figures 3.4 and 3.5 for pictures of inclinometer as installed in the rebar cage before concrete was poured. See Table 3.1 for inclinometer tilt sensor elevations.

Figure 3.4 Inclinometer as Installed in the Test Pile

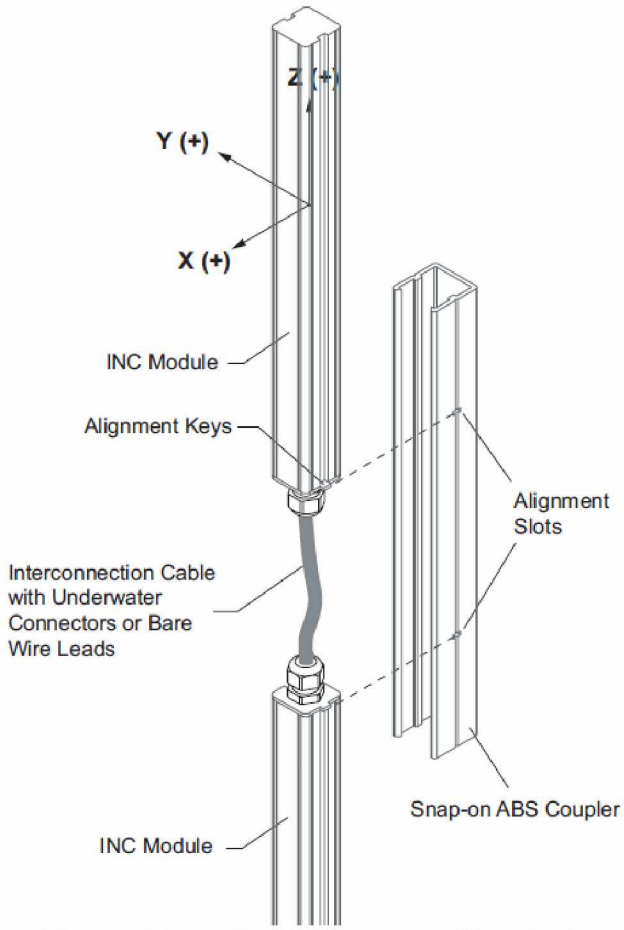

Figure 3.5 Inclinometer setup (Geodaq)

3.2.3 Soil and Pile Temperatures

The piles were tested in the both the frozen and unfrozen condition. In the frozen condition, the temperature of the soil is important. Not only is the depth of the frozen soil layer important but also, the temperature of the soil has a significant impact on soil strength. In order to accurately measure soil temperatures, thermistors, which measure temperature, were placed throughout each test pile (north test pile and south test pile) and in a soil string located 20 feet away from the test piles. The accuracy of the thermistors is ± 0.1 degrees Celsius. See Table 3.1 for thermistor elevations. The thermistors in the

test piles were placed approximately one inch inside the steel pipe jacket. All three soil strings were read throughout the winter by U.S. Army Cold Regions Research and Engineering Laboratory (CRREL) as an attachment to the meteorological station at the test site.

3.3 Data Acquisition System

A Campbell CR9000X (Campbell 2010) data acquisition system was selected for this study. It is capable of monitoring static loads, dynamic, earthquake and blast loads. The data acquisition system provided 5 volts of precision power to the gages by using 9060 Excitation cards. The cards used to read the gages were CR9050 Analog Input w/RTD (RTD-real time data). The program used to code the CR9000X during testing is provided in Appendix B.

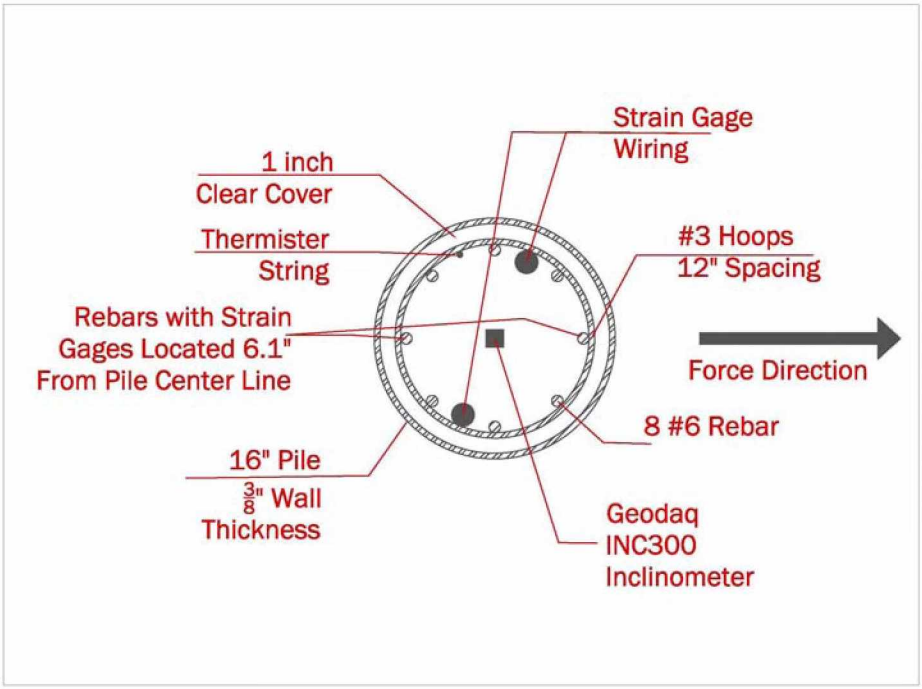

Figure 3.6 Pile Instrumentation Cross Section

Table 3.1 Gage Location / Elevations as Tested

North Pile as Tested		South Pile as Tested	
Elevation from Ground Surface (in)	Gage at Elevation	Elevation from Ground Surface (in)	Gage at Elevation
59.75	LMT 1	59.75	LMT 1
53.75	Inc & Therm	52.50	Inc & Therm
49.75	LMT 2	49.75	LMT 2
41.75	Inc & Therm	40.50	Inc & Therm
40.25	LMT 3	40.25	LMT 3
29.75	Inc & Therm	28.50	Inc & Therm
28.25	LMT 4	28.25	LMT 4
17.75	Inc & Therm	16.50	Inc & Therm
16.25	LMT 5	16.25	LMT 5
5.75	A0, B0, Inc & Therm	4.50	A0, B0, Inc & Therm
4.25	LMT 6	3.00	LMT 6
-6.25	A1, Inc & Therm	-7.50	A1, Inc & Therm
-18.25	A2, B2, Inc & Therm	-19.50	A2, B2, Inc & Therm
-30.25	A3, Inc & Therm	-31.50	A3, Inc & Therm
-42.25	A4 & B4	-43.50	A4 & B4
-48.25	Inc & Therm	-49.50	Inc & Therm
-54.25	A5 & B5	-55.50	A5 & B5
-60.25	Inc & Therm	-61.50	Inc & Therm
-66.25	A6 & B5	-67.50	A6 & B5
-72.25	Inc & Therm	-73.50	Inc & Therm
-78.25	A7 & B6	-79.50	A7 & B6
-84.25	Inc & Therm	-85.50	Inc & Therm
-90.25	A8 & B7	-91.50	A8 & B7
-96.25	Inc & Therm	-97.50	Inc & Therm
-102.25	A8	-103.50	A8
-108.25	Inc & Therm	-109.50	Inc & Therm
-114.25	A10 & B9	-115.50	A10 & B9
-120.25	Inc & Therm	-121.50	Inc & Therm
-126.25	A10	-127.50	A10
-132.25	Inc & Therm	-133.50	Inc & Therm

Table 3.1 Continued - Gage Location / Elevations as Tested

North Pile as Tested		South Pile as Tested	
Elevation from Ground Surface (in)	Gage at Elevation	Elevation from Ground Surface (in)	Gage at Elevation
-138.25	A12 & B11	-139.50	A12 & B11
-150.25	A13, Inc & Therm	-151.50	A13, Inc & Therm
-162.25	A14, Inc & Therm	-163.50	A14, Inc & Therm
-174.25	A15, B15 Inc	-175.50	A15, B15 Inc
-186.25	A16, Inc & Therm	-187.50	A16, Inc & Therm
-198.25	A17 & Inc	-199.50	A17 & Inc
-210.25	A18, Inc & Therm	-211.50	A18, Inc & Therm
-222.25	A19, Inc & Therm	-223.50	A19, Inc & Therm
-234.25	Inc & Therm	-235.50	Inc & Therm

Abbreviations

- Inc – inclinometer Therm – thermistor
- A# - Tensile Strain gage
- B# - Compressive Strain gage

4 Site Selection and Pile Installation

The criteria for selecting a test site included the following items:

1) A thick layer of seasonally frozen soil

2) Silty soil with high moisture content;

3) On or near the University of Alaska Fairbanks campus;

4) Permafrost lower then bottom of the test piles;

5) Easily accessible by pile driving equipment.

Several sites throughout the Fairbanks area were explored as possible test sites. Initially the permafrost depth for each site was evaluated to insure that the test site would meet the criteria that the piles were not embedded in permafrost. The site selected for pile testing was the Farmers Loop Permafrost Research Site. Prior to selecting this site, the site was hand probed to insure that the depth of the permafrost would be below the bottom tip of the pile. The test site is owned and operated by the U.S. Army Corps of Engineers Cold Regions Research and Engineering Laboratory (CRREL) and it is also an ASCE dedicated research site. The test site is located in Fairbanks, Alaska at mile 0.9 Farmers Loop Road approximately 8 miles from the University of Alaska Fairbanks campus.

4.1 Site Selection and Soil investigation

As part of the selection of the test site on Farmers Loop Road, a preliminary soil investigation was completed. Shallow test holes were dug and the permafrost table was located at several places at the site. The shallow holes were dug by hand and the permafrost table was found by working a half-inch diameter rod into the soil until refusal

of the rod was reached. The location that was selected is North 64^0 52.520'. West 147^0 40.391'. This is approximately 75 feet from the CRREL test site meteorological station. Preliminary investigation revealed a thin gravel layer overlaying silt and a permafrost table located at approximately 20 - 22 feet below ground surface. A drill rig was brought in and soil borings were taken at the proposed location for the two test piles and the reaction pile. See Figure 4.1.

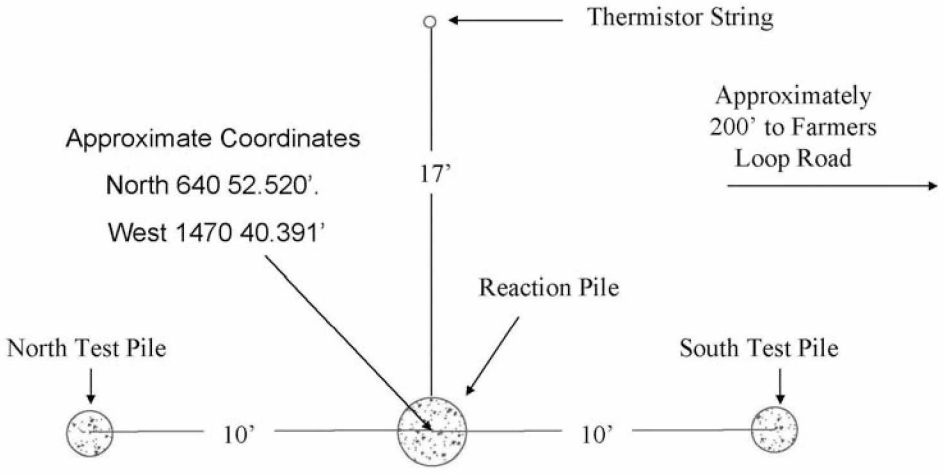

Figure 4.1 Site Map

Three bore holes were drilled at the test site on July 24, 2008. The bore holes were drilled at the proposed location of piles. Bore hole #1 was drilled at the proposed location of the south test pile, bore hole #2 was drilled at the proposed location of the reaction pile, and bore hole #3 was drilled at the proposed location of the north test pile. The bore holes were logged by Mikhail Kanevsky, Ph.D. in Permafrost Geology, Research Assistant Professor at University of Alaska Fairbanks. For the SPT Testing continues samples were taken. Four blow counts were recorded in the bore logs for each

test; for SPT values the middle two blow counts should be taken. A 300 lb hammer was used; a hammer efficiency of 60% is typical for this drill rig. See Appendix C for boring logs.

4.2 Pile Installation

The test piles were driven in August of 2008, using a vibratory hammer mounted to a crane. See Figure 4.2

Figure 4.2 Pile Installation

The bottoms of the piles were left open during installation. After installation soil was removed from the inside of the pile using a smaller pile with a flap at the bottom of it (soil removal apparatus). See Figure 4.3

Figure 4.3 Small Soil Removal Apparatus

The soil removal apparatus was vibrated into the soil; when the apparatus was removed the flap at the bottom retained the soil. While this method of soil removal was effective for removing most of the soil from inside the pile, it was not effective for removing soil stuck the walls of the pile. In an attempt to remove the soil stuck inside the pile walls, the soil removal apparatus was repeatedly lowered and vibrated into the piles. After extensive attempts to remove all of the soil from inside of the piles the steel pipe jacket began to sink in the ground; at this point the method of soil removal was immediately

abandoned. The results of the excessive vibration on the pile were: excavation of soil several feet below the bottom of the pile, disturbing the permafrost below the pile, the liquefaction of the soil surrounding the piles, and the piles filling with a mixture of silt and water. Subsequently a large vacuum truck was brought in to remove the rest of the soil and water from inside the piles. The vacuum truck was equipped with a high pressure water jet at the inlet of the vacuum which left the inside of the piles clean and free of soil. The instrumented rebar cages were then lowered into the test piles. The piles were then filled with concrete using a concrete pump truck. Inside of the rebar cage a four inch PVC pipe was installed to allow the ribbed hose from the pump truck to be lowered to the bottom of the test pile without damaging the instrumentation. The PVC pipe and pump truck hose were removed as the concrete was poured. The concrete was not allowed to free fall more then 3 feet inside the test pile. The concrete mix used was a self consolidating mix, test cylinders and concrete beams were taken during testing results are discussed further in Chapter 7.

5 Testing

Cyclic quasi-static lateral loads were applied to two 16-inch diameter steel jacketed reinforced concrete test piles. It was the purpose of this study to evaluate the stiffness change between loads applied to a pile in thawed ground versus the load applied to a pile in seasonally frozen soils. The testing was designed to create a correlation between stiffness of the pile in unfrozen soil and that of a similar pile in a layer of seasonally frozen soil. To date there has been extensive testing on piles in unfrozen soils. There has also been some testing on piles in permafrost, but there has been very little testing on piles in seasonally frozen soils. The testing for this project consisted of three full scale pile tests. The first test was in September 2009 (fall). At the time, the soil was thawed for the full length of the pile. The second test was performed in January 2010. This date was chosen in an attempt to test when the frost depth was approximately half the expected maximum depth of frozen conditions. The final test was conducted in late March 2010 when depth of seasonally frozen soil was nearly at its maximum depth.

5.1 Pile Testing Procedure

There are two standards that provide guidelines for laterally loaded pile testing. The first standard is a draft of a report entitled "Recommendation for Seismic Performance Testing of Bridge Piers." The report was prepared for the Federal Highway Administration (FHWA 2004) in an attempt to standardize bridge pier testing. The other guideline is published by the American Society of Testing and Materials (ASTM). This standard is "ASTM D 3966-07 Standard Test Methods for Deep Foundations under Lateral Load." Since the FHWA 2004 report was specifically drafted for seismic testing

of bridge piers, it was the primary reference used in this study. ASTM D 3966-07 was used where the FHWA report was not specific enough.

According to FHWA 2004 the pile testing falls under type A2, Quasi Static cyclic testing; under the classification of Quasi Static testing. Thus, the effects of inertia can be ignored. While cyclic testing from compression to tension to create asymmetric load conditions is recommended, equipment limitations precluded cycling from tension to compression. The test equipment could only pull the test pile toward the reaction pile. Further, displacement control is recommended by FHWA and was used for cyclic testing of piles. Thus, during September's test, displacement control was used. Displacement control is designed for soils where exceeding the ram stroke usually defines failure or the end of testing. Displacement control was attempted during winter testing. As loads spiked to almost 50 percent of the yield strength of the pile without the pile deflecting 0.1 inches at the ram, it became clear that load control not displacement control should be used for winter testing.

The following recommendations from FHWA shaped the test plan.

1) The initial amplitude should be below yielding of the pile.
2) The subsequent amplitudes should be between 1.25 times and 1.5 times the current amplitude.
3) Three load cycles should be applied for each amplitude.

The loading plan that was used for pile testing is listed in Figures 5.5, 5.10, 5.15. The September test was displacement controlled and the January and March tests were load controlled.

While a constant ram speed throughout the entire loading program is recommended, some variation in loading speed is commonly practiced (FHWA 2004). Obtaining a constant speed throughout the test was extensively explored and in the end it was determined that it was not possible without going to a computerized hydraulic loading system. The loading rate for the pile was variable with a maximum loading speed at the ram of 7 in/min (0.29 cm/sec) for loads less then 22 kips and 1 in/min (0.0423 cm/sec) for loads over 22 kips. These load speeds are only approximations and were obtained using the manufacturer's pump specifications for the pump and the effective area of the hydraulic ram, which is 22.5 square inches. See Figure 5.1 for pump flow chart.

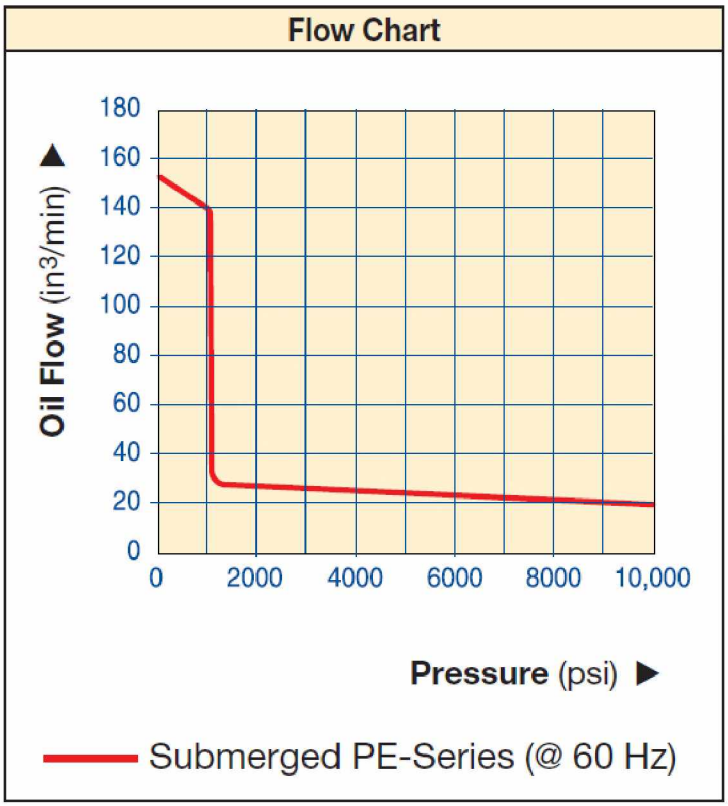

Figure 5.1 Flow Chart for Hydraulic Pump - Enerpac PE – Series Pump; Model PEJ1401B (Enerpac)

5.2 Test Frame Design Construction and Testing

The test frame was designed to meet the requirements set forth by ASTM D 3966-07 and FHWA 2004. The test frame was originally designed using Allowable Stress Design (ASD) methods to limit the amount of stress that each component of the frame was to be subjected to. The estimated yield strength of the pile was 4,400 kip-inches, and the estimated ultimate strength of the pile was 8,700 kip-inches. For the September test, the estimated location of the maximum moment was between 48 and 96 inches below ground surface. Using the equivalent stiffness method and assuming the pile is fixed at 48 inches below grade and that the ram is located 40 inches above grade approximately 90 kips are required to fail the pile. The design capacity of the frame was 120 kips which is 30 percent beyond the estimated capacity of the pile. The frame was also designed with a factor of safety so increased capacity was built in. See Figure 5.2 and 5.3 for test frame design.

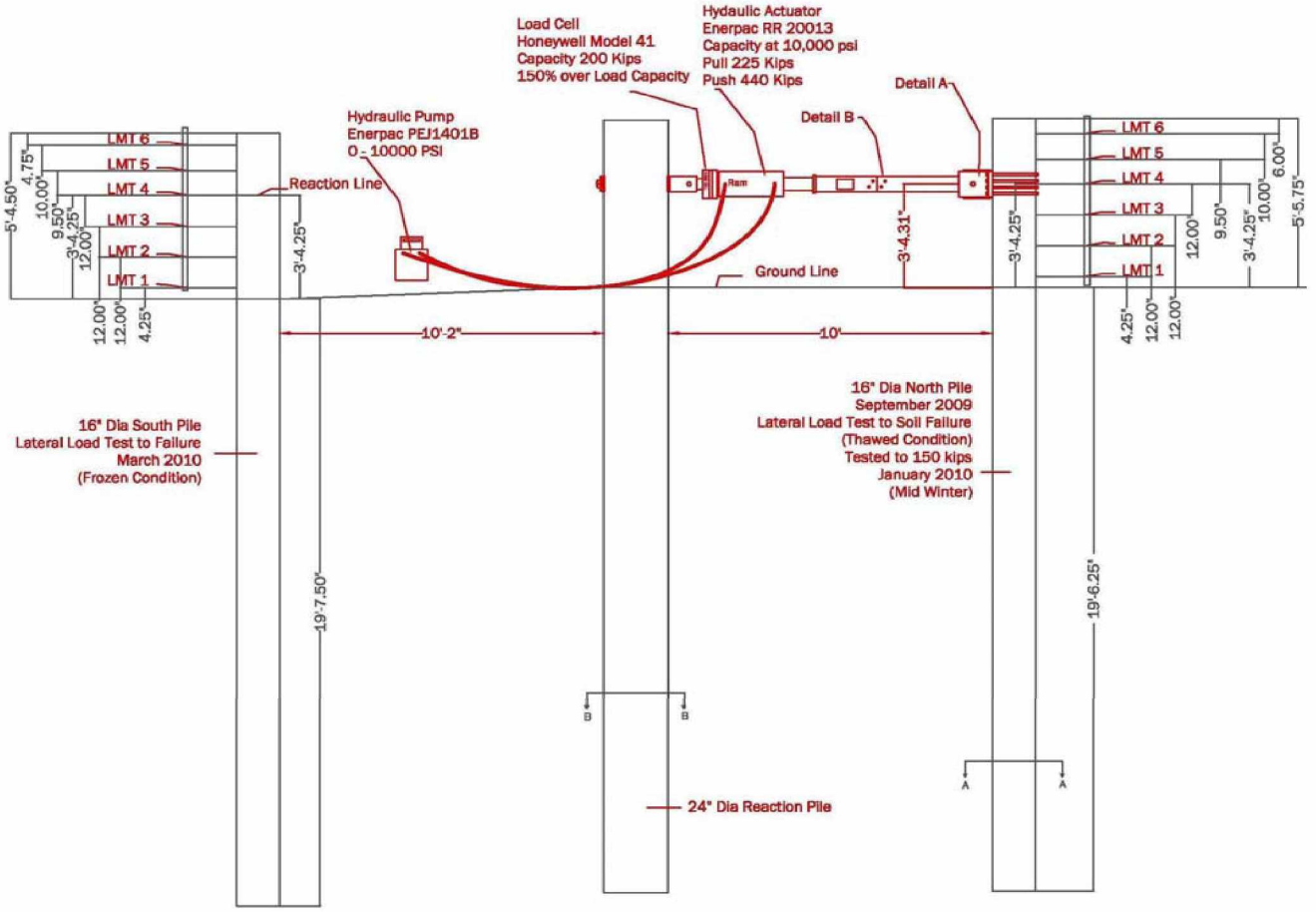

Figure 5.2 Test Frame Overview

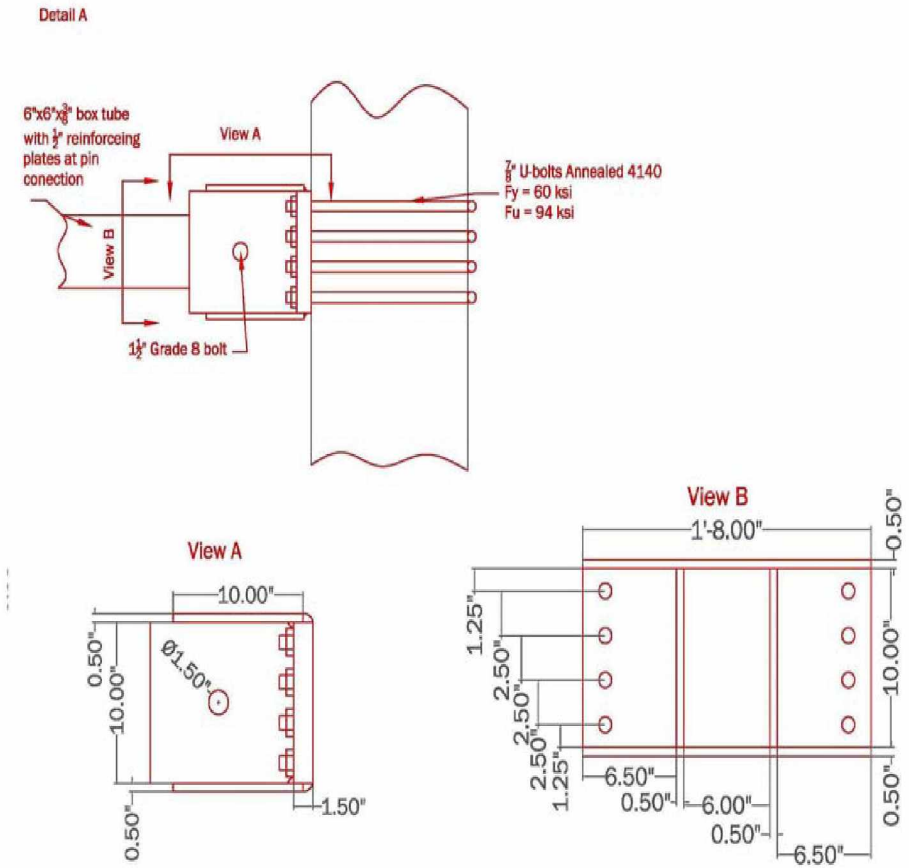

Figure 5.3 Test Pile Connection Detail

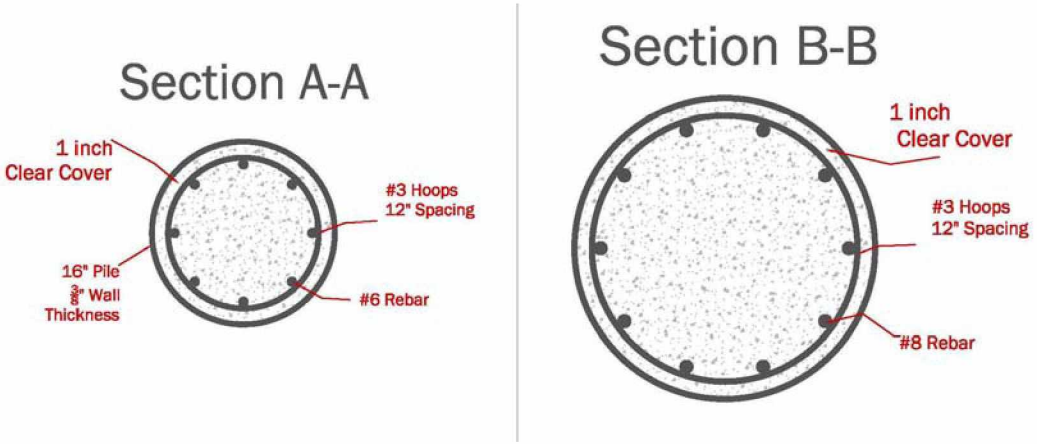

Figure 5.4 Pile As Built

5.3 Pile Testing

5.3.1 September Testing

On September 19, 2009 the north test pile was tested. The weather was overcast and calm, the range in air temperature was from 45-55 degrees Fahrenheit. Displacement control was used throughout the test with the target displacement taken at the elevation of the ram. The first target displacement was 0.15 inches. Successive target displacements were 1.5 times the previous displacement until 2.4 inches. Then, successive target displacements were 1.25 times the previous displacements. Target displacements in Figure 5.5 were used for the test with the pile being pushed back into the upright position after each load cycle. Before testing began, all instrumentation was zeroed by taking an average reading in the unloaded condition and subtracting it from the gage reading. Shortly after testing began, it was determined that data was not being collected. This was at the third displacement increment (increment 0.37 inches). At this point, we unloaded, re-zeroed and restarted testing. After the first few initial cycles, the pile was held in place

for a period of at least 30 seconds. This was done in an attempt to give the inclinometer sufficient time to measure and record the centerline deflection of the pile. See Figure 5.6 for cyclic load vs. deformation at the point of loading. Testing was stopped when ram stroke reached capacity at a test pile displacement of 5.7 inches. While this displacement is less then the full capacity of the hydraulic ram, 13 inches, due to the cyclic testing and extremely soft soil, the reaction pile was slowly jacked toward the test pile throughout the course of the test, it was moved father then the test pile was at the end the test see Figure 5.8. Failure occurred in the soil and there were no visual signs of yielding of the test pile. See Figure 5.7 – 5.9 for pictures of final load cycle of September test. The soil gap formed in front of the pile caused by plastic soil deformation is quantified in Figure 5.21.

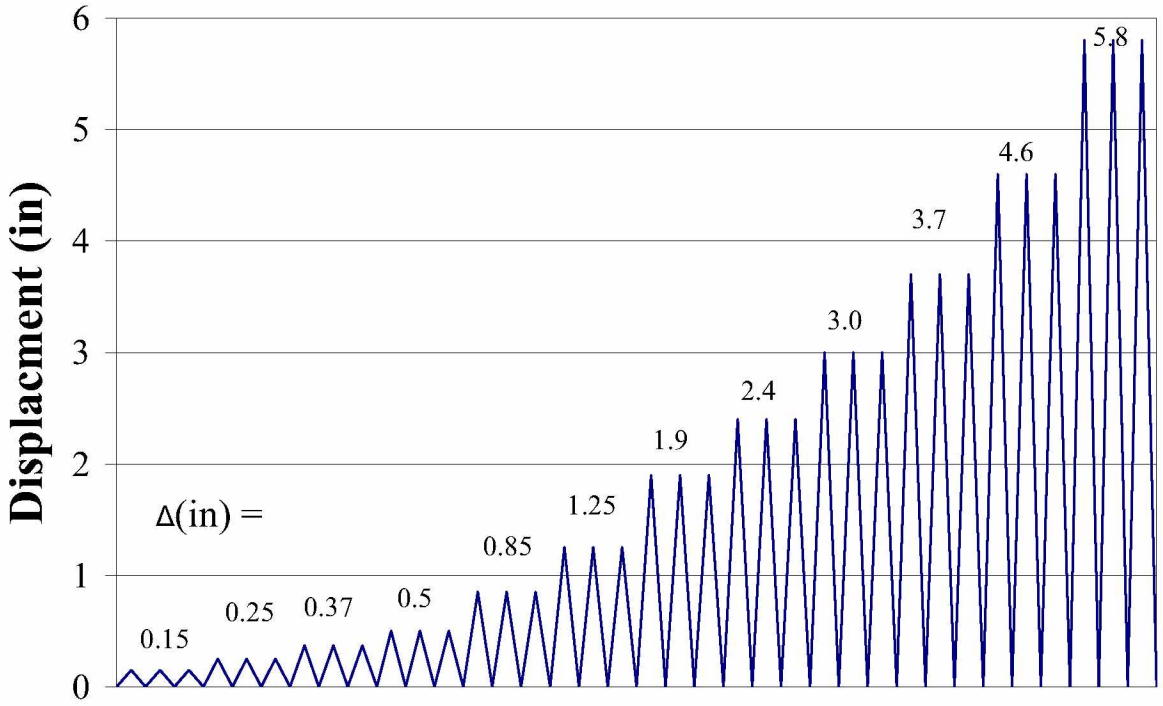

Figure 5.5 September Target Displacement Increments

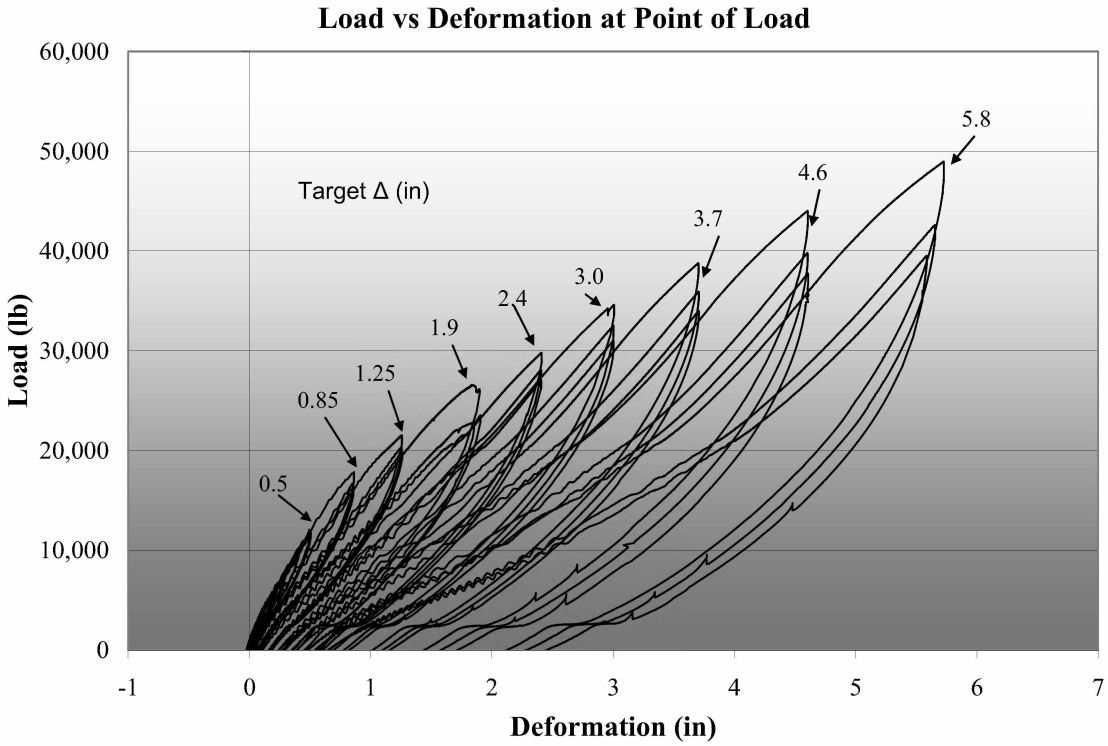

Figure 5.6 September Cyclic Load vs Deformation at Point of Load

Figure 5.7 Test Pile at Final September Load Increment

Figure 5.8 Reaction Pile at Final September Load Increment

Figure 5.9 Plastically Deformed Soil in Front of Test Pile after Final Loading and Unloading

5.3.2 Pile Rehabilitation

In September 2009, we performed the first cyclic laterally loaded pile test. This was on the north 16-inch diameter steel jacketed reinforced concrete test pile. The test loads were applied using displacement control as a criteria for each load increment. During testing, load was applied by pulling the test pile towards the reaction pile until the desired deflection (measured at the load cell) was reached. This was followed by pushing the reaction pile back until the displacement was zero. This was considered cycle. This was repeated three times.

At the next load step, load was applied until displacement at the load cell was a the next target displacement, see Figure 5.5. This continued until failure. In the case of the September test, the soil deformed to the point that ram stroke was exhausted. Failure occurred in the soil and the structural capacity of the pile was not reached. After the test the pile was returned to a vertical position and held there until the soil around the pile relaxed and stayed vertical without any applied lateral load. It was decided that it would be beneficial to test this pile again when seasonal frost was at approximately half of full frost depth.

The soil surrounding the pile after the fall test was plastically deformed and there was a gap between the soil and the pile, see Figure 5.9. At the recommendation of the principal investigator and with the approval of DOT Bridge Design and the funding agencies, sand was placed in the gap and a pencil vibrator was used to liquefy the soil close to the ground surface until the sand was vibrated to fully fill the gap. The extent of

this liquefaction of the soil affected approximately six inches of soil perpendicular to the front of the pile and six feet below the ground surface.

5.3.3 Snow Conditions at the Test Site

In order to obtain the maximum frost depth at the test site, snow was removed from around the south pile. A review of the literature revealed that if snow was removed from around the test pile for a radius of approximately 10 feet, the frost would penetrate evenly around the test pile (Nicholson and Granberg 1973). Snow was removed after each accumulation of four inches of snow depth. Snow was left undisturbed around the north pile to insulate the ground surface and keep the frost depth to a minimum. It was estimated from 2008-2009 frost data that there would be maximum of approximately 6 to 8 feet of frost depth at the pile site if snow cover was left in place. This was assuming winter conditions would be similar.

5.3.4 January Testing

The January test was performed on the rehabilitated north test pile. In the beginning of January 2010 the frost depth was just over 3 feet on the north pile. Snow was removed from around the north test pile. Testing started on January 6. Displacement control was initially used, but when loads spiked to almost 50 percent of the yield strength of the pile before the first target deflection of 0.15 inches was reached, it became clear that displacement control would not work for winter testing. Testing was stopped and a load control test plan was developed.

The load plan for January testing was as follows. The first target load was 5 kips; successive target loads were 1.5 times the previous load until 50 kips, then successive

target loads were 1.25 times the previous load. See Figure 5.10 for loading schedule used for the January test.

Before resuming testing, data from the first cycle was reviewed to make sure that all readings were within a reasonable range. Off scale strain readings were gathered for approximately half of the strain gages during initial testing. Testing was stopped at this point and it was several days before the problem was corrected. During this time temperatures plunged to well below -40 degrees Fahrenheit. Based on past experience with equipment operation during extremely cold weather, the decision was made to delay testing until the daily low temperature was above -20 degrees Fahrenheit.

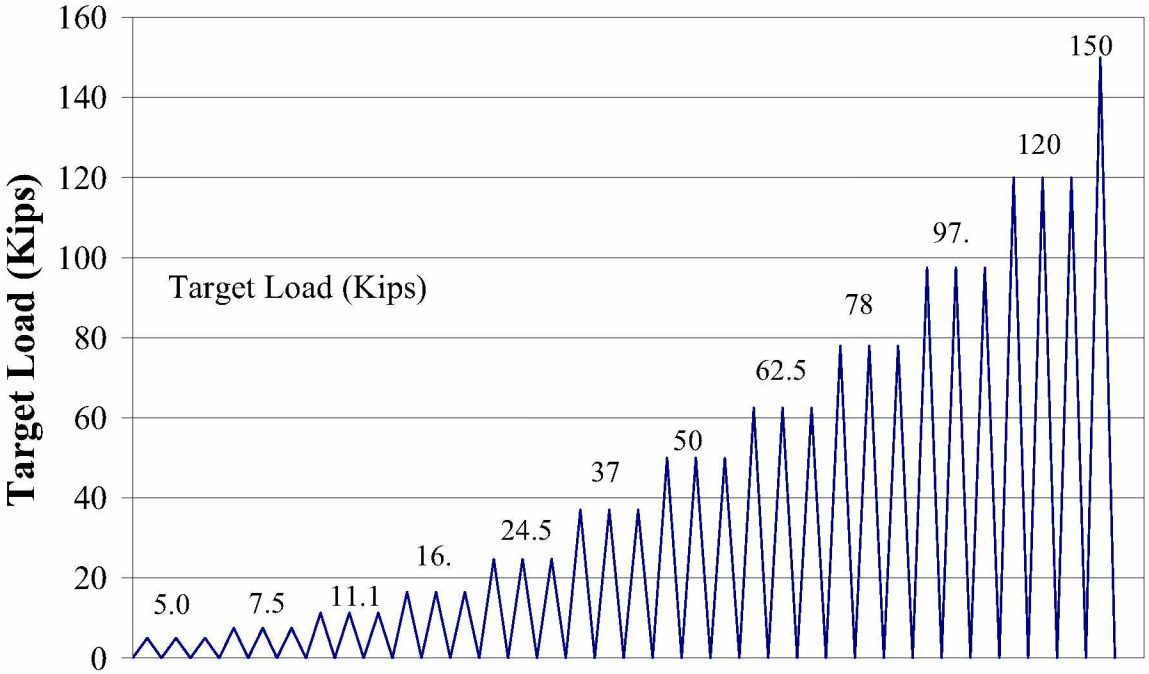

Figure 5.10 January Target Load Increments

The results of the January 6 testing also revealed that the pile in the frozen soil was really stiff. A needle valve had to be added between the hydraulic pump and the

cylinder so that the speed of the cylinder could be slowed so that the load steps could be accurately achieved. It is estimated that the load rate for the pile test during the January test did not exceed 1 in/min (0.0423 cm/sec).

On January 18, 2010 testing resumed on the North Test Pile. The weather was sunny and calm. Temperatures during testing ranged from -20 degrees to -9 degrees Fahrenheit. During the 11 days between January 6 and January 18, the weather was extremely cold and with the protective snow cover removed, the frost depth next to the north test pile increased to nearly 4.5 feet see Figure 5.11.

The increase in stiffness of the pile from the unfrozen condition during the September test to the frozen condition of the January test was substantial. During January's test the pile was loaded to 120 kips, the design capacity of the test frame; without any apparent yielding of the test pile and without the formation of a gap between the pile and the soil. Since none of the components of the test frame showed signs of failure and the frame had a factor of safety, it was decided to load the pile to 150 kips, 30 kips beyond the design limit of the test frame. At this increased load, the connection to the reaction pile and the concrete under the jacket of the reaction pile crushed, see Figure 5.12. Loading for the mid winter test was stopped at this point and the remaining two test cycles at 150 kips were unable to be completed. Load vs. cyclic deformation is plotted in Figure 5.13, a small amount of plastic deformation occurred during the 120 kip and 150 kip load increments.

A small crack in the soil at the base of the pile formed at the 150 kip load increment, see Figure 5.13 but it was less then 1/32 of an inch; no other soil cracking at the base of the pile was noticed.

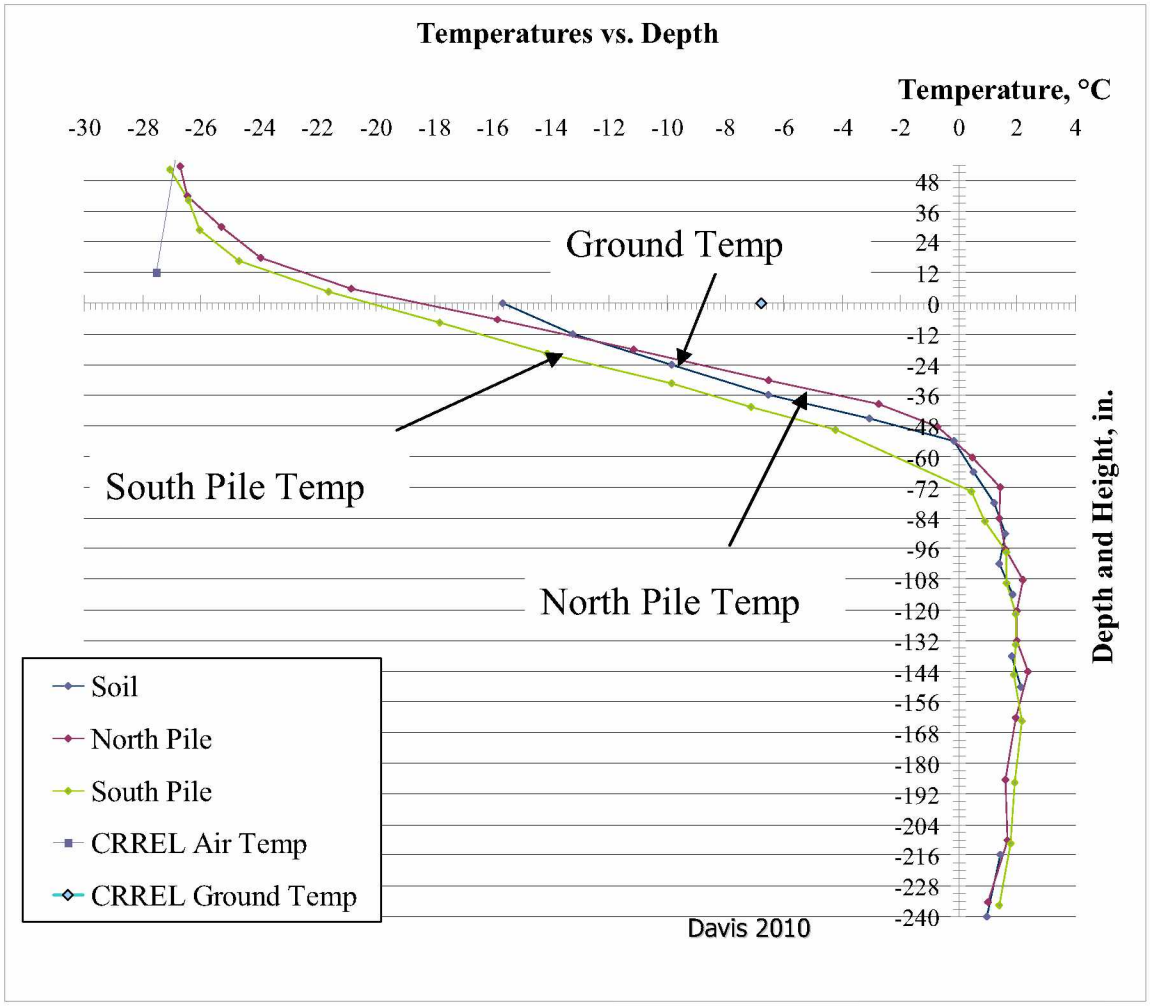

Figure 5.11 Temperatures with Depth January 18, 2010 (Davis 2010)

Figure 5.12 Bearing Failure of Test Frame at Reaction Pile.

Figure 5.13 Soil Crack at 150 Kips January Test

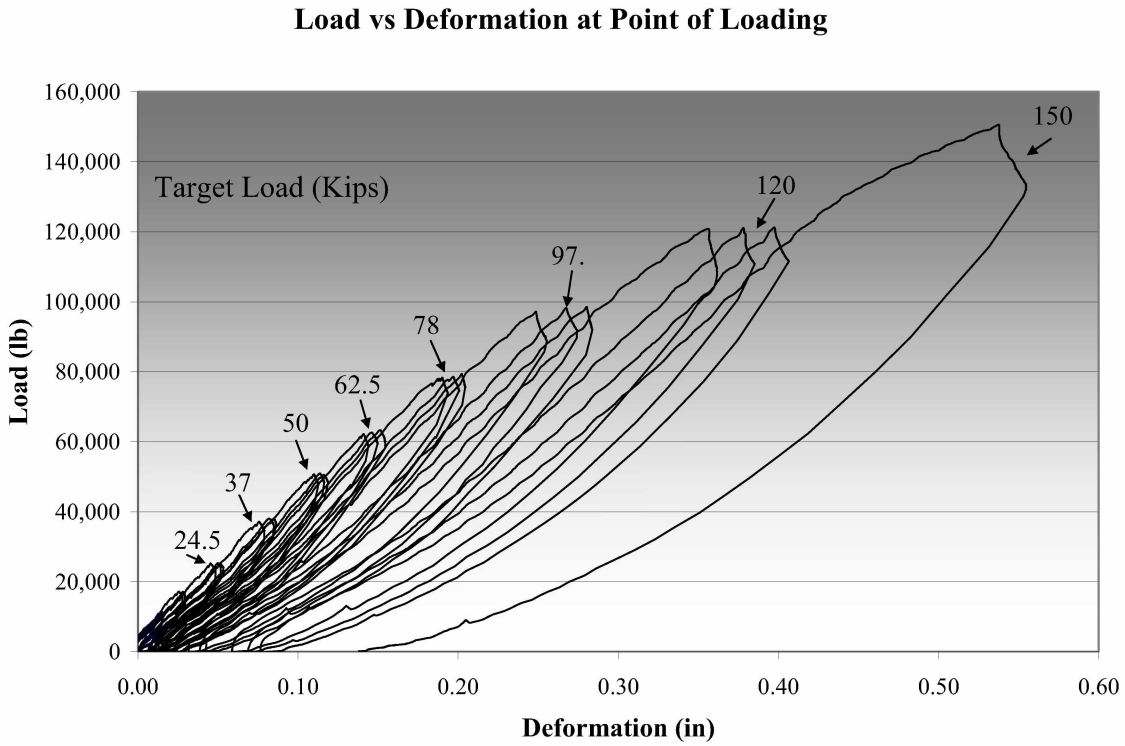

Figure 5.14 January Cyclic Load vs Deformation at Point of Load

5.4 Test Frame Redesign

During testing in January of 2010 the 120 kip capacity of the test frame was insufficient to fail the pile in the frozen condition. After the January 2010 test, the system was reevaluated using LRFD methods using a design factor of safety of 1.0. Since the spring test was the last pile test and the frame wouldn't be needed for future testing it was determined that it would be acceptable if parts of the test frame went in to plastic deformation. The modifications of the test frame were limited to: increasing the bearing surface at the hinge on the test pile side of the reaction frame and increasing the size of the bearing plate at the reaction pile. With a these modifications the frame's capacity was raised to 226 kips, the maximum capacity of the hydraulic loading cylinder.

No changes were made to the test pile-load frame interface and the changes made to the fame didn't have any effect on the results of future testing other then increasing the capacity of the load frame.

5.5 March Testing

On March 24, 2010 the south pile was tested. The weather was sunny with a slight breeze. Site temperatures ranged from 19 to 25 degrees Fahrenheit. Testing equipment was set up the night before and testing of the pile began around 1 p.m. The load plan for March testing is as follows. The first target load was 5 kips, successive target loads were 1.5 times the previous load until 50 kips. Then successive target loads were 1.25 times the previous load; see Figure 5.15 for loading schedule used for the March test. For the test there were approximately 90 inches of frost. See Figure 5.16.

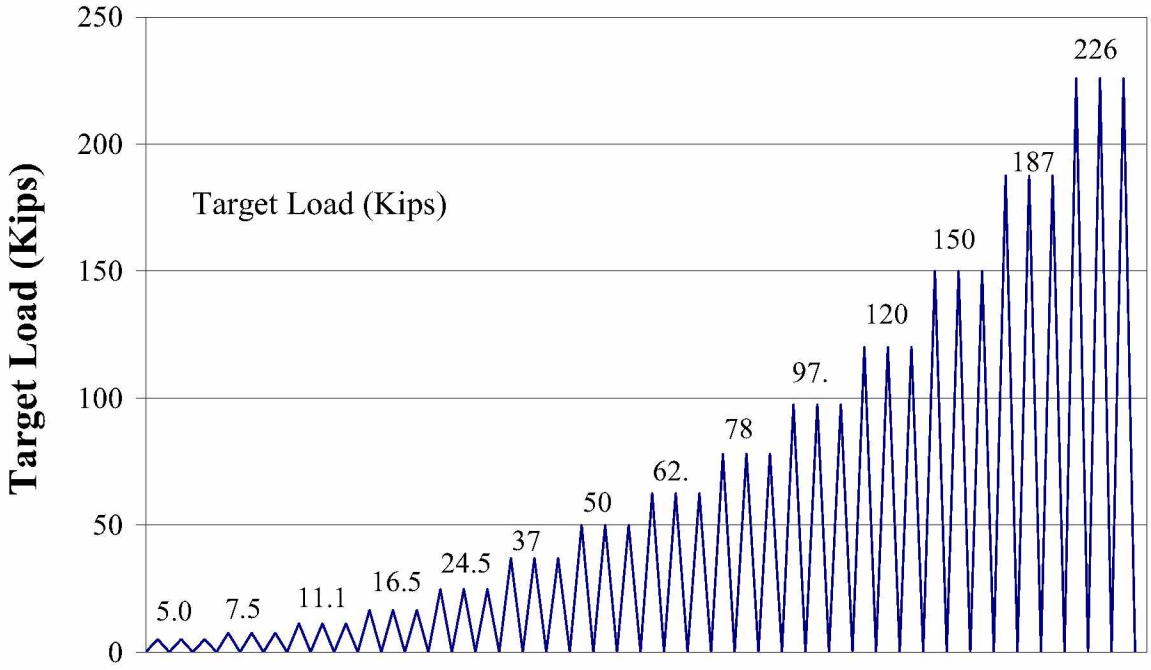

Figure 5.15 March Target Load Increments

During the low loading of the test pile, load steps below 50 kips load; loading speed was again was reduced by use of a needle valve. The hydraulic pump would be pulsed and the needle valve would slow the rate at which fluid would flow into the ram. During the larger loads above 62 kips, the needle valve was not used and it is reasonable to assume the rate of loading at the ram would be equal to that of flow volume of the pump divided by the effecting area of the ram about 1 in/min (0.0423 cm/sec). This neglects movement of the reaction pile but is a best estimate of the speed at which the pile was loaded.

Cracking noise of the concrete started at 50 kips and gradually increased throughout the test. Plastic deformation started to be noticeable above 120 kips of load. Figures 5.17 show load-deformation behavior of the pile throughout the entire test and Figure 5.18 shows the cyclic behavior of the pile at low deformations. Once large plastic deformation started to occur above 160 kips of load, cracking/popping noise began to increase rapidly and it is theorized that this noise was the de-bonding of the steel/concrete bonds inside the pile. This theory can not be proved with out further investigation inside the pile. As plastic deformation of the pile started to take place during the first cycle of the 187 kip load increment the amount of energy it took to load the pile increased. For cycles # 2 & 3 at the 187 kip load increment the plastic deformation had already occurred and increased deformation was smaller at these cycles, see Figure 5.17. On the first cycle at the 226 kip load, step plastic deformation of the pile continued and the hydraulic pump overheated at approximately 199 kips and loading for that cycle was stopped. The strain gage at 6.25 inches below ground surface on the

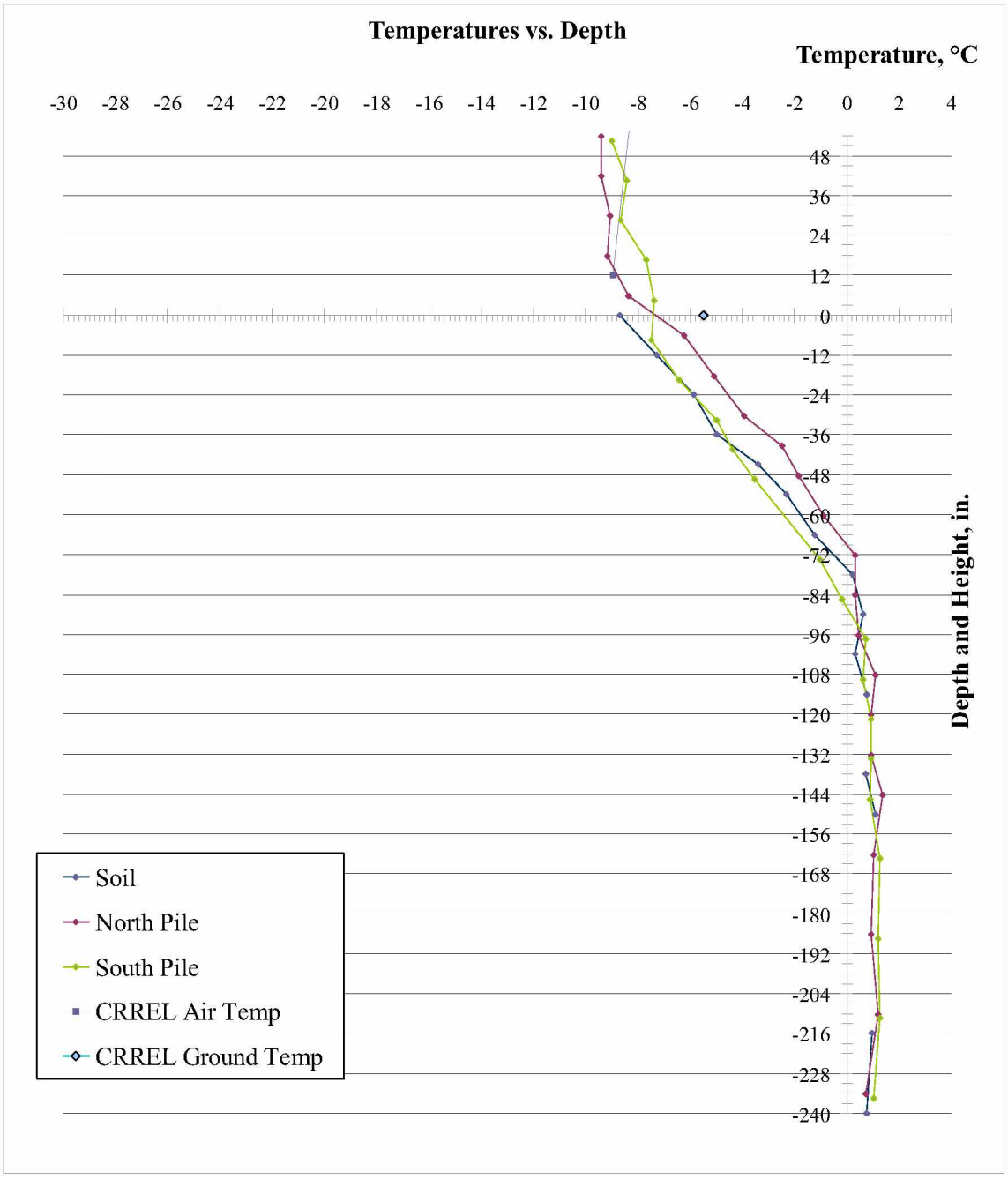

Figure 5.16 Temperatures with Depth March 24, 2010 (Davis 2010)

tension side of the pile went off scale due to strain readings over 28,000 micro strain. On the second cycle of the 226 load step rotation at the plastic hinge that formed just below the ground surface became so extreme that the pile was tilted over 12 degrees. At 207 kips the U-bolts holding the hinge onto the test pile slipped up the test pile, see Figure 5.19. Testing was stopped at this point and a third cycle at 226 kips was not completed. The soil gap in front of the pile caused by plastic deformation of the soil is quantified in Figure 5.22. Figure 5.20 is a picture of the soil gap in the unloaded condition after the 207 kip load step.

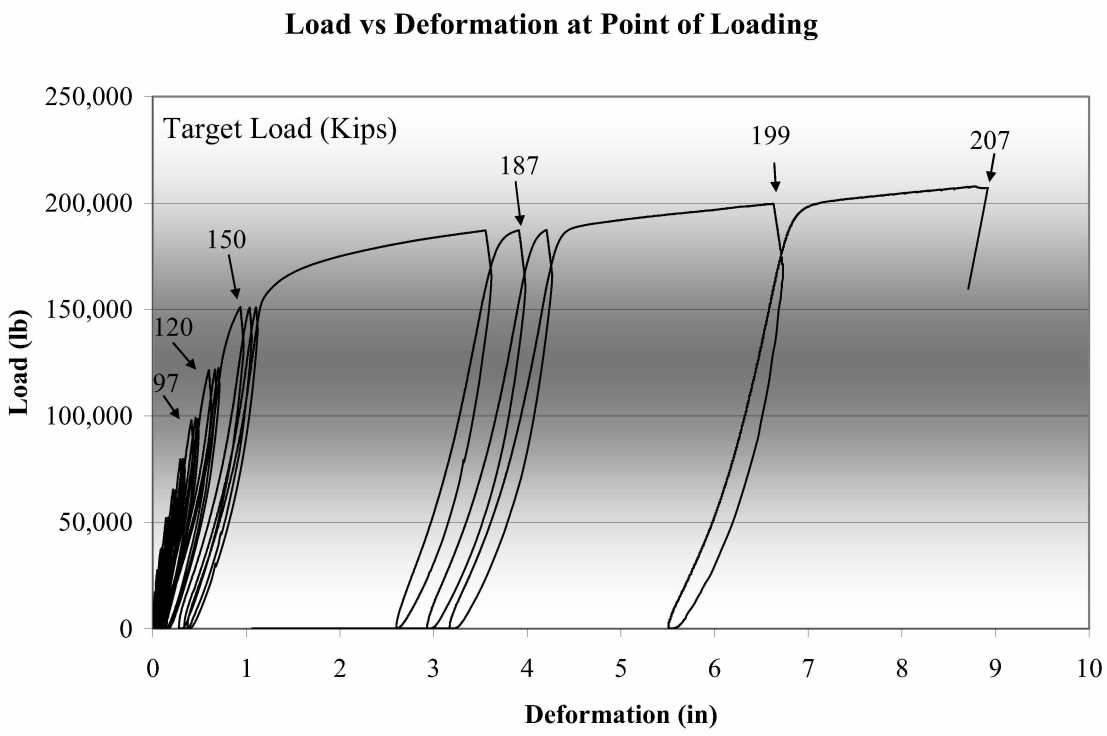

Figure 5.17 March Cyclic Load vs. Deformation at Point of Load 0 to 207 kips

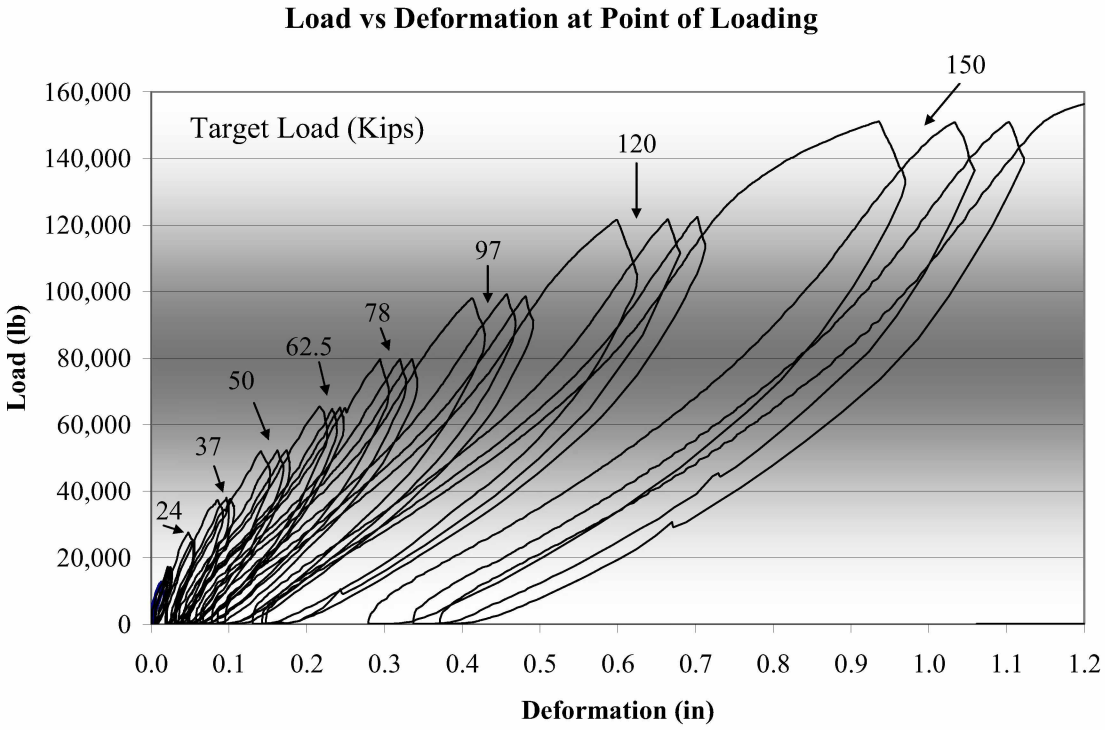

Figure 5.18 March Cyclic Load vs. Deformation at Point of Load 0-150 Kips

Figure 5.19 207 Kips Final Loading of the South Pile

Figure 5.20 207 Kips Unloaded Plastically Deformed Soil Gap in Front of Test Pile

5.6 Formation of Soil Gap

The gap left by plastic deformation of the soil is summarized in Figures 5.21 and 5.22 for September and March respectively. Figures 5.21 and 5.22 are an estimation of the gap based on photographs taken during testing. Figure 5.23 is a diagram of measurement locations. During March testing, several tension cracks were formed. This cracking is summarized in Figure 5.24. The gap formed in January testing was not summarized as it was insignificant.

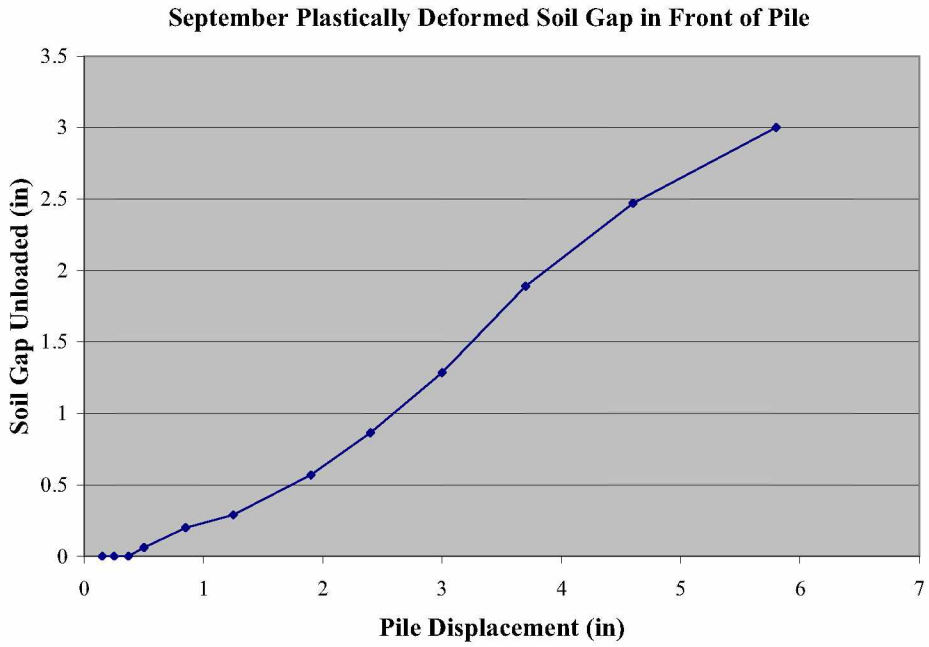

Figure 5.21 Plastically Deformed Soil Gap in Front of Pile September Test

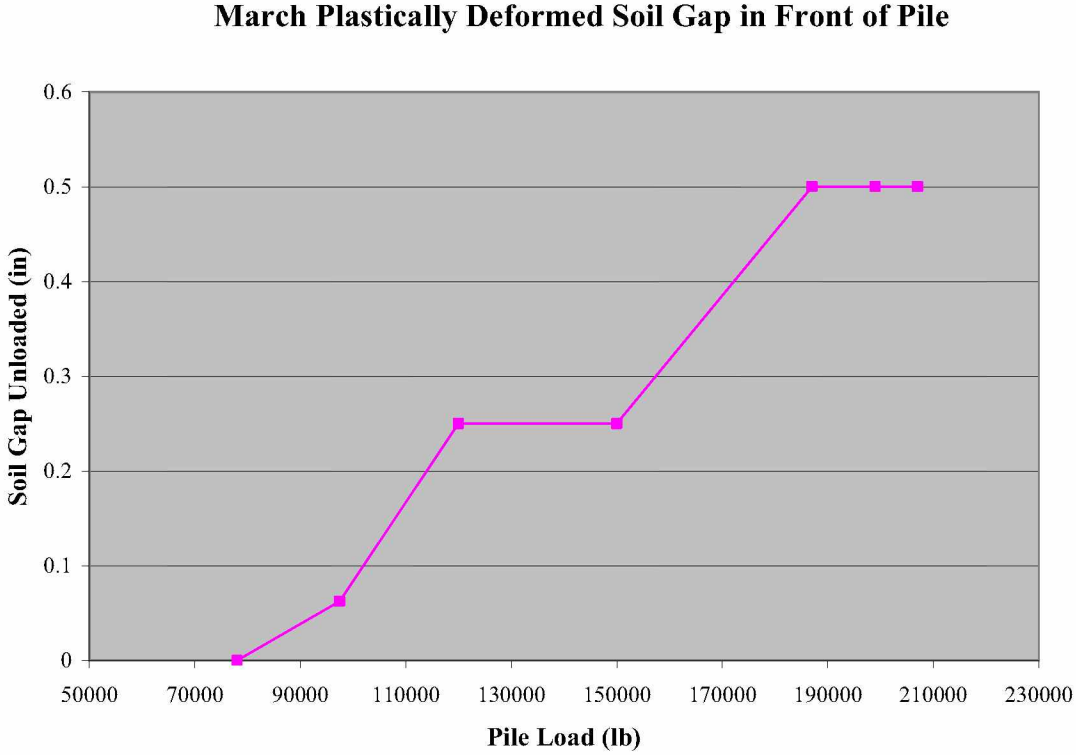

Figure 5.22 Plastically Deformed Soil Gap in Front of Pile March Test

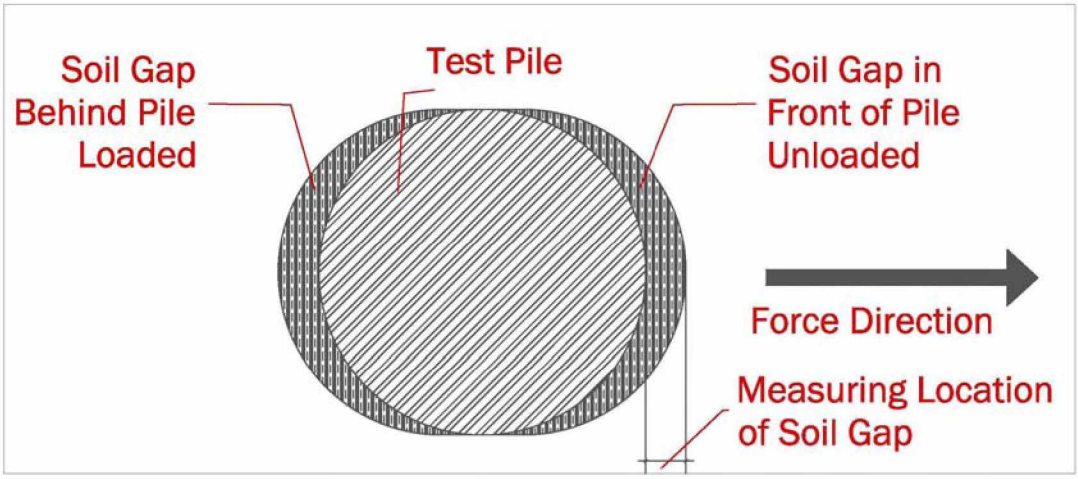

Figure 5.23 Soil Gap Location

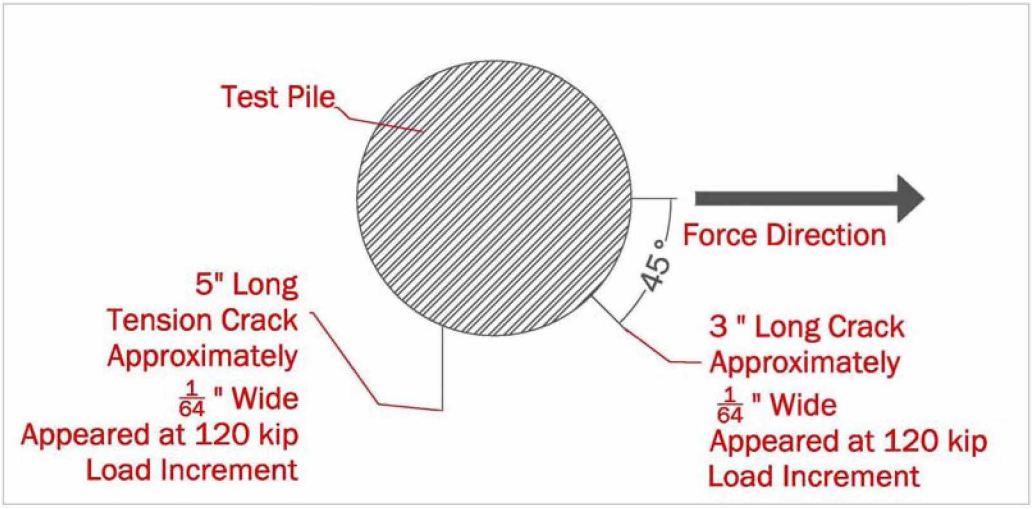

Figure 5.24 March Soil Cracking Summarized

6 Soil Properties

The soils investigation for this project consisted of three bore holes dug at the test site. Lab testing was limited to classifying the soil at the site. The following soils tests were done on soil samples taken at the site: moisture content, sieve analysis, hydrometer analysis and plasticity index. A literature review was done on Fairbanks silt and information was obtained for frozen and unfrozen Fairbanks silt.

6.1 Classifying the Soil

Three bore holes were drilled at the test site on July 24, 2008. The holes were placed in the future location of the test piles, bore hole #1 was drilled in the location of the south test pile, bore hole # 2 was drilled in the location of the reaction pile, bore hole #3 was drilled in the location of the north test pile. See Appendix C for bore logs. Moisture contents were taken at different depths, see Figure 6.1. Standard Penetration Testing (SPT) testing was done as soils were sampled. For the SPT Testing continues samples were taken. Four blow counts were recorded in the bore logs for each test; for SPT values the middle two blow counts should be taken see Figure 6.2. A 300 lb hammer was used and a hammer efficiency of 60 percent is typical for this drill rig.

Sieve analysis (ASTM C136-06) and Hydrometer (ASTM D 422-63) testing were done on soil samples taken from bore holes and samples taken from test holes dug by hand, see Appendix C. Soil was classified according to ASTM D2487 (Coduto 2001) The bore logs for bore hole #1 in the current location of the south test pile indicates a gravel layer extended to a depth of 1 meter. This is believed to be

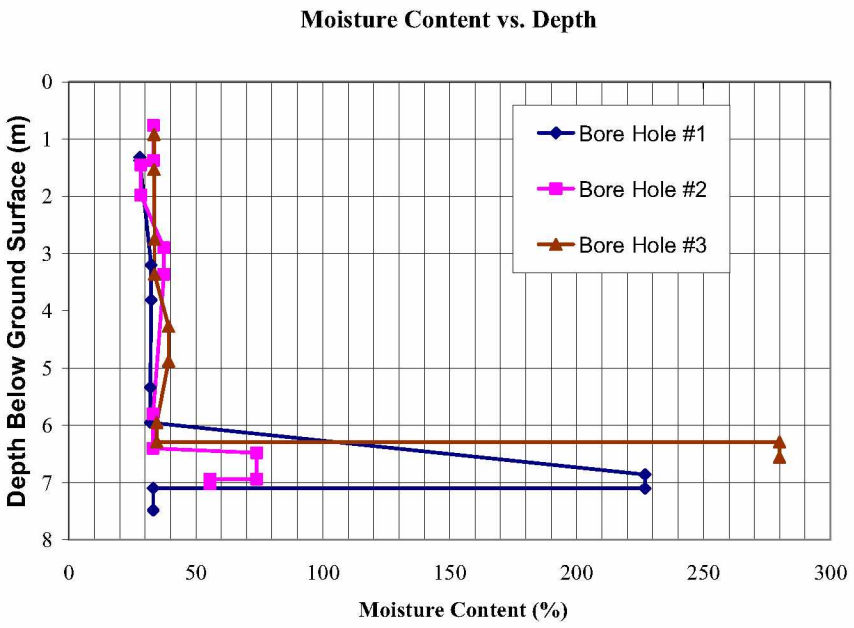

Figure 6.1 Moisture Contents 7/24/2008 Soil Borings

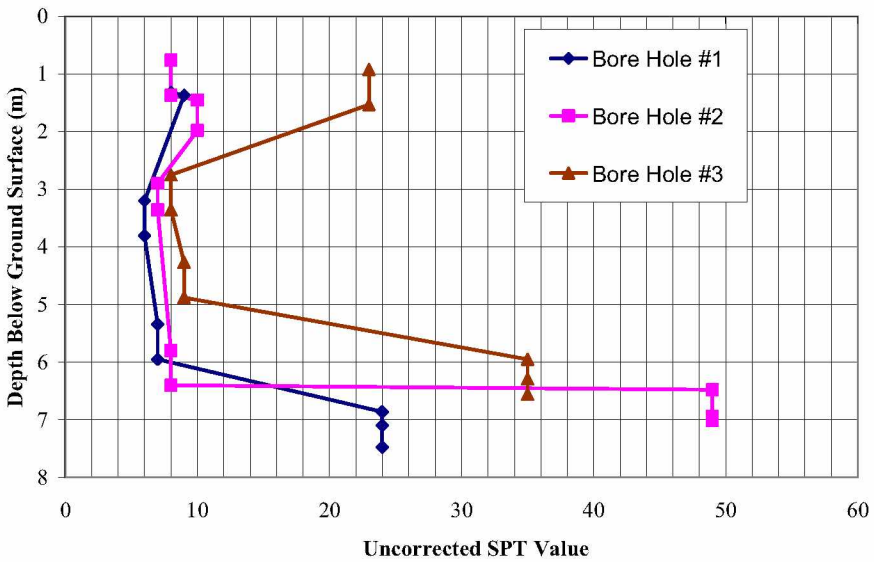

Figure 6.2 Uncorrected SPT Values 7/24/2008 Soil Borings

incorrect. A later soil investigation by hand revealed that there was gravel on top of the silt, but the depth of the gravel layer was only 12 inches. The gravel found was

well graded (GW). The soil throughout the remaining length of the pile can be classified as non-plastic silt (ML) see Figure 6.3.

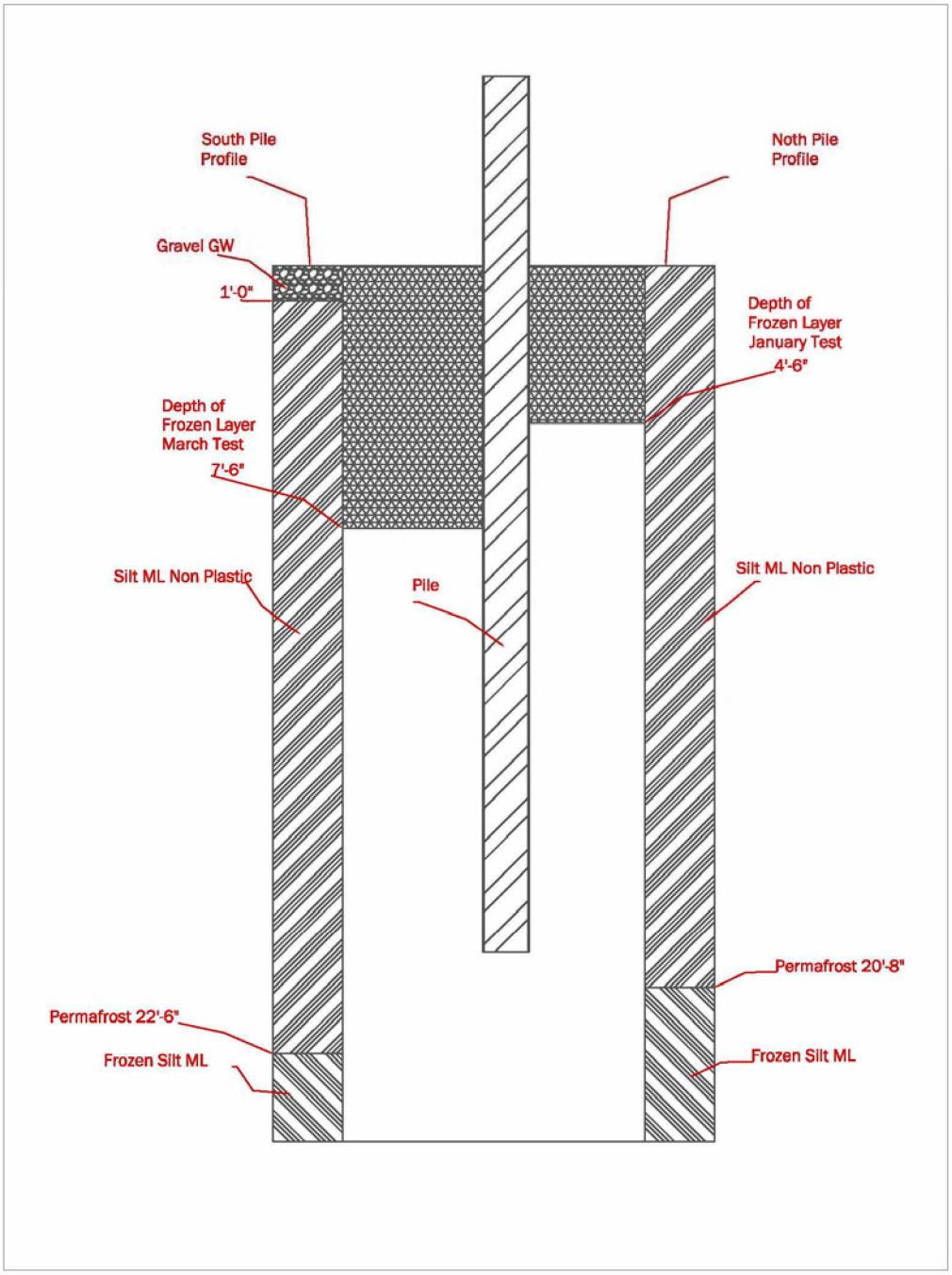

Figure 6.3 Soil Profile (Horizontal distance not to scale)

6.2 Shear Wave Velocity Testing

Shear Wave Velocities at the site were also taken as part of a different research project in the summer of 2009 and the winter of 2010. The work is not yet published, preliminary results are given in Table 6.1 and Figure 6.5. The University of Arkansas (UARK) in conjunction with the University of Alaska Fairbanks (UAF) is doing a micro grid of Fairbanks, Alaska. The UAF professor leading the project is Dr Kenan Hazirbaba; the UARK professor leading the project is Dr. Brady Cox; the UARK PhD student that did the winter testing was Clint Wood.

Figure 6.4 Shear Wave Velocity Testing at the Site Winter 2010

Table 6.1 Shear Wave Velocity Preliminary Results

Shear Wave Velocity Test Data							
Layer No.	Thickness (m)	Depth to bottom (m)	P-wave Velocity (m/s)	Shear Wave Velocity (m/s)	Poisson's Ratio	Unit Weight (kN/m3)	Vs 30 (m/s)
1	1.2	1.2	180	100	0.3	16	296
2	5.2	6.4	230	120	0.3	17	
3	7.6	14	850	430	0.33	18	
4	16.5	30.5	1090	550	0.33	19	

Note Maximum depth of the profile is approximately equal to maximum experimental wavelength/two

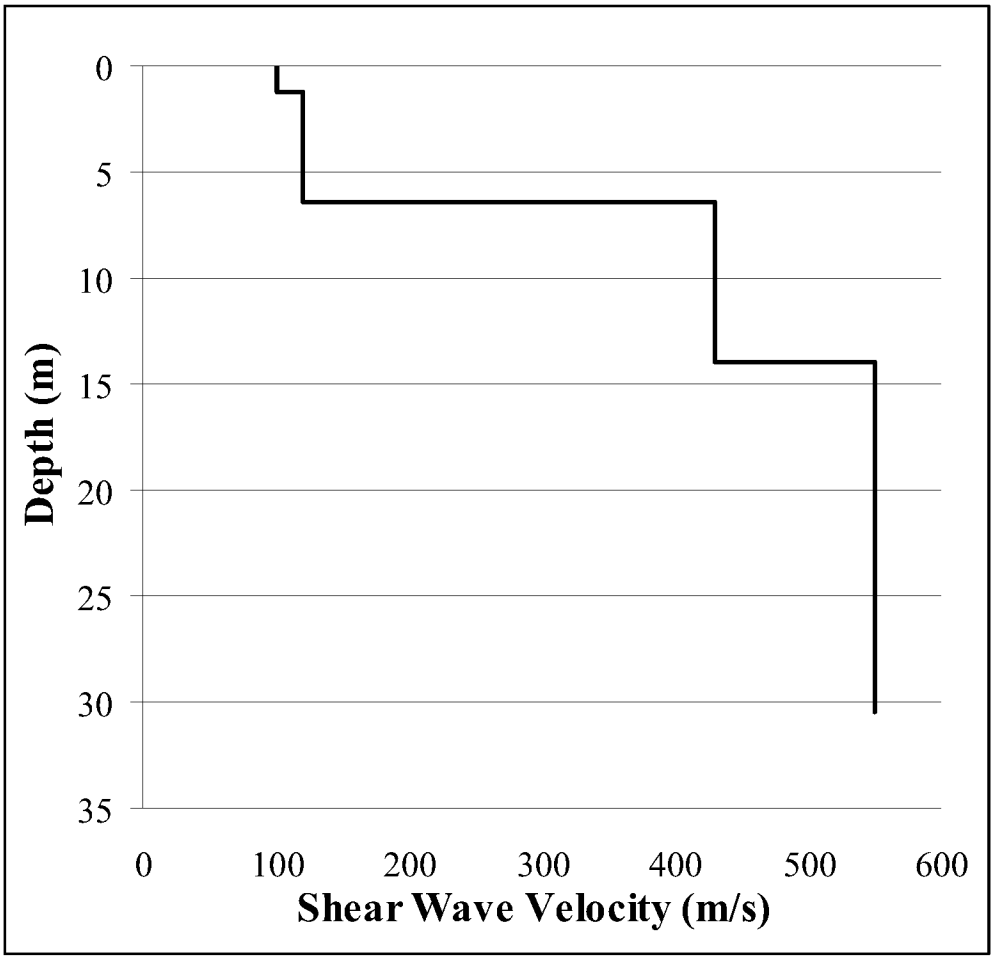

Figure 6.5 Preliminary Shear Wave Velocity Profile

7 Pile Flexural Behavior and Experimental Results

This chapter presents tests results for three different laterally loaded pile tests. Each test was conducted using cyclic quasi-static laterally applied loads to a 16-inch diameter steel jacketed reinforced concrete pile. The three tests were performed in September 2009 on the north pile (fall; fully thawed); January 2010 on the rehabilitated north pile (winter, frozen soils were 4.5 ft deep); and March 2010 on the south pile (spring, frozen soils were 7.5 ft deep).

Two analytical methods for evaluating the test results were requested by AKDOT. These methods were examined as part of the study of the experimental data. The first method is a simplistic method that is well established. The method is based on the idea that this complicated problem can be simplified as a pile with a fixed end in the ground and a free end above the ground. In this method, the soil above the depth of equivalent fixity is neglected and the soil below the depth of equivalent fixity is considered infinitely rigid (Coduto 2001). The second method is more complicated. It is based on the idea that the soil adjacent to the pile may be approximated by discretely spaced springs. This method is essentially a beam on elastic or inelastic foundation where soil resistance is approximated by discretely spaced springs. For this analysis, LPile (Reese et al. 2004), a finite difference program, was used to develop a sufficiently accurate soil springs for use in predicting the experimental pile deformations.

7.1 Material Properties

7.1.1 Concrete Strength

Compressive strength was obtained from uniaxial compression tests the testing conformed to ASTM C39 2005 and was done 28 days after the pour (Davis 2010). Compressive strength properties are presented in Table 7.1. Tensile strength for the concrete was obtained from flexural beam testing. These tests conformed to AASHTO T 23 and the analysis conformed to AASHTO T 22. Results are listed in Table 7.2. While split tension testing on concrete cylinders was conducted, it is not presented in the report.

Table 7.1 Concrete Compressive Strength and Modulus of Elasticity

Test Specimen	*A*	*B*	*C*
$Diameter_1$ (in)	4.005	4.004	3.999
$Diameter_2$ (in)	3.99	3.995	3.995
$Diameter_{average}$ (in)	3.998	4.000	3.997
Ultimate Load (lb)	67,960	64,462	62,515
Area (in^2)	12.55	12.56	12.55
Ultimate Stress (psi)	5,415	5,131	4,982
40% Ultimate Stress (psi)	2,166	2,052	1,993
40% Ultimate Strain (in/in)	0.000711794	0.000331166	0.000505099
Secant Modulus (psi)	3,042,945	6,197,496	3,945,563
Chord Modulus (psi)	2,940,401	4,819,008	3,895,641
Average Secant Modulus (psi)	4,395,335		
Average Chord Modulus (psi)	3,885,017		
Average Compressive Strength (psi)	5,176		
ACI Modified Concrete Modulus (psi)	3,724,031		
Unit Weight (pcf)	135		

Table 7.2 Concrete Tensile Strength

Load (lb)	*Width (in)*	*Depth (in)*	*Span (in)*	*Modulus of Rupture (psi)*
9225	6.10	6.05	18.00	740
8860	6.10	6.10	18.00	700
8885	6.00	6.10	18.00	715
		Average		718

The chord modulus was chosen as the elastic modulus for the concrete as it is the closest to the ACI modified concrete modulus. Originally the chord modulus for concrete was used but it became apparent that this would not be an accurate representation of concrete at failure. While stress-strain testing was conducted on 28 day concrete due to equipment limitations stress-strain data was only obtained to 3500 psi. The results of this testing are shown in Figure 7.1. To accurately model the stress-strain behavior during testing a model for obtaining the stress-strain behavior of the concrete over the entire strength range of the concrete was needed. The following model was taken from a text by Collins and Mitchell (1991). This expression relating the stress, f_c, and the strain caused by this stress, ε_{cf}, is

$$\frac{f_c}{f'_c} = \frac{n(\varepsilon_{cf} / \varepsilon'_c)}{n - 1 + (\varepsilon_{cf} / \varepsilon'_c)^{nk}} \qquad \text{Equation 7.1.1}$$

where

f'_c = peak stress obtained from a cylinder test

ε'_c = strain when f_c reaches f'_c

n = curve –fitting factor equal to $(E_c/(E_c - E'_c)$

$E'_c = f'_c / \varepsilon'_c$

k = factor to increase the postpeak decay in stress, taken as 1.0 for $(\varepsilon_{cf}/ \varepsilon'_c)$ less than 1.0 and as a number greater the 1.0 for $(\varepsilon_{cf}/ \varepsilon'_c)$ greater then 1.0

Also, since all of the above properties were not known, the following equations were given for normal weight concrete.

$$n = 0.8 + \frac{f'_c}{2500} \text{ (psi)} \qquad \text{Equation 7.1.2}$$

$$\varepsilon'_c = \frac{f'_c}{E_c} * \frac{n}{n-1} \qquad \text{Equation 7.1.3}$$

$$k = 0.67 + \frac{f'_c}{9000} \text{ (psi)} \qquad \text{Equation 7.1.4}$$

The stress-strain relationship that was obtained by the above equations was compared to experimental data and the results are plotted below in Figure 7.1. From the stress-strain relationship, a modulus of elasticity was calculated for any particular strain; see Figure 7.2.

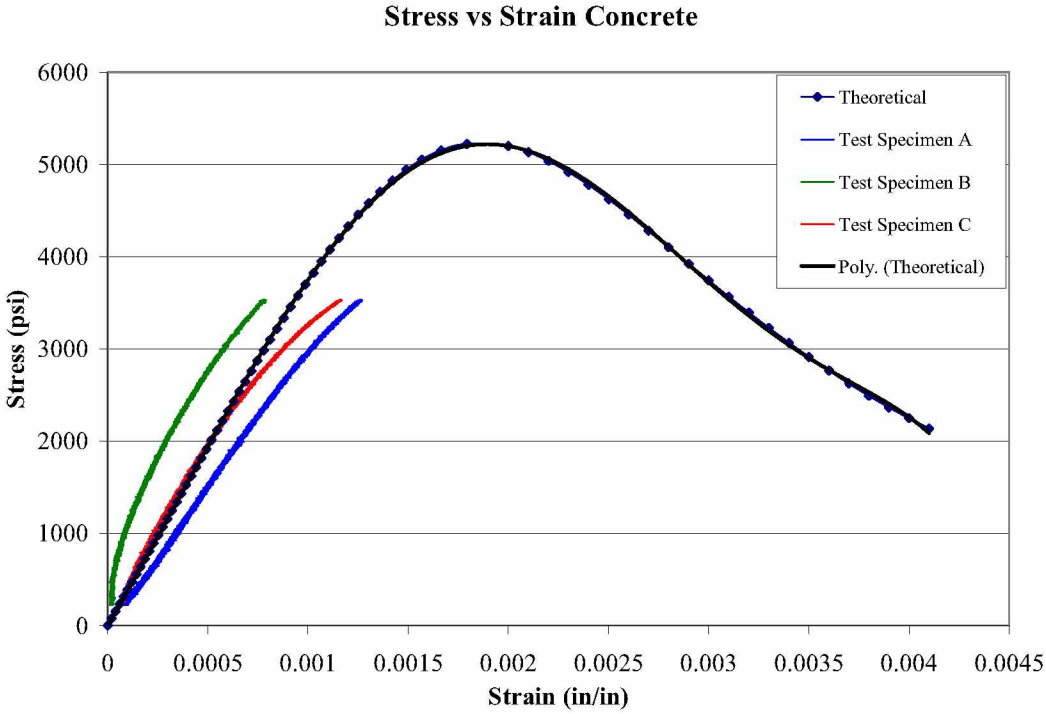

Figure 7.1 Concrete Stress Strain Behavior Experimental and Theoretical

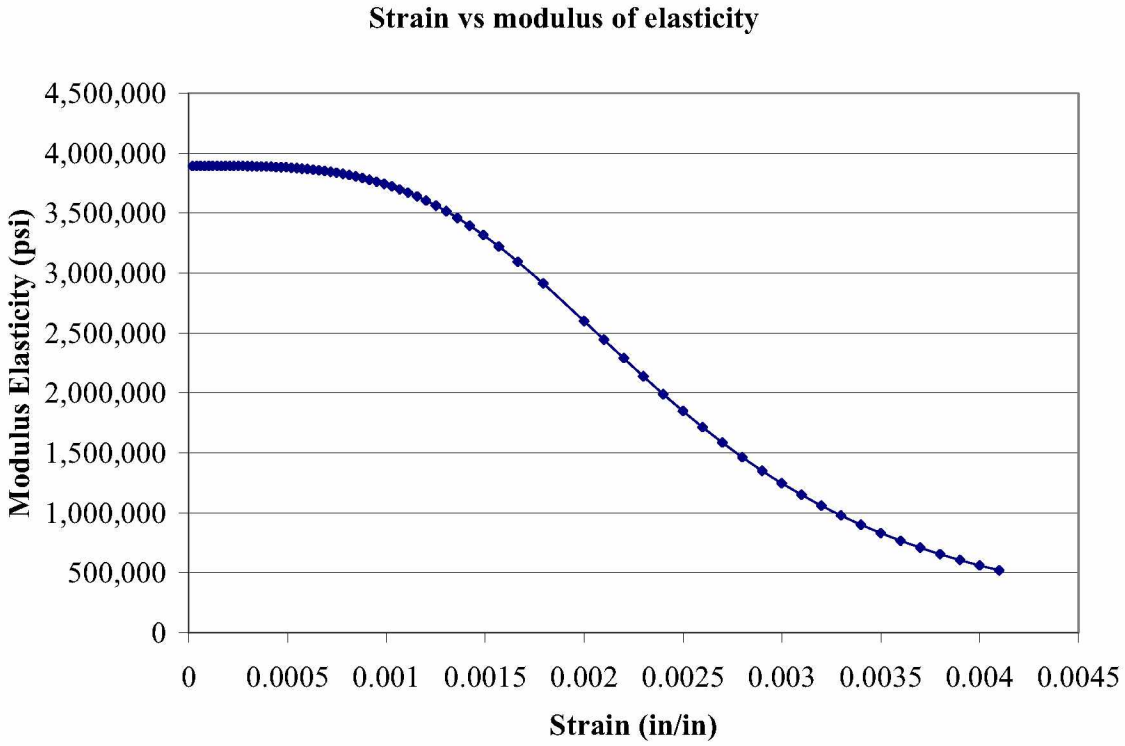

Figure 7.2 Concrete Strain vs. Modulus of Elasticity

7.1.2 Steel Strength

Tensile strength was based on three test specimens for both the steel pipe jacket and the rebar; the testing was done by Quality Inspection & Testing, Inc. The testing conformed to ASTM A370. See Table 7.3 for steel pipe jacket tensile strength and Table 7.4 for rebar tensile strength.

Table 7.3 Pipe Jacket Tensile Strength

E_{sj} =	28,946,889	psi
σ_{yield} =	57,243	psi
$\sigma_{Ultimate}$ =	71,674	psi
% Elongation	28.03	%

Table 7.4 Reinforcing Bars Tensile Strength

E_s =	30,610,801	psi
σ_{yield} =	76,531	psi
$\sigma_{Ultimate}$ =	105,612	psi
% Elongation	26.50	%

7.2 Flexural Stiffness of the Pile

The flexural stiffness of a steel pile is nearly constant until the elastic limit is reached. The properties of steel in tension and compression are nearly identical and the material is linear elastic; the properties of concrete are not. The tensile strength of concrete is only about 10 percent of the compressive strength and the material is not linear elastic. So the flexural stiffness of a composite pile, composed of both steel and concrete varies depending on the load/moment applied to the pile.

The flexural stiffness of the pile was based on the assumption that at a given point on a reinforcing bar, the strain between in the reinforcing bar and the concrete are equal. Further, the same assumption was made at the interface between the concrete and the steel jacket. In other words, it was assumed that the concrete did not slip with respect to the steel jacket. Based on these assumptions, a program was written to approximate moment versus strain (moment versus curvature). The program utilizes numerical integration to evaluate the stiffness change. The moment –strain was calculated by diving the pile into 300 parallel slices. In order to insure sufficient accuracy, the calculate values were compared using less slices. A desired strain level would be then applied to the tension side of the pile and to the compressive side of the pile. Strain was assumed to be linear from the tensile side of the pile to the compressive side of the pile.

The strain at each slice of the pile was then calculated and the stress-strain behavior for the steel and concrete was used to calculate the force of each slice. For the analysis, the concrete in each slice was considered un-cracked until subjected to a strain that could cause cracking. After the cracking strain was reached, the concrete will be considered cracked and the tensile capacity of the concrete will be zero. Using an iterative process the strain on the compressive side of the pile would be changed until the summation of forces in both the tensile and compressive zones of the pile would be equal to zero. After equilibrium was reached the moment needed to cause the strain at the outer edges in the pile was calculated using summation of moments about the edge of the pile. The methodology was based on the following assumptions:

- Plane sections before bending remain plane after bending;
- Steel jacket and concrete are fully bonded;
- Reinforcing bars and concrete are fully bonded;
- Concrete stress is determined from stress-strain curve;
- Concrete tensile strength is considered zero after being subjected to a strain sufficient to cause cracking;
- Steel stress is determined from its modulus of elasticity;

The following equation was then used to find the flexural stiffness of the pile at a given strain level.

$$EI = \frac{M \bullet c}{\varepsilon} \qquad \text{Equation 7.2.1}$$

where:

EI = flexural stiffness

M = moment used to calculate flexural stiffness at the particular point

ε = tensile or compressive strain

c = distance to the neutral axis from the out most tensile or compressive fiber

This was process was repeated for the range of strain levels the pile was subjected to in testing and the flexural stiffness and correlating moment were found. To simplify analysis flexural stiffness vs. moment is plotted in Figure 7.3 and flexural stiffness vs. strain in reinforcing bars is plotted in Figure 7.4.

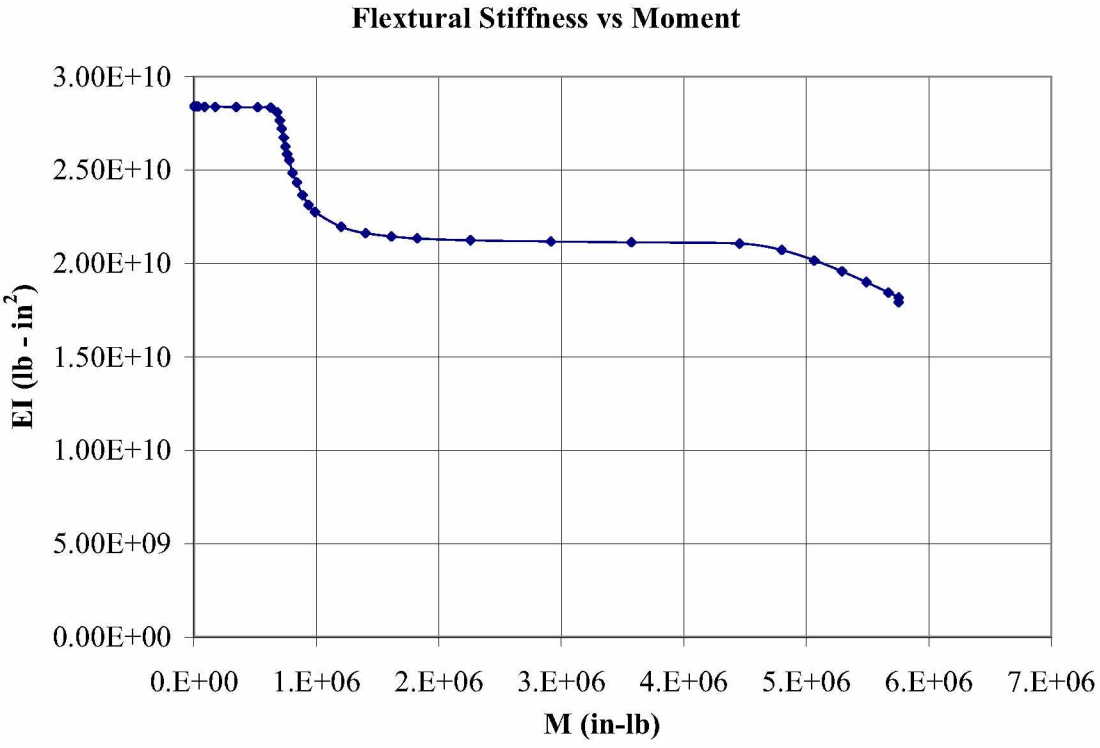

Figure 7.3 Flexural Stiffness vs. Moment

The analysis was checked for a pre-cracked pile section using a transformed section analysis done by hand using fewer slices, this crude analysis (pre-cracked

transformed section) was only done to verify that the model was producing realistic results. The results were very close with the flexural stiffness from strain compatibility (computer program described above) equal to 28.3 million kips per inch and the flexural stiffness from transformed section equal to 27.9 million kips per inch. The slight error between the two methods can be partially attributed to the number of slices used for each analysis. In the strain compatibility analysis, a computer program was written and 300 slices were used. The transformed section analysis was performed by hand and the concrete in the pile was only divided into 15 slices for transformation and the results were comparable.

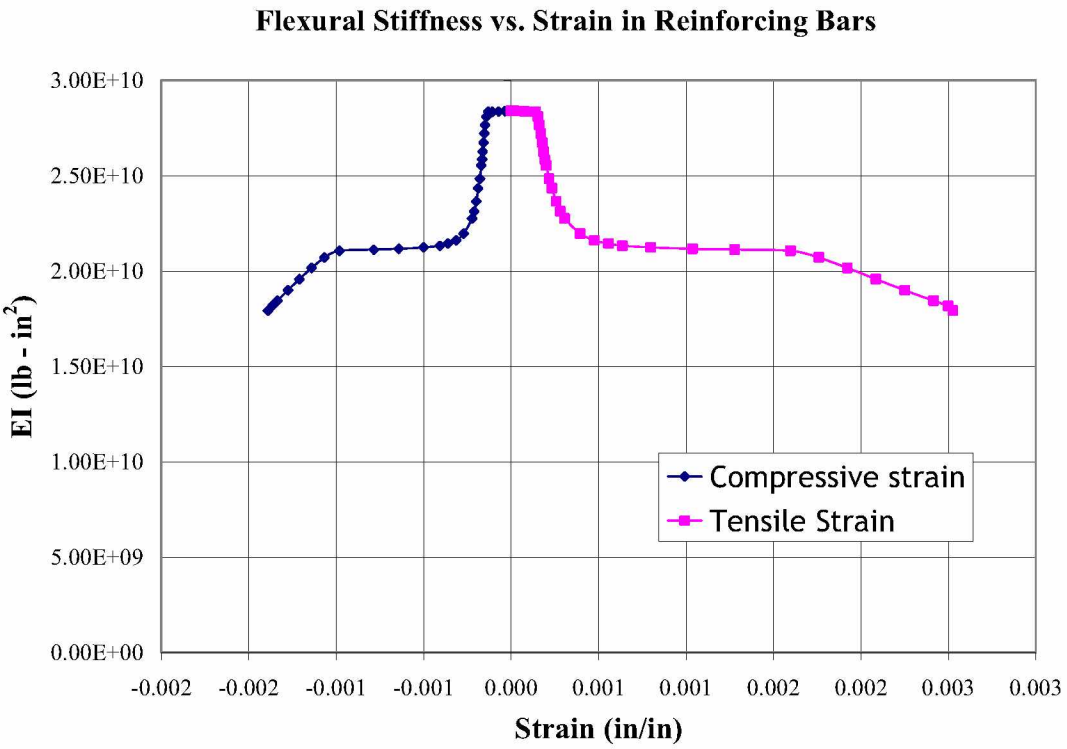

Figure 7.4 Flexural Stiffness vs. Strain in Reinforcing Bars

7.3 Pull Over Analysis

7.3.1 Experiment Results

Considerer that the load frame was installed at 40.25 inches above the ground line, see Figure 7.5. At that height, both the load cell (applied load) and transducer displacement are read. Results for three load cycles are presented in Figures 7.6 - 7.8. In Average loads and deflections are presented in Figure 7.9.

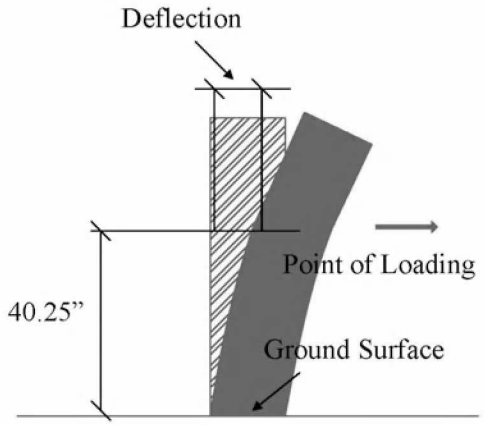

Figure 7.5 Location of Deflection Measurement

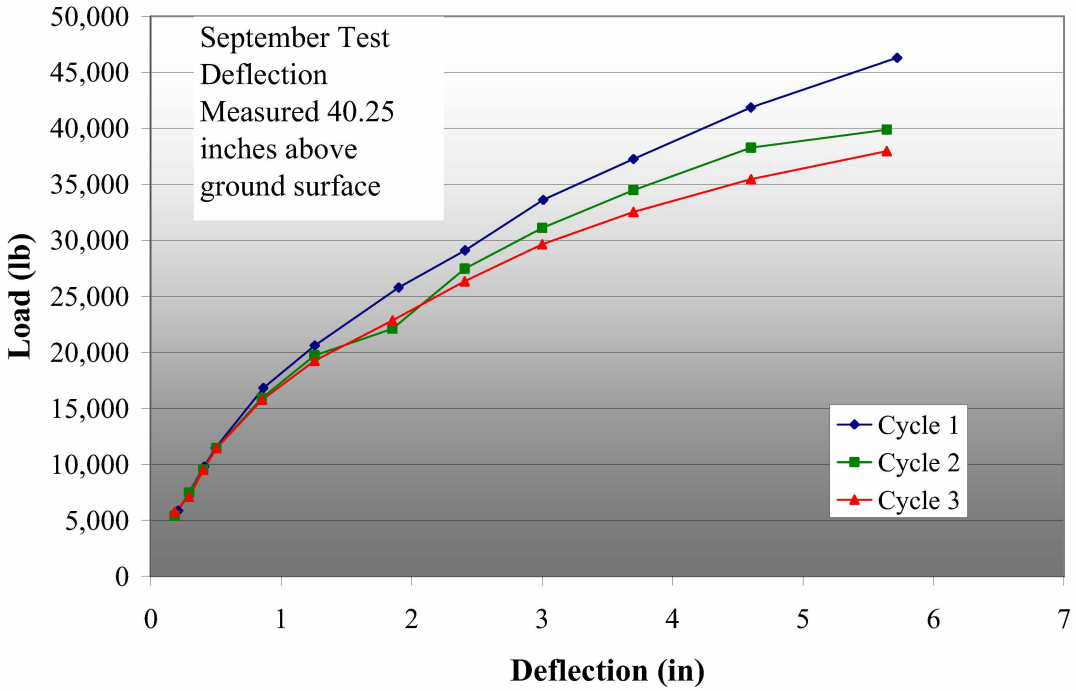

Figure 7.6 September Pile Test Pull Over Analysis

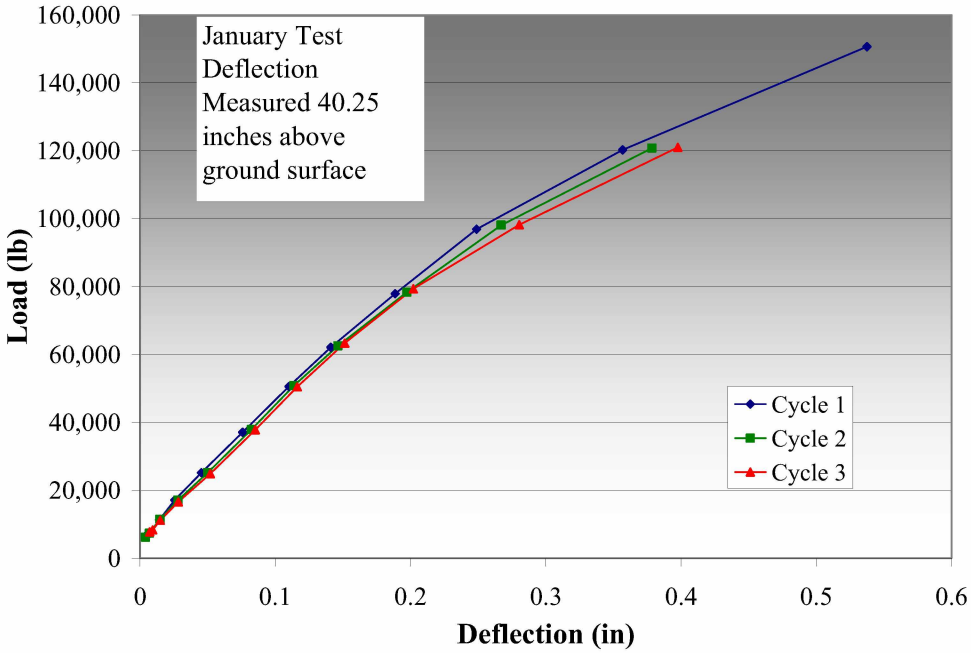

Figure 7.7 January Pile Test Pull Over Analysis

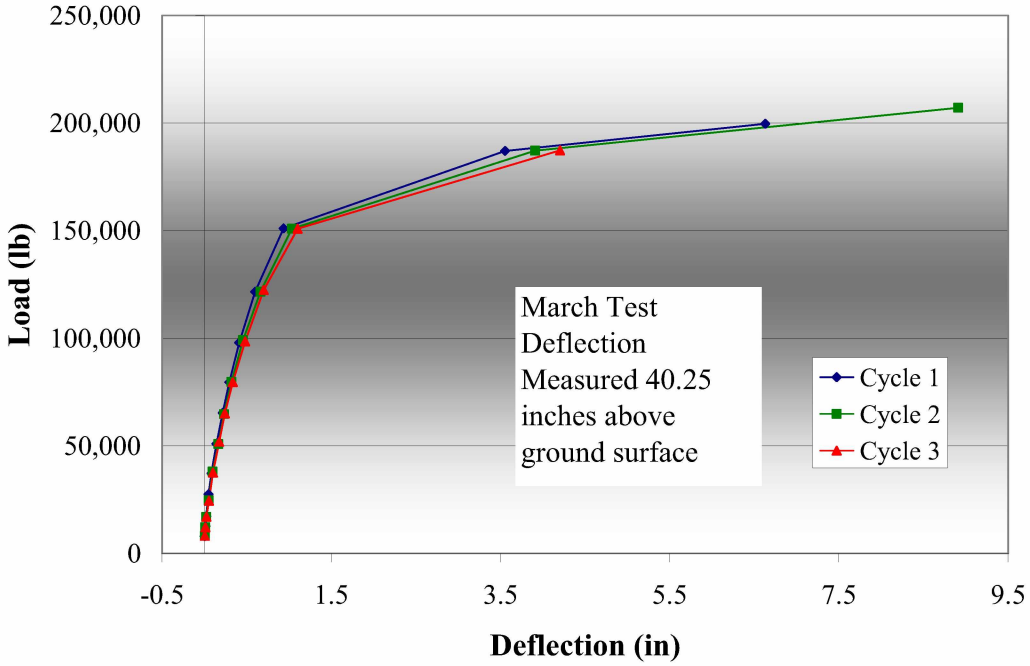

Figure 7.8 March Pile Test Pull Over Analysis

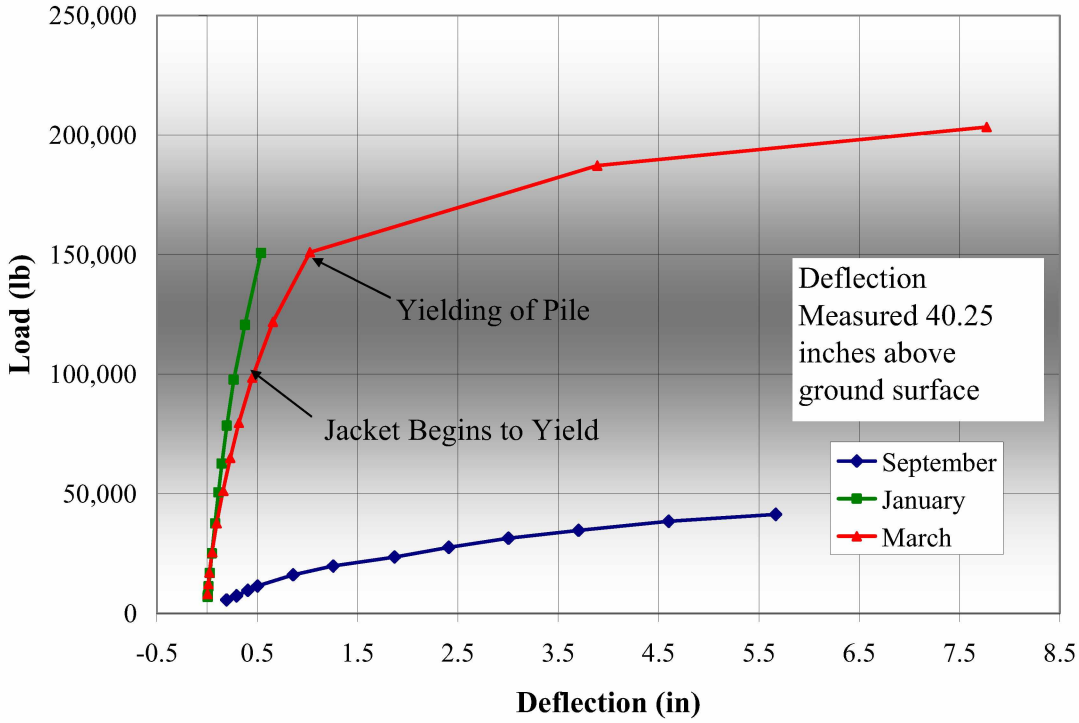

Figure 7.9 September, January, and March Pile Test Pull Over Analysis

7.4 Depth to Fixity Analysis

Results from lateral pile tests have in the past been described in terms of depth of fixity (Coduto 2001). There are several ways of finding equivalent depth of fixity. The first method uses equations of bending to approximate the distance from the point of load application to an equivalent fixed depth, similar to a cantilever beam. The second method uses the location of the maximum moment as the location for the depth of fixity.

7.4.1 Depth to Fixity Flexural Analysis

In the depth to fixity analysis, the pile is modeled as a cantilever beam where the soil above the depth of fixity is ignored and the soil below the depth of fixity is considered infinitely rigid (Coduto 2001). The deflection at the end of a cantilever beam is described.

$$\Delta = \frac{PL_e^{\,3}}{3EI} \qquad \text{Equation 7.4.1}$$

where:

Δ = deflection at point of loading

P = load

EI = flexural stiffness

L_e = distance from load to fixed end

The depth of fixity is typically measured from the ground surface. The pile stiffness (EI) is based on test results for the material properties (E, concrete stress-strain values, tensile strength), measured load and the corresponding calculated moment of intertia, and the measured deflection at the location of the load. Thus, rearranging the variables in the

above equation and by subtracting the distance from the point of load to the ground surface the depth of fixity can be found.

$$L_f = (L_e - L) = (\frac{3EI\Delta}{P})^{1/3} - L \qquad \text{Equation 7.4.2}$$

where:

L_f = depth of fixity measured from the ground surface

L_e = distance from point of loading to the depth of fixity

L = distance from point of loading to ground surface

Figure 7.10 presents the load vs. depth of fixity for September, January and March pile tests. This analysis is only valid for elastic behavior of the pile. During the last two load increments of the March test, a plastic hinge formed below the soil surface; since this analysis is not valid beyond the elastic zone of the pile they are not included in this analysis. See Figure 7.11 for pile behavior during testing and a diagram of the depth to fixity analysis.

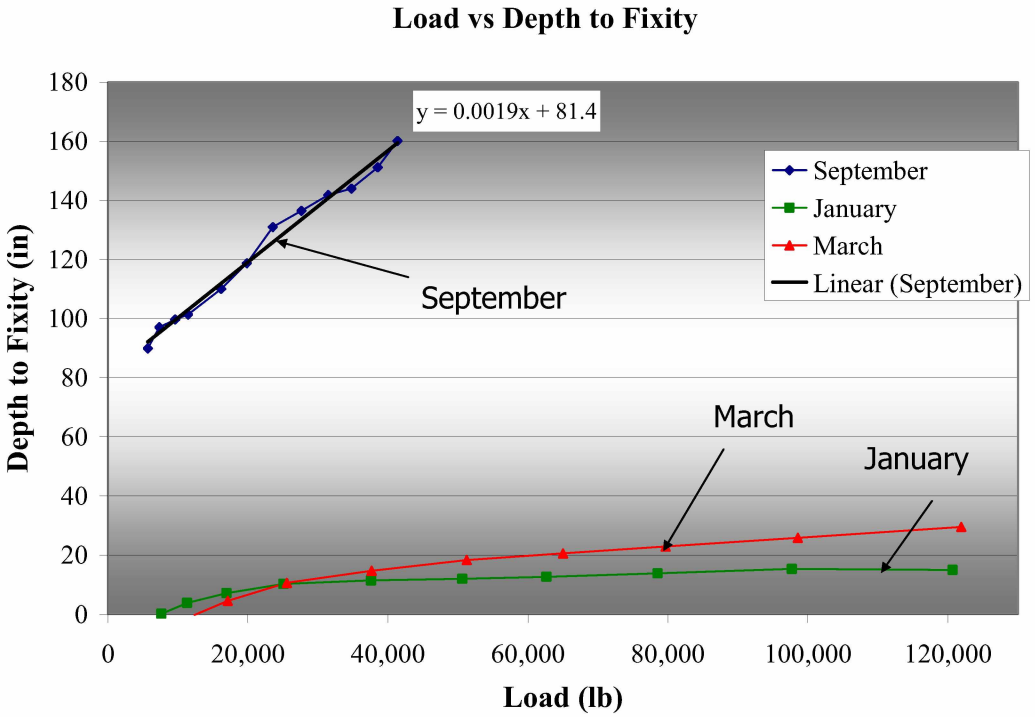

Figure 7.10 Load vs. Depth of Fixity

The results show that depth to fixity during March when the frost depth was at its greatest was actually lower then depth of fixity during January when frost depth was not as deep. This could be attributed to several factors. The stiffness of silt increases as temperature decreases and there is a one foot layer of gravel that has a low moisture content above the silt surrounding the south pile; this layer of gravel is not present on the north test pile.

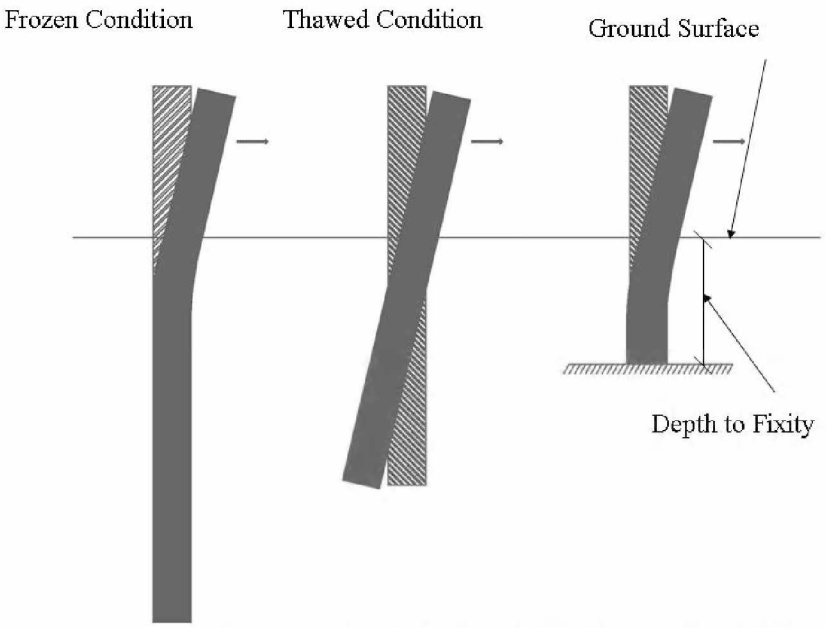

Figure 7.11 Pile Short and Long Foundation Behavior and Depth to Fixity

7.4.2 Depth to Fixity Maximum Moment Analysis

Depth of fixity was also calculated by the method of locating the maximum moment. The location of the maximum strain corresponds to the maximum moment, so strain data from testing was used to find the maximum moment. In Figures 7.12 - 7.14 strain vs. depth is plotted for each test increment. All load steps are plotted on the same graph.

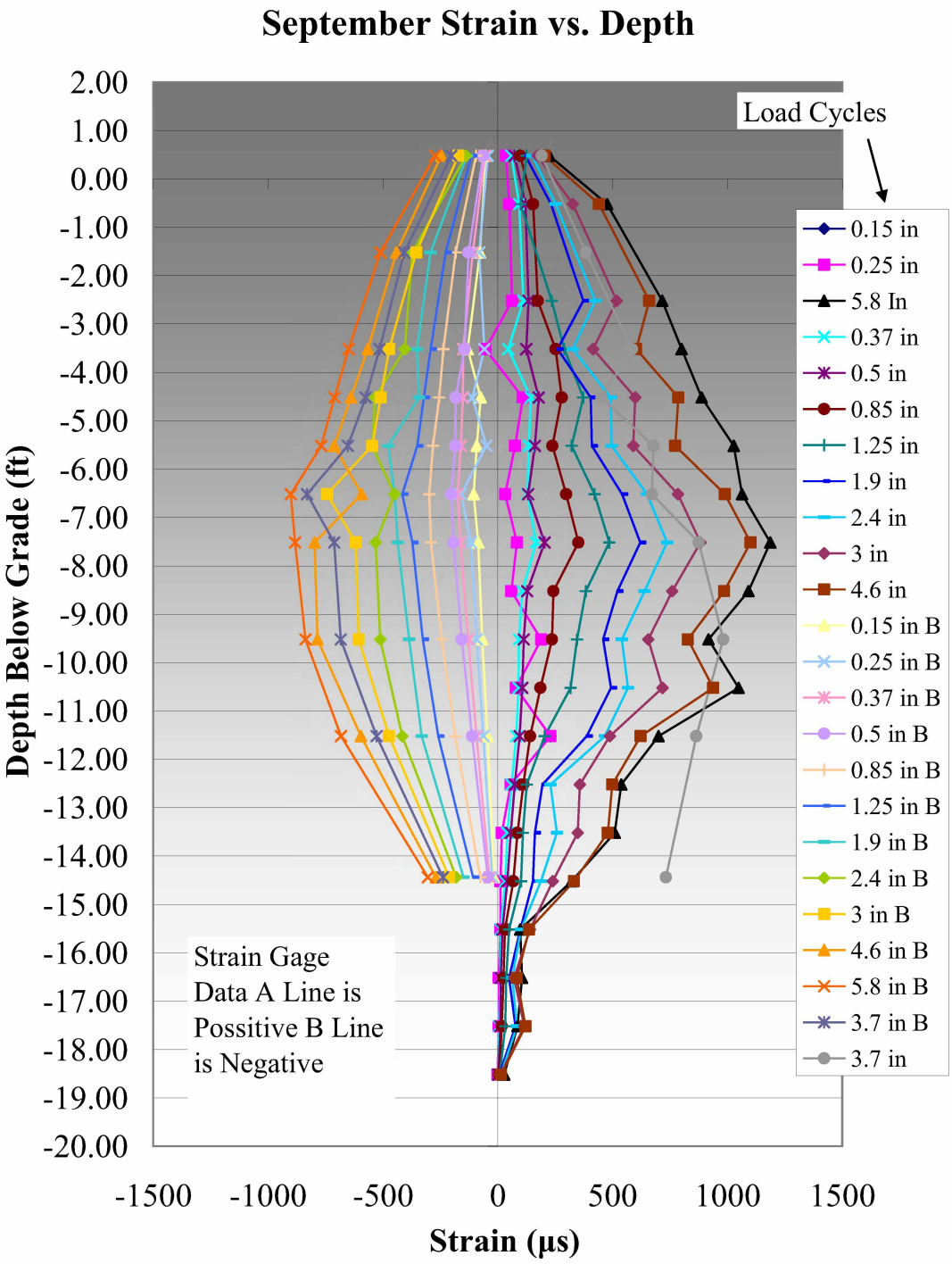

Figure 7.12 September Pile Test Strain vs. Depth

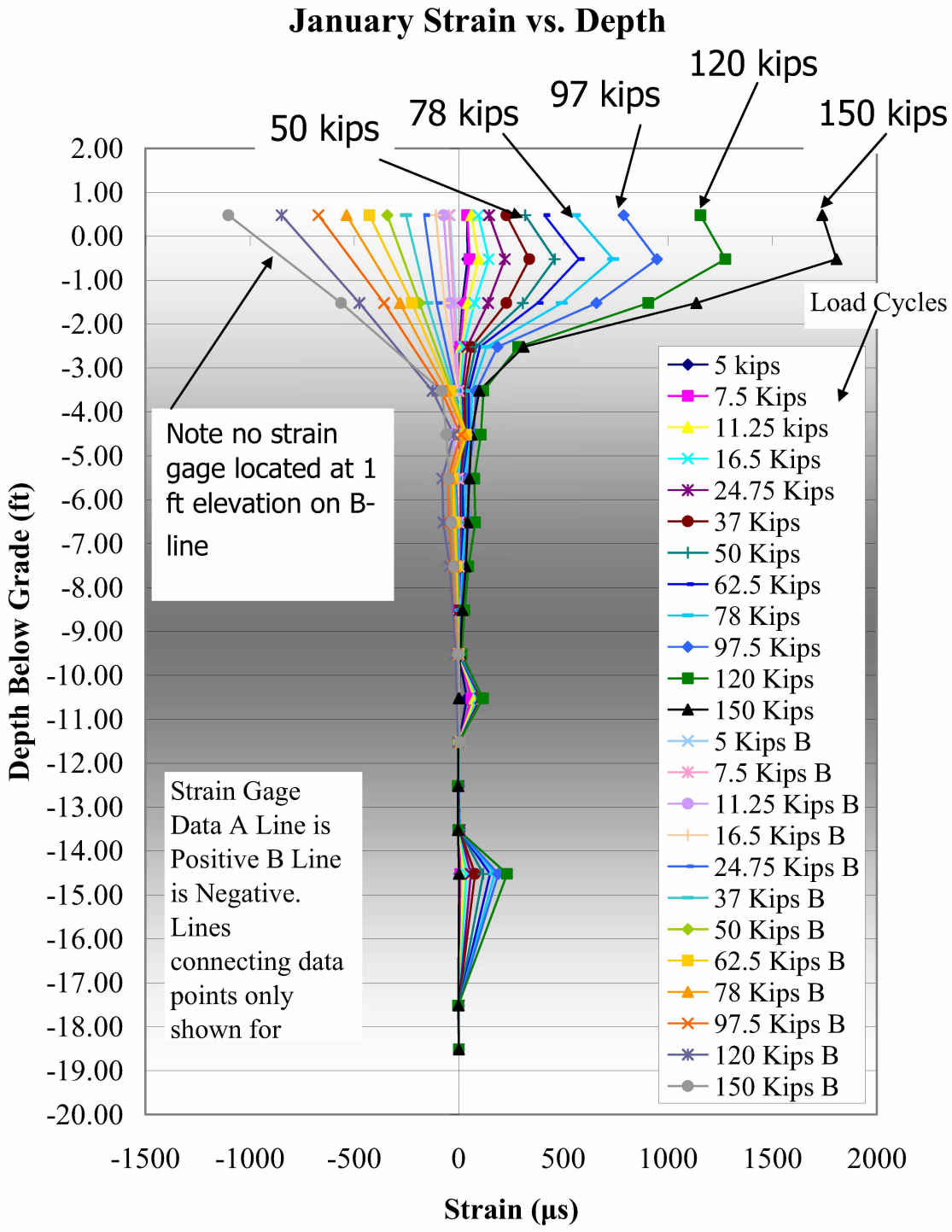

Figure 7.13 January Pile Test Strain vs. Depth

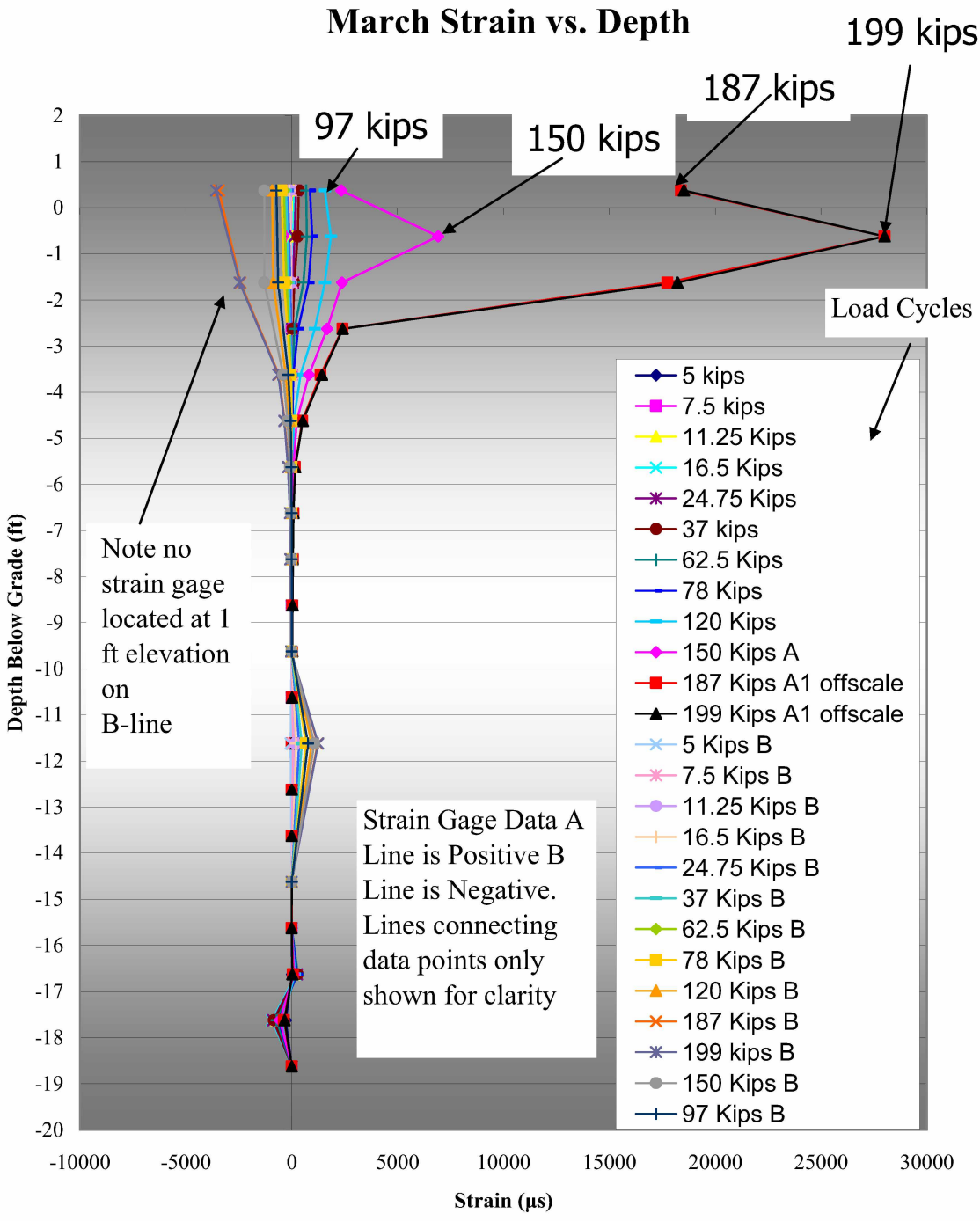

Figure 7.14 March Pile Test Strain vs. Depth

For the September test, the pile response was that of a short foundation with the pile acting like rigid beam rotating through the soil; see Figure 7.11. The strain data for the September test was noisy and the location of maximum strain for the September test was not as clear as for the January and March tests see Figures 7.12 - 7.14. This is a result of the pile acting more like a rigid body in a soft soil then as a pile bending about a specific point. The depth of fixity for the September test can be approximated between six and nine feet below ground surface.

For January pile testing, the pile response was that of a deep (long pile) foundation with the pile bending and the toe of the pile not moving. Strain readings from the tension side of the pile indicated that the location of maximum strain is was between ground surface and 12 inches below ground surface. The maximum strain occurred at six inches below ground surface. On the compression side of the pile there was not a strain gage located at six inches below ground surface. Both tension and compression strains at six inches above ground surface and eighteen inches below ground surface have the similar strains; remember the neutral axis of the pile has shifted toward the compression side of the pile at higher loads. The maximum strain for the January test occurred between the ground surface and 12 inches below ground surface.

For March pile testing, the pile response was again that of a deep foundation with the pile bending and the toe of the pile not moving. Strain readings from the tension side of the pile indicated that the location of maximum strain was between the ground surface and eighteen inches below ground surface. Again, the maximum strain was six inches below ground surface. On the compression side of the pile there was no strain gage

located six inches below ground surface. Again, like the March tests, both tension and compression strains at six inches above ground surface and eighteen inches below ground surface have the similar strains; remember the neutral axis of the pile has shifted toward the compression side of the pile at higher loads. The maximum strain for the March test occurred between the ground surface and 12 inches below ground surface.

7.5 Soil Spring Model

Soil springs have been used extensively for modeling the lateral displacement of piles. LPile Plus version 5.0.40 (LPile) was used for the following analysis (Reese et al. 2004). LPile is essentially a beam on elastic or inelastic foundation; the soil resistance is approximated by discretely spaced springs. LPile uses a numerical approximation method based on finite difference. The software was used to develop empirical soil springs that would accurately predict the experimental results for the piles embedded in silt and located at the CRREL test site. In the model, the pile was divided into 276 one-inch long sections. A point load was applied approximately 40 inches above the ground surface. The soil springs begin at the ground surface and are located at each node between the one inch pile sections. The analysis takes into account the nonlinear behavior of the steel and concrete pile. The stiffness of the pile at different bending moments is calculated and then applied to the loaded pile. In Figure 7.15 the bending stiffness vs. bending moment from LPile is compared to that computed by strain analysis. LPile has a large database of soil springs that have been suggested by past research and

full scale pile testing. Nonlinear soil springs can also be input into the model to create soil springs for unusual soil conditions.

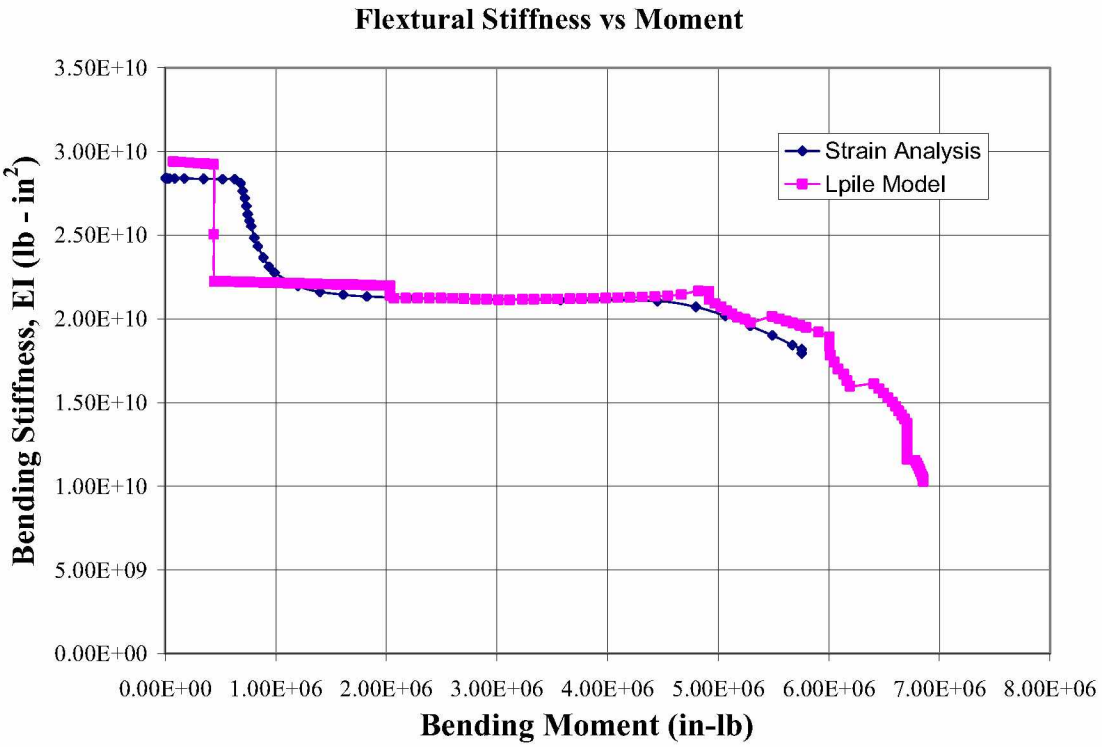

Figure 7.15 Bending Stiffness vs. Bending Moment

7.5.1 Thawed Soil Springs

The modulus of subgrade reaction varies with the stiffness of the soil. In the thawed condition, the soil at the test site is a very lose nearly saturated silt. Initially the soil springs were created by inputting friction angle and cohesion for Fairbanks silt (Nidowicz 1981) into the silt model that is built into LPile. The silt springs based on the soil properties were far too stiff for the silt at the test site. A different model was needed. A literature review was done; the results are summarized below.

In TM 5, a design manual published by the US Army Corps of Engineers, a recommendation modulus of subgrade reaction is given for concrete floor slabs subjected to heavy loads. Theses values were created for vertical loads on the soil. For silts with more than 29 percent moisture content at more than 90 percent compaction, the recommended modulus (K_s) is 50 (lb/inch^3). For soils that are not at over 90 percent compaction, it is recommended to reduce the value by 50 lb/inch^3 but the value should no be lower then 25 (lb/inch^3). To get from the modulus of subgrade reaction to the stiffness of the soil spring the following equation was used.

$$K_{spring} = K_s B \qquad \text{Equation 7.5.1}$$

Where:

K_s = modulus of subgrade reaction form TM 5 (in lb/in^3)

B = width of the foundation (in)

K_{spring} = the stiffness spring (lb/in) per inch of pile

The soil springs created from this method are plotted in Appendix D

A second modulus was derived from shear wave velocity testing done at the site. In order to get the modulus of subgrade reaction, the following equations were used. From Kramer (1996)

$$G_{\max} = \rho V_s^{\,2} \qquad \textbf{Equation 7.5.2}$$

Where:

ρ = mass of soil

V_s = shear wave velocity

G_{max} = Maximum Shear Modulus

Gmax is the maximum shear modulus of a soil and is found by dynamic testing. From the Electric Power Research Institute's (EPRI) manual on estimating soil properties, design correlations are given to get from G_{max} to a modulus of subgrade reaction for cohesive soils; the calculations are as follows. Seed and Idriss (1970) recommended that the static shear modulus, G, is 5-10 percent of G_{max} for sands (EPRI 1990). For undrained loading of cohesive soils Young's modulus is approximated as

$$E = 3G \qquad \textbf{Equation 7.5.3}$$

Where:

E = Young's Modulus for soils

G = 5 to 10% G_{max}

Vesic (1961) proposed the following model to go from E to modulus of subgrade reaction (EPRI 1990).

$$K_s = \left(\frac{0.65}{B}\right) * \left(\frac{EB^4}{E_f I_f}\right)^{\frac{1}{12}} \left(\frac{E}{1-\upsilon^2}\right) \qquad \textbf{Equation 7.5.4}$$

Where:

K_s = modulus of subgrade reaction

B = width of the foundation

E = Young's modulus for the soil

E_fI_f = flexural stiffness of the foundation

The modulus of subgrade reaction is then multiplied by the width of foundation and the length of the foundation that the soil spring will represent. In the LPile model used to model the test pile, the pile was broken into one-inch sections with springs located at each node. Each soil spring represented a one-inch length of the pile. The springs created from shear wave velocity testing are plotted in Figure 7.16

The calculated spring stiffness was a starting point for modeling. The modulus of subgrade reaction does not provide an upper end for the compressive strength of the silt. Using the different soil modulus, the strength possible for the silt would be up to 250 psi over a distance of 5 inches, but it is unlikely that that strength could be obtained in this soft soil. The shape of the soil springs for the model started as listed above and through an iterative process spring values were adjusted to match the experimental behavior. After several iterations and adjustments, springs were found that would accurately represent the behavior of the pile. The springs are plotted in Figure 7.16. Springs computed from above method are plotted for comparison in Appendix D

Lpile linearly interpolates between the soil springs specified at each elevation. A printout of the output file can be found in Appendix A. In the file, spring values are given every 1 foot throughout the length of the pile. A pull over analysis was done in the LPile model with the silt springs. The results are plotted in Figure 7.17. Results from the model were also compared to the deflected shape of the pile from testing the results are plotted in Figures 7.18, 7.19 and Appendix D

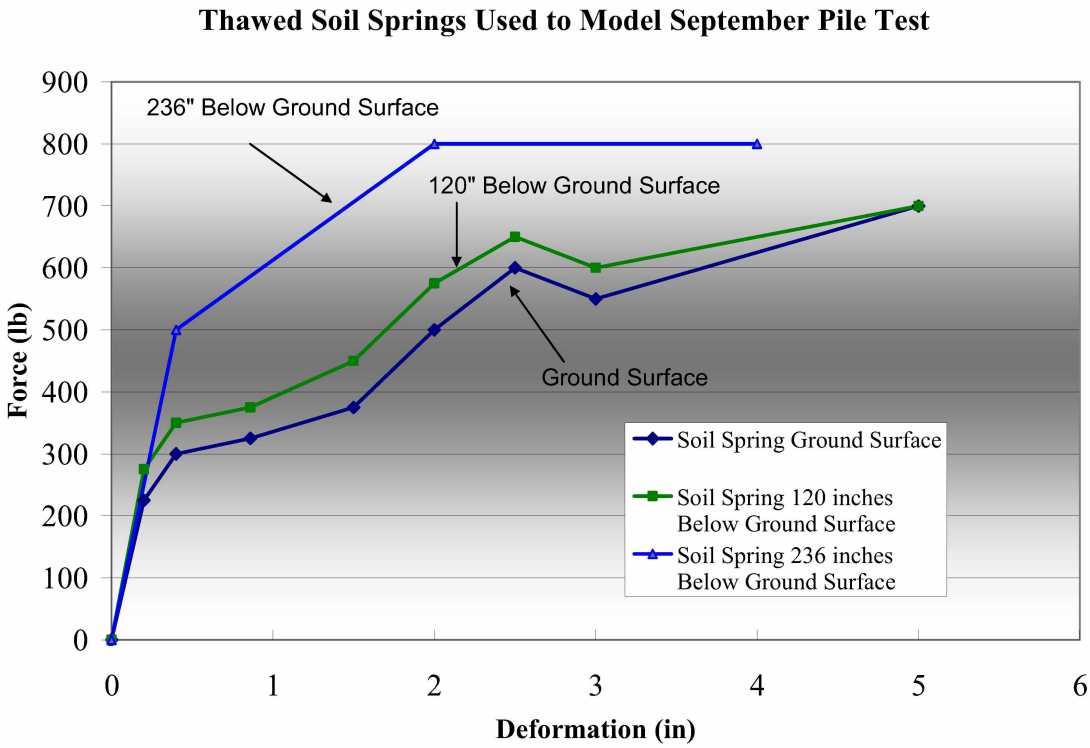

Figure 7.16 Soil Springs Used to Model September Test

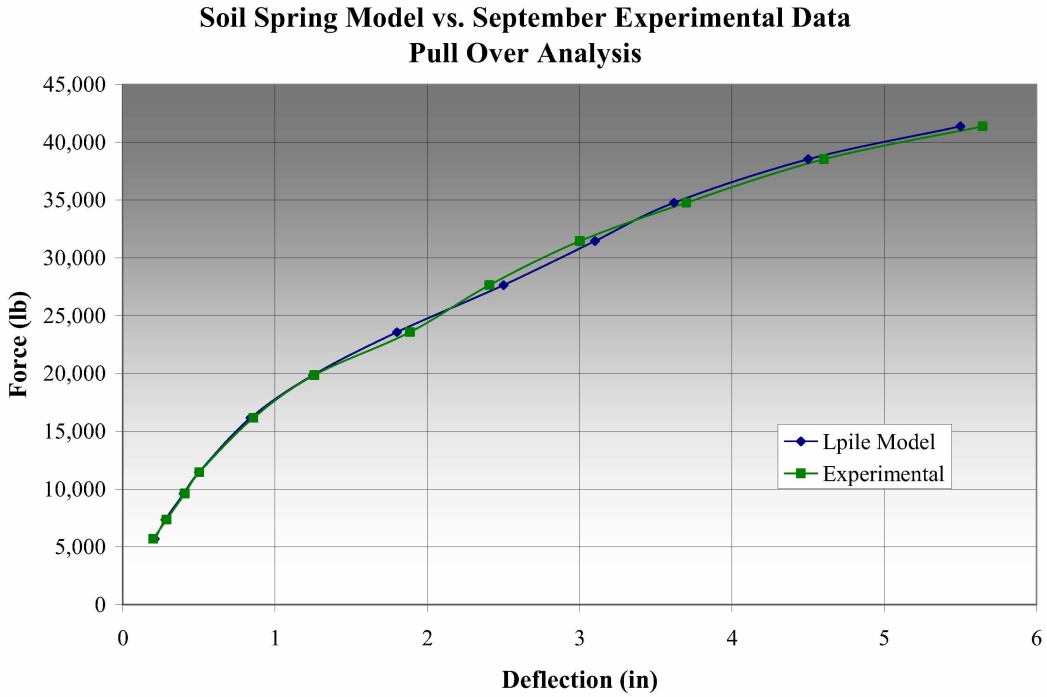

Figure 7.17 Pullover Analysis Model Predicted, and Experimental

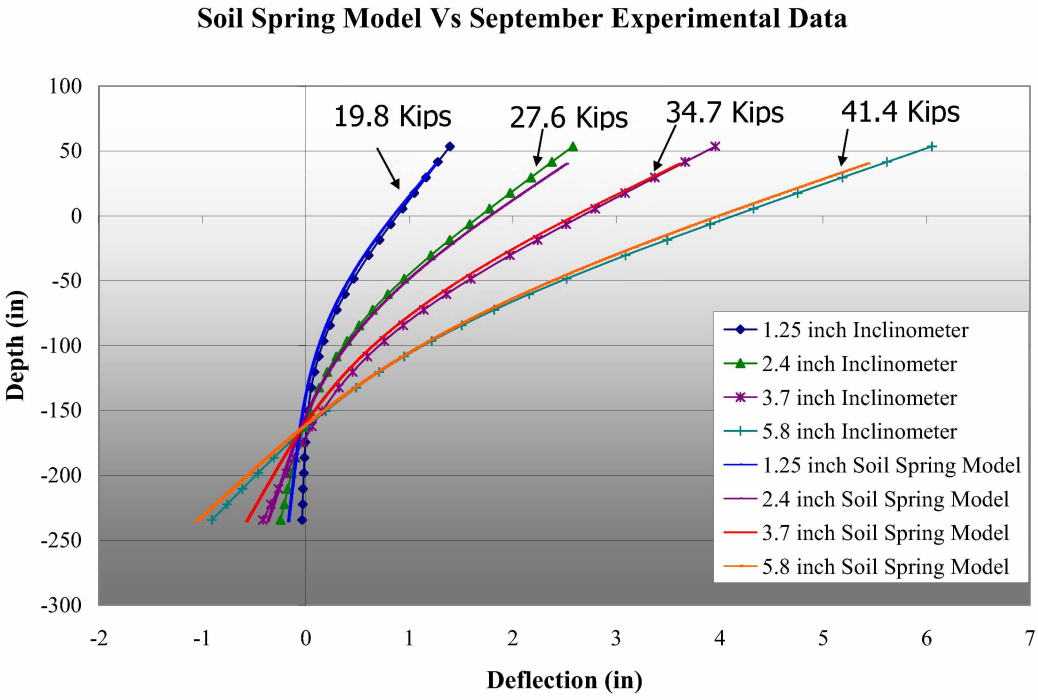

Figure 7.18 Deflected Shape Model Predicted, and Experimental

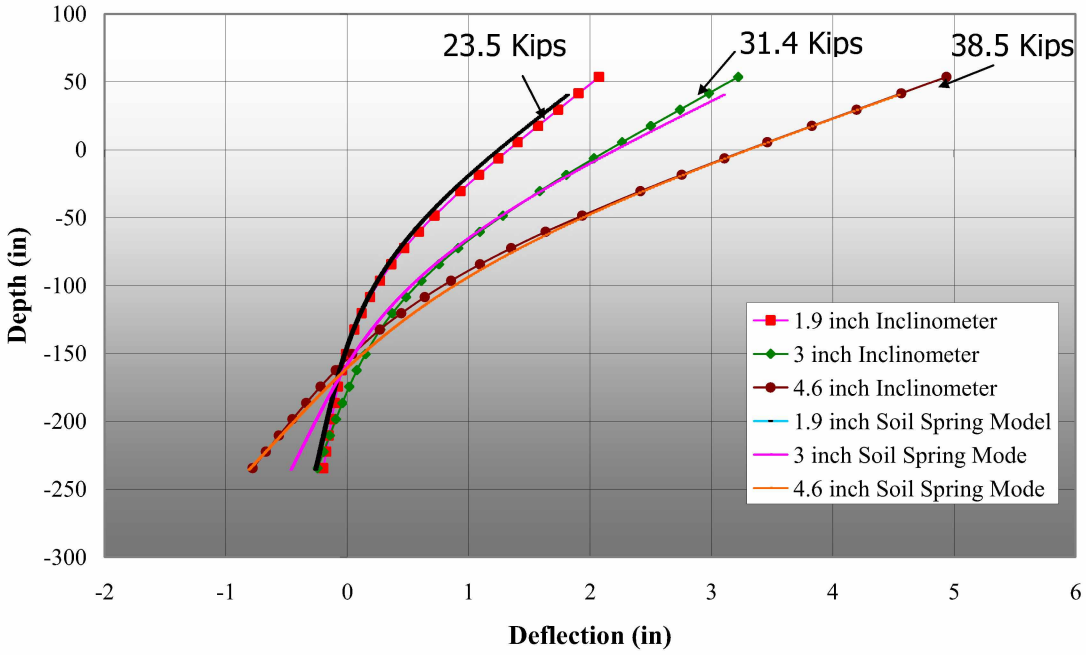

Figure 7.19 Deflected Shape Model Predicted, and Experimental

7.5.2 Frozen Soil Springs

The modulus of subgrade reaction for frozen soils has not been extensively explored. While there has been strength testing on frozen silts there has not been an accurate model created that will describe the frozen soil using a soil spring to model full scale pile testing. LPile was again used to model the pile soil interaction. Since LPile did not have a built in model for frozen silt or any frozen soil, a spring that would accurately model the frozen soil was developed. As a starting point, a literature review was done see Chapter 2. The properties listed in Tables 7.5 and 7.6 (Haynes and Karalius 1977) were used to model the frozen Fairbanks silt.

Table 7.5 Properties of Frozen Fairbanks Silt (Haynes and Karlaluis 1977)

Water Content (%)	*Temp. (C)*	*Applied Strain Rate (s^{-1})*	*Displacement Rate (in/min) 6 inch tall sample*	*Dry Density (pcf)*	*Peak Strength (psi)*
43.5	-10	0.00557	2.0052	73.79	1422.82
42.6	-10	0.00123	0.4428	74.79	1031.22
41.7	-10	0.000115	0.0414	75.54	697.63

Table 7.6 Properties of Frozen Fairbanks Silt (Haynes and Karaluis 1977)

Water Content (%)	*Temp. (C)*	*Applied Strain Rate (s^{-1})*	*Initial Yield Strength (psi) σ_y*	*Initial Tangent Modulus E_i (psi)*	*50 % Strength Modulus E_i (psi)*
43.5	-10	0.00557	1095.03	Unknown	250915
42.6	-10	0.00123	835.42	301678	174045
41.7	-10	0.000115	570.00	387251	216106

Soil springs were then found using Equation 7.5.4. Although this equation is for thawed soils, it is a starting point for going from a modulus of elasticity to a modulus of subgrade

reaction. Values for these springs are listed in Table 7.8. Results produced were nowhere near what was found during lateral load testing.

Table 7.7 Modulus of Subgrade Reaction from Haynes and Karaluis Silt Properties

Water Content (%)	*Temp. (C)*	*Applied Strain Rate (s-1)*	*Modulus of Subgrade Reaction for Soil (lb/in^3)*	*Spring Siffness for Pile (lb/in)*
43.5	-10	0.00557	10064	161032
42.6	-10	0.00123	6772	108345
41.7	-10	0.000115	8561	136977

The soil springs were modified until the LPile model performed similar to the experimental behavior that was seen during March field testing; see Figure 7.20 for springs used for March modeling.

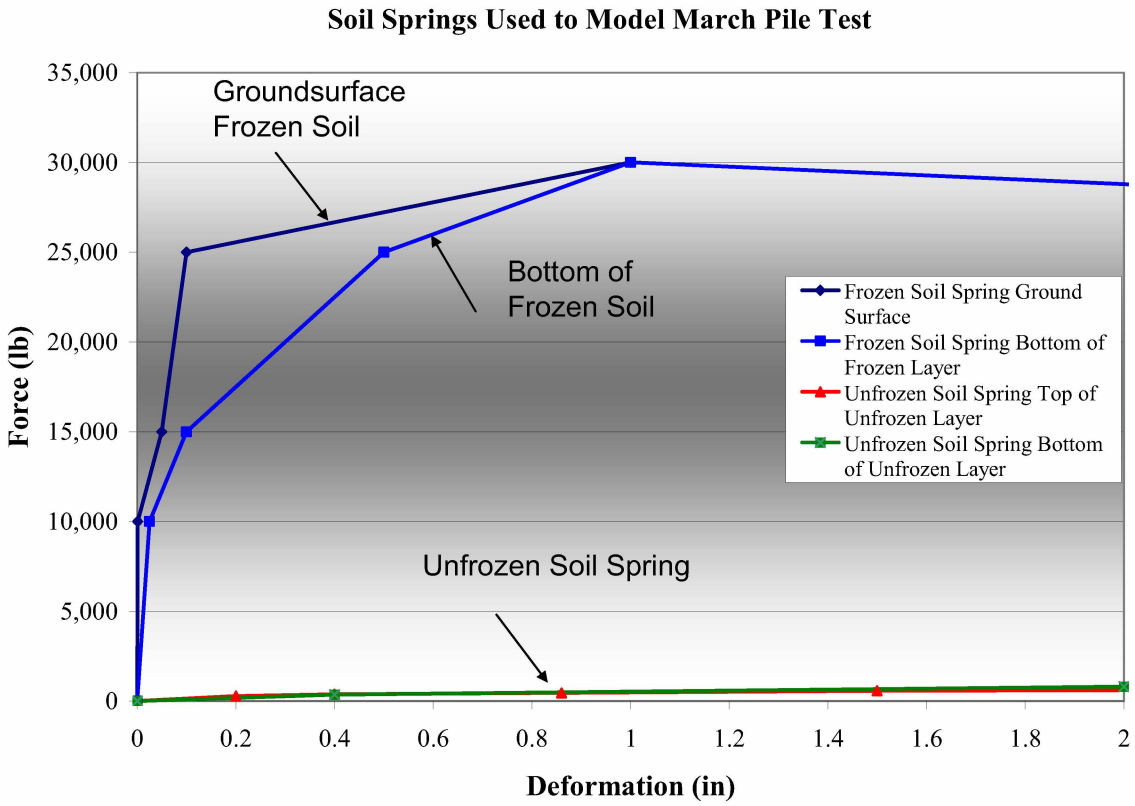

Figure 7.20 Soil Spring Used to Model March Pile Test

While experimental data was collected until the end of testing, this analysis is limited to the 120 kip load increment. For the model, strain data was used to match the model to experimental data. LPile outputs deflection, moment, shear and soil reaction with depth. In order to convert the moment from the Lpile model into an equivalent strain at the tensile rebar, the A-line strain gages, the moment flexural program was again used. A plot of moment vs. tensile strain at A-line gages was created; see Figure 7.21 a sixth order polynomial trend line was fitted through the data. The equation was then used to convert moment from the model into equivalent tensile strain and compare it to the experimental data.

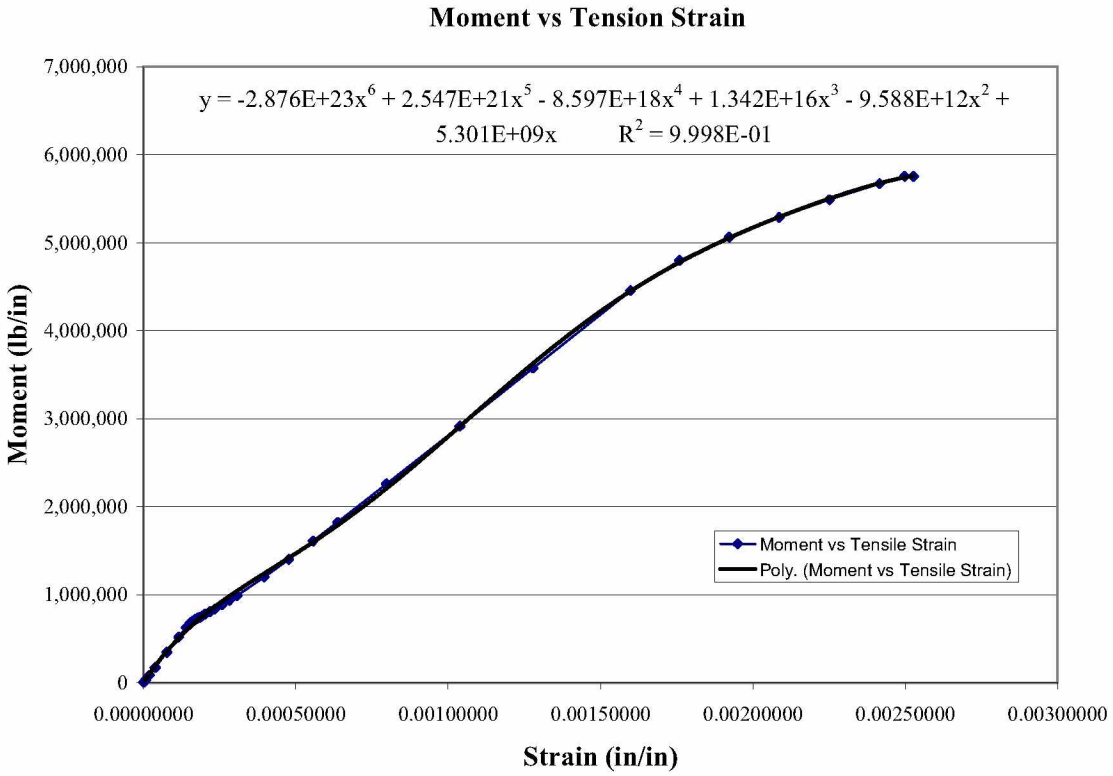

Figure 7.21 Experimental Tensile Rebar Strain vs. Moment in Test Pile

The results of the model are plotted in Figure 7.22 and 7.23. While the results of the experimental data do not line up perfectly with the experimental data, they are within an acceptable range of error. Possible sources of this error are the rebar cage not being perfectly centered in the pile and differences between pile properties modeled and actual.

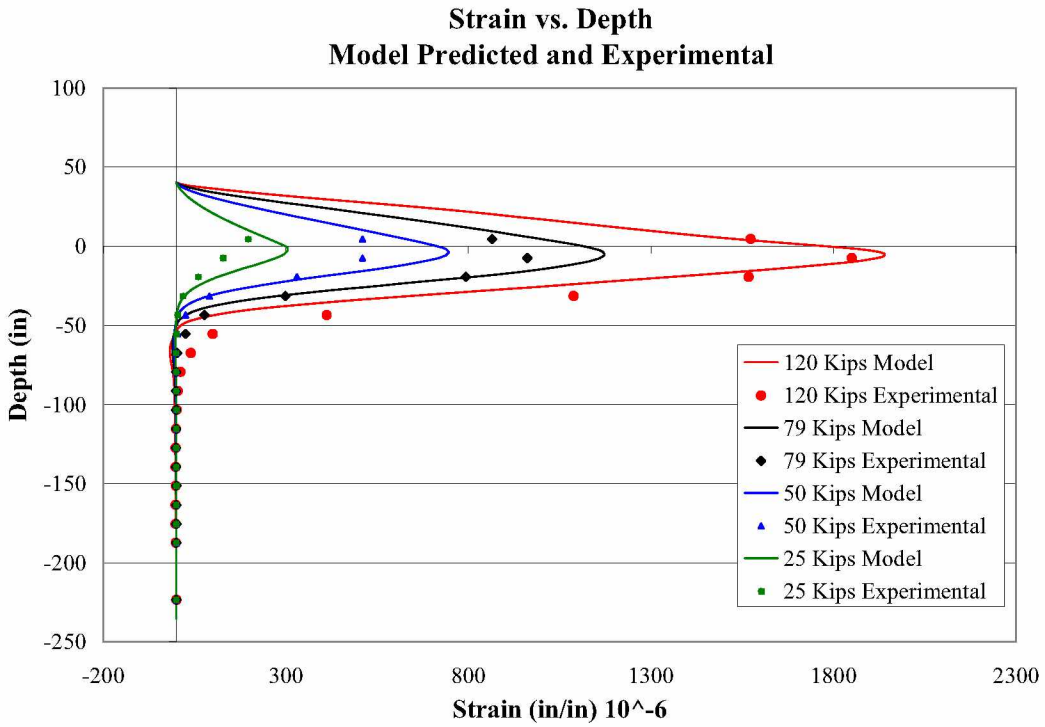

Figure 7.22 Strain, Model Predicted and Experimental

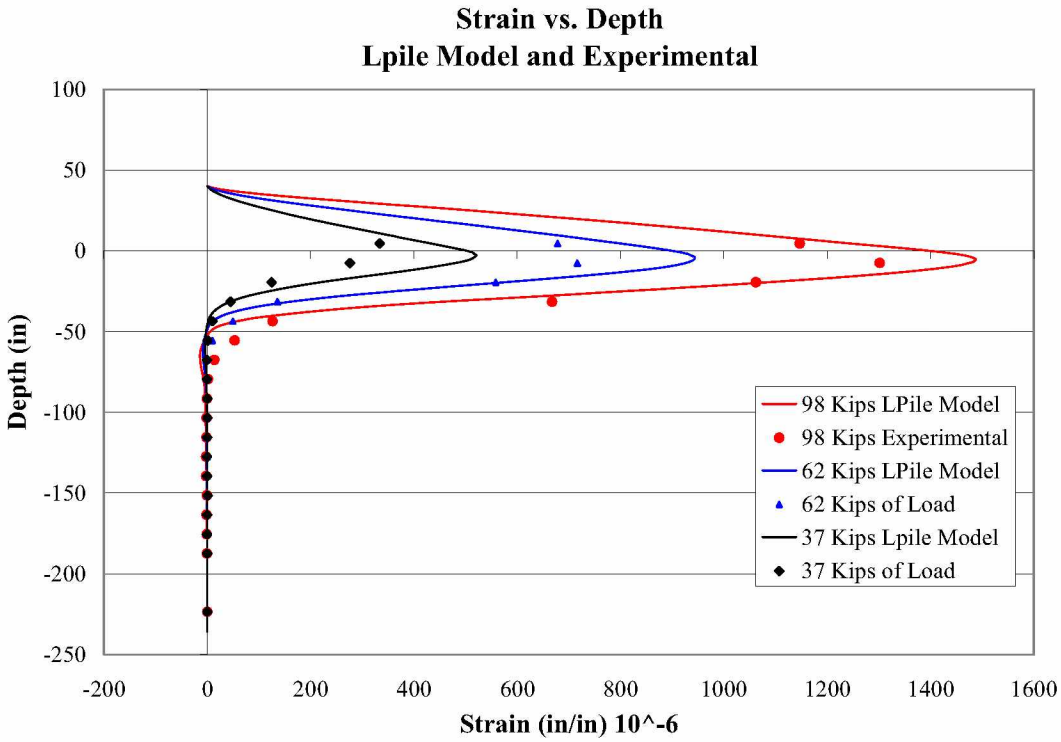

Figure 7.23 Strain, Model Predicted and Experimental

8 Findings

The pile tested in thawed conditions experienced short foundation behavior. The pile rotated about a point below subgrade see Figure 8.1; the toe of the pile kicked and failure of the system occurred in the soil. During frozen conditions the pile was extremely stiff and the pile experience a bending type failure that is typical of deep foundation behavior. During both the January and March tests, the location of the maximum moment was within 0.75 pile diameters of the ground surface for the 16-inch diameter pile in Fairbanks silt or Fairbanks silt with a foot of gravel on top. During March testing, a plastic hinge in the pile formed approximately 6-12 inches below the ground surface. Figure 8.2 is a picture of the yielded south pile.

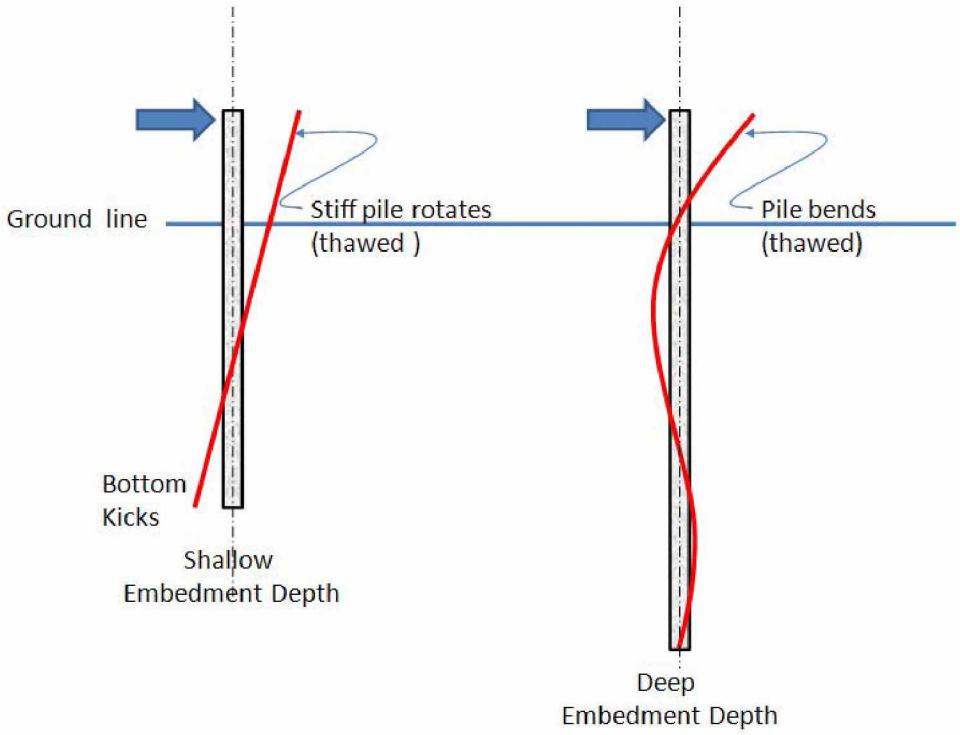

Figure 8.1 Short Pile Embedment vs Deep Pile Embedment

Figure 8.2 Excavation of South Pile Tested March 2010

Two analytical methods for evaluating test results were requested by AKDOT; these were to be based on experimental test results. The first is a simplistic method that is well established. The method simplifies the problem by using a depth of an equivalent fixity to approximate a complicated problem. In this method, the soil above the depth of equivalent fixity is neglected and the soil below the depth of equivalent fixity is considered infinitely rigid (Coduto 2001). The second method is more complicated and uses soil springs to approximate the behavior of the pile. This is essentially a beam on elastic or inelastic foundation; the soil resistance is approximated by discretely spaced springs. For this analysis, LPile (Reese et al. 2004) was chosen to perform the analysis.

LPile uses a numerical approximation method based on finite difference. The software was used to develop a set of soil springs that would accurately predict the experimental results of the pile.

8.1 Depth to Fixity

The results of lateral pile tests have in the past been described in terms of depth to fixity. There are several ways of finding the equivalent depth of fixity. The first method uses equations of bending to approximate the distance from the point of load application to an equivalent fixed depth, similar to a cantilever beam. The second method uses the location of the maximum moment as the depth of fixity. Table 8.1 summarizes the results. The two methods produced comparable results. While there were differences between the two methods in the thawed condition, this can be attributed to the pile rotating through the extremely soft soils during summer testing, see Figure 8.1. Results from the flexural analysis are no longer valid after the formation of a plastic hinge and are not shown for loads larger then 120 kips. The results from this analysis also become less accurate as the pile rotates in the ground. Thus, results for the fall (thawed) test are not shown for loads over 30 kips. The depth of equivalent fixity shifted up 8-10 feet during winter testing in comparison to summer testing. When designing for a worst-case winter depth of fixity for pushover analysis it is safe to assume that the depth of fixity is located at or within 0.75 diameters of the ground surface, for a similar pile in similar soil conditions.

Table 8.1 Depth to Fixity 16 inch Diameter Steel Jacketed Reinforce Concrete Pipe Pile, Embedded in 19.5 feet of Fairbanks Silt

Depth of Frost	*Thawed Soil (September)*		*4.5 Foot Layer of Seasonally Frozen Soil (January)*		*7.5 Foot Layer of Seasonally Frozen Soil (March)*	
Load (kips)	*Depth from Equivalent Stiffness Method (ft)*	*Depth from Location Maximum Moment (ft)*	*Depth from Equivalent Stiffness Method (ft)*	*Depth from Location Maximum Moment (ft)*	*Depth from Equivalent Stiffness Method (ft)*	*Depth from Location Maximum Moment (ft)*
10	8-9	5-11	0-1	0-1	0-1	0-1
25	10-12	5-11	0-1	0-1	0-1	0-1
30	10-12	5-11	0-1	0-1	0-1	0-1
78			1-2	0-1	1-2	0-1
120			1-2	0-1	1-2	0-1
150				0-1		0-1
190				0-1		0-1
200				0-1		0-1

8.2 Soil Springs

Soil springs were calculated for both the frozen and unfrozen conditions. Initially, an attempt was made to use existing soil spring data from the LPile database. However, these spring values provided a poor comparison between the predicted P-Y curves and the measured P-Y curve data. Therefore, empirical evaluated springs were developed to match the experimental results. The springs used to model the frozen soil are show Figures 7.16 & 7.20 and in Appendix D. The spring stiffness needed to model the pile increased by two orders of magnitude, from thawed to frozen. The force required to displace the soil spring 0.5 inches went from 310 lb in summer conditions to over 27,500 lb in frozen conditions. This spring represents the equivalent soil force for a 1 inch pile section of the pile.

8.3 Quantify Stiffness Increase and Moment of Maximum Moment

The calculated yield and ultimate strength are 4,400 kip-inches and 8,700 kip-inches respectively. During September, the north 16-inch diameter pile was tested and during this test, it experienced short foundation behavior. That is, the toe of the pile kicked and the pile rotated through the soil; failure occurred in the soil not in the pile. During the January and March tests, the north pile (January test) and the south pile (March test) the pile behaved as a long foundation. In January, it was determined that the capacity of the load frame was inadequate to fail the pile. During that test, the pile steel jacket started to yield above 100 kips. This corresponds to an effective length of 45 inches, force * effective length= yield capacity. Based on the expected yield capacity of the pile this corresponds to an equivalent depth to fixity of 5 inches below ground surface. By the end of the third cycle at 120 kips plastic deformation was around 0.09 inches at the point of loading; after the first cycle of 150 kips approximately 0.14 inches of plastic deformation occurred at the loading. This plastic deformation of the pile itself corresponds to calculated yield and ultimate strength of the pile with the corresponding depth to fixity of 5 inches.

During March testing, the steel jacket started to yield above 100 kips of load, this again corresponded to a depth to fixity of 5 inches below grounded surface, calculated based on the assumptions stated above. By the end of the third cycle at 120 kips, plastic deformation was around 0.15 inches at the point of loading; after the first cycle of 150 kips approximately 0.3 inches of plastic deformation occurred at the loading. This

stiffness difference could be due to the difference in soil conditions. In the top one foot of the soil, the south pile has a one foot layer of gravel fill. While the north pile had some 1 to 2 inch cobbles mixed in with the silt in the top 8 inches of soil, the material was over 80 percent silt. This difference could also be partially attributed to the difference in soil temperature, during the January test the lowest recorded soil temperature was -18 degrees Celsius. During March testing the lowest soil temp was -8 degrees Celsius.

The March test was stopped when the rotation in the plastic hinge that formed just below ground surface became too great and the U-bolts that attached the test frame to the test pile slipped up the pile. Total displacement at the point of loading was 8.9 inches under a load of 207 kips. The ultimate moment placed on the pile during testing based on the location of the plastic hinge 6-12 inches below ground surface was 9,570 to 10,800 kip-in, which was 10 to 25 percent more than the estimated ultimate pile capacity.

In comparison to summer testing, shear demand in the pile increased from 42 kips to 207 kips; a 409 percent increase. Yielding of the test pile was not obtained during summer testing with a maximum displacement of 5.7 inches at the point of loading. While the pile started to plastically deform during the January testing it was not taken beyond the ultimate capacity of the pile. During March testing, the displacement capacity at yield measured 0.75 inches at the point of loading. The force required to yield the pile was approximately150 kips. The stiffness increase from summer to winter was significant. Since the pipe rotated in the summer condition, the displacement capacity was not compared.

9 Conclusions

AKDOT funded this study to find the upper limit of stiffness for a typical AKDOT bridge pile foundation in a seasonally frozen soil. This research quantifies that stiffness increase for 16 inch, steel-jacketed, steel reinforced concrete piles embedded in frozen and unfrozen silts.

As soils freeze the stiffness and strength of the soil increases. So, if a pile is embedded in soil and it freezes, the stiffness of the foundation system increases. As a result, depth to equivalent fixity is reduced and the distance the top of the pile can displaced before the pile failure (displacement capacity) is also reduced.

Sixteen inch diameter steel jacketed reinforced concrete piles embedded in frozen soil were subjected to cyclic quasi-static lateral load tests. The results of these tests showed that the piles behaved similar to the same piles modeled as a fix cantilever beam with the location of the fixed end being just below ground surface. Shear demand for piles in frozen soil versus piles in thawed soil increased over 400 percent. Depth of fixity of the pile was within 0.75 pile diameters of the ground surface during the winter and 8 diameters for the summer. Results were similar for two conditions: a 16 inch diameter pile in Fairbanks silt and Fairbanks silt with a 1 foot layer of gravel fill atop the ground surface. The stiffness increase from summer to winter was notable: in summer the unfrozen soil was easily compressed out of the way. In the winter, as water in the soil froze, it became extremely stiff.

For earthquake design as an upper design limit, the depth of equivalent fixity is often used as a design parameter. In this case, the pile may be considered fixed at the

ground surface for a frozen silt in interior Alaska. For a 16 inch diameter steel jacketed, reinforced concrete pile in similar soil conditions, it is accurate to assume that the pile is fixed at or within 0.75 pile diameters of the ground surface. For the thawed condition, the pile experienced short foundation behavior; with the pile simply rotating through the soil. As a result the depth of fixity for a long foundation system still must be determined by other methods. In this study, the depth of pile embedment precluded finding an equivalent depth of fixity. Failure in the thawed soil needs further study.

Soil springs used to model the pile in frozen soils are significantly stiffer than those that represent the thawed or unfrozen soils. The spring stiffness needed to model the pile increased by two orders of magnitude, from thawed to frozen. For a soil spring representing the top few inches of soil and a 1 inch long pile section, the force required to displace the soil spring 0.5 inches went from 310 lb in summer conditions to over 27,500 lb in frozen conditions.

9.1 Suggestions for further research.

Data Processing

- Pushover Analysis for Winter Condition Using Software that can accommodate Plastic Material behavior.
- Create Soil Springs for to simulate January testing.
- Percent degradation for cycle of three loads or displacement.

Further Pile Tests

- Full scale testing of similar piles in gravel and sand
- Full scale pile test in thawed Fairbanks silt

References

AISC (2005) "Steel Construction Manual", 13th edition American Institute of Steel Construction. 13th

American Society of Civil Engineers (ASCE), (2005) "ASCE/SEI 7-05, Minimum Design Loads For Building and Other Structures." United States.

Andersland, O. B., Anderson, D. M., (1978) Geotechnical Engineering for Cold Regions." *Ice Pressures and Bearing Capacity*, L.W. Gold, New York, NY. 516.

Campbell Scientific. (2010) "CR9000x Modular Measurement and Control System" <http://www.campbellsci.com/cr9000x> (Jan. 2010)

Coduto, D. P., (2001). "Foundation Design Principles and Practices 2nd edition." *Deep Foundations Lateral Load Capacity,* Upper Saddle River, New Jersey, 594-595.

Collins, M. P., Mitchell, D. (1991). "Prestressed Concrete Structures." Material Properties, Prentice Hall, Englewood Cliffs, New Jersey, 61-65

Cox, C. R., Reese L. C., and Grubbs, B. R., (1974). "Field Testing of Laterally Loaded Piles in Sand." Proceedings of Sixth Annual Offshore Technology Conference, Houston TX.

Crowther, G. S. (1990). "Analysis of Laterally Loaded Piles Embedded in Layered Frozen Soil." Journal of Geotechnical Engineering, 116(7), 1137-1152.

Davis, D., (2010). "Effect of frost depth on the effective length of bridge piles." MS thesis, University of Alaska Fairbanks., Fairbanks, AK.

Electric Power Research Institute (EPRI), (1990). "Manual on Estimating Soil Properties for Foundation Design." *Elastic Deformability*, Cornell University, Ithaca, New York 5(1-26).

Enerpac Hydraulics. 2009. web address - http://enerpac.com/files/catalogues/PE_pump_326US.pdf

Foriero, A., St-Laurent, N., and Ladanyi, B., (2005). "Laterally Loaded Pile Study in Permafrost of Northern Quebec, Canada." Journal of Cold Regions Engineering, 19(3), 61-84.

Geodaq, (2006) "Geodaq INC300 series inclinometer data sheet." www.geodaq.com (Mar. 2006)

Haynes, F.D., Karalius, J.A. and Kalafut, J. (1975) Strain rate effect on the strength on the strength of frozen silt. USA CRREL Research Report 350. AD 021981.

Haynes, F.D., Karalius, J. A. (1977). "Effect of temperature on the strength of frozen silt." CRREL Report 77-3, Cold Regions Research and Engineering Laboratory. Hanover, New Hampshire.

Kramer, S. L. (1996). "Geotechnical Earthquake Engineering." *Stress-Strain Behavior of Cyclicality Loaded Soils*, Prentice Hall, Upper Saddle River, New Jersey, 232-233.

Linell, K. A. 1973. Long-term effects of vegetative cover on permafrost stability in an area of discontinuous permafrost. Permafrost 2nd international conference, Yakutsk, U.S.S.R.

Nicholson, F.H. and Granberg, H.B. (1973). Permafrost and snowcover relations near Schefferville. In: Permafrost, Second International Conference North American Contribution. Washington, D.C. national Academy of Sciences, pp151-158.

Nidowicz, B., (1981) "Consolidation and Shear Strength Characteristics of Fairbanks Silt." MS thesis University of Alaska Fairbanks, Fairbanks, AK

Reese, L.C., Wang, S.T., Isenhower, W.M., Arrellaga, J.A., (2004) "Computer Program LPile Plus version 5.0." Ensoft Inc. Austin, Texas.

Reese, L. C., Welch, M., (1975). "Lateral Loading of Deep Foundations in Stiff Clay." Journal of the Geotechnical Engineering Division, 101(GT7), 633-649.

Rowley, R.K., (1973). "Vertical and Lateral Pile Load Tests in Permafrost." Proc., 2nd Int. Conf. Permafrost, Yakitsk, North Am. Contrib., pp712-721

Seed, H. B., Idriss, I. M., (1970). "Soil Moduli and Damping Factors for Dynamic Response Analysis." Report EERC 70-10, University of California, Earthquake Engineering Research Center, Berkeley,

Sritharan, S., White, D. J., Suleman, M. T., (2004) "Bridge Column Foundations-Soil-Interaction Under Earthquake Loads in Frozen Conditions." *Proc. World Conference on Earthquake Engineering*, Vancouver, Canada., paper # 3425

Stevens, H.W. (1973). Viscoelastic properties of frozen soils under vibratory loads. North American Contribution to the Second International Conference on Permafrost, pp 400-409. Yakutsk, U.S.S.R.

Suleiman, M.T., Sritharan, S., White, D.J., (2006). "Cyclic Lateal Load Response of Bridge Column-Foundation-Soil Systems in Freezing Condition." Journal of Structural Engineering, 132(11) 1745-1754.

US Army Core of Engineers (USACE), (1987) "Departments of the Army and the Air Force Technical Manual." *Concrete Floors Slabs on Grade Subjected to Heavy Loads* "TM 5-809-12" 4-2.

U.S. Army Corps of Engineers (USACE), Permafrost Division (1950). "Investigation of military construction in Arctic and Subarctic regions 1948-1950"; Main report, and appendix III – Design and construction studies in at Fairbanks research area. ACFEL Tech. Rep. 28

U.S. Department of Transportation Federal Highway Administration (FHWA), "Recommendations for Seismic Performance Testing of Bridge Piers." first edition draft, December 2004, Mclean Vermont.

Yang, Z., Xiong, F., Xu, G., Hulsey, J. L., Marx, E. E., (2008). "Seasonal Freezing Effects on the Lateral Behavior of Steel Pipe Piles" Proc. 14th World Conference on Earthquake Engineering, Beijing, China,

Yuanlin Zhu., Carbeee David. L. (1984). "Uniaxial Compressive Strength of Frozen Silt under Constant Deformation Rates." US Army Corps of Engineers Cold Regions Research and Engineering Laboratory. Hanover, New Hampshire 03755 (U.S.A.)

Yuanlin Zhu., Carbeee David. L. (1987). "Tensile Strength of frozen Silt." CRREL Report 87-15, US Army Corps of Engineers Cold Regions Research and Engineering Laboratory. Hanover, New Hampshire (U.S.A.)

Vaziri, H., Han, Y., (1991). "Full-Scale Field Studies of the Dynamic Response of Piles Embedded in Partially Frozen Soils." *Canadian Geotechnical Journal*, 28(5), pp708-718.

Vesic, A. S., (1961). "Beams on Elastic Subgrade and the Winkler Hypothesis", Proceedings of, 5th International Conference on Soil Mechanics and Foundation Enginering, Vol. 1, Paris, 845-850

LPILE Plus for Windows, Version 5.0 (5.0.39)

Analysis of Individual Piles and Drilled Shafts
Subjected to Lateral Loading Using the p-y Method

This program is licensed to:

Jacob Horazdovsky
University of Alaska Fairbanks

Path to file locations: C:\Documents and Settings\Jakey\My Documents\Research\Lpile\New Analysis\Winter Moment Line up\Final Analysis\
Name of input data file: Final Analysis 05052010.lpd
Name of output file: Final Analysis 05052010.lpo
Name of plot output file: Final Analysis 05052010.lpp
Name of runtime file: Final Analysis 05052010.lpr

Time and Date of Analysis

Date: May 5, 2010 Time: 23:26:43

Problem Title

16 inch test pile in Silt

Program Options

Units Used in Computations - US Customary Units: Inches, Pounds

Basic Program Options:

Analysis Type 3:
- Computation of Nonlinear Bending Stiffness and Ultimate Bending Moment Capacity with Pile Response Computed Using Nonlinear EI

Computation Options:
- User-specified p-y curves used in analysis
- Analysis does not use p-y multipliers (individual pile or shaft action only)
- Analysis assumes no shear resistance at pile tip
- Analysis for fixed-length pile or shaft only
- Analysis includes computation of foundation stiffness matrix elements
- Output pile response for full length of pile
- Analysis assumes no soil movements acting on pile
- Additional p-y curves computed at specified depths

Solution Control Parameters:
- Number of pile increments = 276
- Maximum number of iterations allowed = 100
- Deflection tolerance for convergence = 1.0000E-05 in
- Maximum allowable deflection = 1.0000E+02 in

Printing Options:
- Values of pile-head deflection, bending moment, shear force, and soil reaction are printed for full length of pile.
- Printing Increment (spacing of output points) = 1

Pile Structural Properties and Geometry

Pile Length = 276.00 in

Depth of ground surface below top of pile = 40.00 in

Slope angle of ground surface = 0.00 deg.

Structural properties of pile defined using 2 points

Point	Depth X in	Pile Diameter in	Moment of Inertia in**4	Pile Area Sq.in	Modulus of Elasticity lbs/Sq.in
1	0.0000	16.00000000	963.0000	201.0000	29000000.
2	300.0000	16.00000000	963.0000	201.0000	29000000.

Please note that because this analysis makes computations of ultimate moment capacity and pile response using nonlinear bending stiffness that the above values of moment of inertia and modulus of are not used for any computations other than total stress due to combined axial loading and bending.

Soil and Rock Layering Information

The soil profile is modelled using 3 layers

Layer 1 is modelled using user-specified p-y curves
Distance from top of pile to top of layer = 40.000 in
Distance from top of pile to bottom of layer = 130.000 in

Layer 2 is modelled using user-specified p-y curves
Distance from top of pile to top of layer = 130.000 in
Distance from top of pile to bottom of layer = 132.000 in

Layer 3 is modelled using user-specified p-y curves
Distance from top of pile to top of layer = 132.000 in
Distance from top of pile to bottom of layer = 276.000 in

(Depth of lowest layer extends 0.00 in below pile tip)

Effective Unit Weight of Soil vs. Depth

Effective unit weight of soil with depth defined using 6 points

Point No.	Depth X in	Eff. Unit Weight lbs/in**3
1	40.00	0.05300
2	130.00	0.05300
3	130.00	0.05300
4	132.00	0.05300
5	132.00	0.05300
6	276.00	0.05300

Shear Strength of Soils

Shear strength parameters with depth defined using 0 points

Point No.	Depth X in	Cohesion c lbs/in**2	Angle of Friction Deg.	E50 or k_rm	RQD %

Notes:

(1) Cohesion = uniaxial compressive strength for rock materials.
(2) Values of E50 are reported for clay strata.
(3) Default values will be generated for E50 when input values are 0.
(4) RQD and k_rm are reported only for weak rock strata.

User-specified p-y Curves

User-specified p-y curves defined using 6 curves.

User-specified curve number 1 at depth =   40.000in

Point No.	y in	p, lbs/in
1	-48.0000	-15000.000
2	-1.0000	-30000.000
3	-0.1000	-25000.000
4	-0.0500	-15000.000
5	-0.0090	-10000.000
6	0.0000	0.000
7	0.0090	10000.000
8	0.0500	15000.000
9	0.1000	25000.000
10	1.0000	30000.000
11	48.0000	15000.000

User-specified curve number 2 at depth = 130.000in

Point No.	y in	p, lbs/in
1	-48.0000	-15000.000
2	-1.0000	-30000.000
3	-0.1000	-25000.000
4	-0.0500	-15000.000
5	-0.0250	-10000.000
6	0.0000	0.000
7	0.0250	10000.000
8	0.1000	15000.000
9	0.5000	25000.000
10	1.0000	30000.000
11	48.0000	15000.000

User-specified curve number 3 at depth = 130.000in

Point No.	y in	p, lbs/in
1	-48.0000	-15000.000
2	-4.0000	-15000.000
3	-2.0000	-15000.000
4	-1.0000	-15000.000
5	0.0000	0.000

6	1.0000	15000.000
7	2.0000	15000.000
8	4.0000	15000.000
9	48.0000	15000.000

User-specified curve number 4 at depth = 132.000in

Point No.	y in	p, lbs/in
1	-48.0000	-4000.000
2	-4.0000	-4000.000
3	-2.0000	-3200.000
4	-1.0000	-1600.000
5	0.0000	0.000
6	1.0000	1600.000
7	2.0000	3200.000
8	4.0000	4000.000
9	48.0000	4000.000

User-specified curve number 5 at depth = 132.000in

Point No.	y in	p, lbs/in
1	-48.0000	-100.000
2	-0.4000	350.000
3	-0.2000	275.000
4	0.0000	0.000
5	0.2000	275.000
6	0.4000	350.000
7	0.8600	375.000
8	1.5000	450.000
9	2.0000	575.000
10	2.5000	650.000
11	3.0000	600.000
12	48.0000	800.000

User-specified curve number 6 at depth = 276.000in

Point No.	y in	p, lbs/in

1	-48.0000	-1600.000
2	-4.0000	-800.000
3	-2.0000	-800.000
4	-0.4000	-350.000
5	0.0000	0.000
6	0.4000	350.000
7	2.0000	800.000
8	4.0000	800.000
9	48.0000	1600.000

Loading Type

Static loading criteria was used for computation of p-y curves.

Pile-head Loading and Pile-head Fixity Conditions

Number of loads specified = 1

Load Case Number 1

Pile-head boundary conditions are Shear and Moment (BC Type 1)
Shear force at pile head = 62500.000 lbs
Bending moment at pile head = 0.000 in-lbs
Axial load at pile head = 0.000 lbs

(Zero moment at pile head for this load indicates a free-head condition)

Output of p-y Curves at Specified Depths

---

p-y curves are generated and printed for verification at 18 depths.

Depth No.	Depth Below Pile Head in	Depth Below Ground Surface in
1	40.000	0.000
2	51.000	11.000
3	63.000	23.000
4	75.000	35.000
5	87.000	47.000
6	99.000	59.000
7	111.000	71.000
8	123.000	83.000
9	135.000	95.000
10	147.000	107.000
11	159.000	119.000
12	171.000	131.000
13	183.000	143.000
14	195.000	155.000
15	207.000	167.000
16	219.000	179.000
17	236.000	196.000
18	276.000	236.000

Depth of ground surface below top of pile = 40.00 in

Computations of Nominal Moment Capacity and Nonlinear Bending Stiffness

---

Number of sections = 1

Pile Section No. 1

The sectional shape is a circular shaft with steel casing.

Outside Diameter	=	16.0000	in
Wall thickness of steel shell	=	0.3750	in
Cross-sectional area of shell	=	18.40777	in**2
Moment of inertia of steel shell	=	5.62084E+02	in**4

Material Properties:

Compressive Strength of Concrete	=	5.176	kip/in**2
Yield Stress of Reinforcement	=	77.	kip/in**2
Steel shell or core yield stress	=	57.	kip/in**2
Modulus of Elasticity of Reinforcement	=	29000.	kip/in**2
Cover Thickness (edge to bar center)	=	1.375	in
Number of Reinforcing Bars	=	8	
Area of Single Bar	=	0.44000	in**2
Number of Rows of Reinforcing Bars	=	5	
Area of Steel	=	21.928	in**2
Area of Shaft	=	201.062	in**2
Percentage of Steel Reinforcement	=	10.906	percent
Unfactored Axial Squash Load Capacity	=	2111.22	kip

Distribution and Area of Steel Reinforcement

Row Number	Area of Reinforcement in**2	Distance to Centroidal Axis in
1	0.440	6.250
2	0.880	4.419
3	0.880	0.000
4	0.880	-4.419
5	0.440	-6.250

Axial Thrust Force = 0.00 lbs

Bending Moment in-lbs	Bending Stiffness lb-in2	Bending Curvature rad/in	Maximum Strain in/in	Neutral Axis Position inches	Max. Concrete Stress psi	Max. Steel Stress psi
73488.34130	2.939534E+10	0.00000250	0.00001906	7.99999809	78.24821663	453.12514

		Final Anal
146809.23293	2.936185E+10	0.00000500
219962.67489	2.932836E+10	0.00000750
292948.66717	2.929487E+10	0.00001000
365767.20978	2.926138E+10	0.00001250
438418.30271	2.922789E+10	0.00001500
438418.30271	2.505247E+10	0.00001750
444885.00564	2.224425E+10	0.00002000
500284.22807	2.223485E+10	0.00002250
555636.47200	2.222546E+10	0.00002500
610941.73742	2.221606E+10	0.00002750
666200.02434	2.220667E+10	0.00003000
721411.33275	2.219727E+10	0.00003250
776575.66265	2.218788E+10	0.00003500
831693.01405	2.217848E+10	0.00003750
886763.38695	2.216908E+10	0.00004000
941786.78134	2.215969E+10	0.00004250
996763.19723	2.215029E+10	0.00004500
1051693.	2.214090E+10	0.00004750
1106575.	2.213150E+10	0.00005000
1161411.	2.212211E+10	0.00005250
1216199.	2.211271E+10	0.00005500
1270941.	2.210331E+10	0.00005750
1325635.	2.209392E+10	0.00006000
1380283.	2.208452E+10	0.00006250
1434883.	2.207513E+10	0.00006500
1489437.	2.206573E+10	0.00006750
1543944.	2.205634E+10	0.00007000
1598403.	2.204694E+10	0.00007250
1652816.	2.203754E+10	0.00007500
1707182.	2.202815E+10	0.00007750
1761500.	2.201875E+10	0.00008000
1815772.	2.200936E+10	0.00008250
1869997.	2.199996E+10	0.00008500
1924175.	2.199057E+10	0.00008750
1978305.	2.198117E+10	0.00009000
2032389.	2.197177E+10	0.00009250
2032389.	2.139357E+10	0.00009500
2069947.	2.123022E+10	0.00009750
2176422.	2.123338E+10	0.00010250
2282974.	2.123697E+10	0.00010750
2389616.	2.124103E+10	0.00011250
2495452.	2.123789E+10	0.00011750

0.00003812	7.99999809	155.79434	906.25028
0.00005719	7.99999809	232.63838	1359.37541
0.00007625	7.99999809	308.78032	1812.50055
0.00009531	7.99999809	384.22017	2265.62569
0.00011437	7.99999809	458.95793	2718.75083
0.00011010	6.66666603	441.97434	3848.54199
0.00012583	6.66666603	503.20412	4398.33370
0.00014156	6.66666603	563.95654	4948.12541
0.00015729	6.66666603	624.23162	5497.91713
0.00017302	6.66666603	684.02933	6047.70884
0.00018875	6.66666603	743.34970	6597.50055
0.00020448	6.66666603	802.19271	7147.29227
0.00022021	6.66666603	860.55837	7697.08398
0.00023594	6.66666603	918.44668	8246.87569
0.00025167	6.66666603	975.85763	8796.66740
0.00026740	6.66666603	1032.79123	9346.45912
0.00028312	6.66666603	1089.24748	9896.25083
0.00029885	6.66666603	1145.22637	10446.04254
0.00031458	6.66666603	1200.72791	10995.83426
0.00033031	6.66666603	1255.75209	11545.62597
0.00034604	6.66666603	1310.29893	12095.41768
0.00036177	6.66666603	1364.36841	12645.20939
0.00037750	6.66666603	1417.96053	13195.00111
0.00039323	6.66666603	1471.07531	13744.79282
0.00040896	6.66666603	1523.71273	14294.58453
0.00042469	6.66666603	1575.87279	14844.37624
0.00044042	6.66666603	1627.55551	15394.16796
0.00045615	6.66666603	1678.76087	15943.95967
0.00047187	6.66666603	1729.48888	16493.75138
0.00048760	6.66666603	1779.73953	17043.54310
0.00050333	6.66666603	1829.51283	17593.33481
0.00051906	6.66666603	1878.80878	18143.12652
0.00053479	6.66666603	1927.62737	18692.91823
0.00055052	6.66666603	1975.96861	19242.70995
0.00056625	6.66666603	2023.83250	19792.50166
0.00058198	6.66666603	2071.21904	20342.29337
0.00060561	6.74981880	2065.89786	20662.99920
0.00062183	6.75274849	2112.34448	21198.47865
0.00065433	6.75866890	2203.98385	22267.98170
0.00068689	6.76468086	2293.94733	23335.48241
0.00071953	6.77079201	2382.22864	24400.91608
0.00075200	6.77499962	2468.17395	25471.06380

		Final Anal
2599276.	2.121858E+10	0.00012250
2702908.	2.119928E+10	0.00012750
2806346.	2.117997E+10	0.00013250
2909591.	2.116066E+10	0.00013750
3012644.	2.114136E+10	0.00014250
3115503.	2.112205E+10	0.00014750
3228323.	2.116933E+10	0.00015250
3335205.	2.117590E+10	0.00015750
3442286.	2.118330E+10	0.00016250
3549602.	2.119166E+10	0.00016750
3657195.	2.120113E+10	0.00017250
3765118.	2.121193E+10	0.00017750
3873439.	2.122432E+10	0.00018250
3982257.	2.123870E+10	0.00018750
4091704.	2.125560E+10	0.00019250
4201970.	2.127580E+10	0.00019750
4313378.	2.130063E+10	0.00020250
4426505.	2.133256E+10	0.00020750
4542651.	2.137718E+10	0.00021250
4667019.	2.145756E+10	0.00021750
4822517.	2.167424E+10	0.00022250
4918186.	2.161840E+10	0.00022750
4918186.	2.115349E+10	0.00023250
4970472.	2.092830E+10	0.00023750
5025204.	2.072249E+10	0.00024250
5075235.	2.050600E+10	0.00024750
5125794.	2.030017E+10	0.00025250
5174179.	2.009390E+10	0.00025750
5242637.	1.997195E+10	0.00026250
5290265.	1.977669E+10	0.00026750
5489050.	2.014330E+10	0.00027250
5552475.	2.000892E+10	0.00027750
5614613.	1.987474E+10	0.00028250
5675931.	1.974237E+10	0.00028750
5736391.	1.961159E+10	0.00029250
5795823.	1.948176E+10	0.00029750
5906493.	1.920811E+10	0.00030750
6005771.	1.891581E+10	0.00031750
6005771.	1.833823E+10	0.00032750
6013916.	1.781901E+10	0.00033750
6047705.	1.740347E+10	0.00034750
6081969.	1.701250E+10	0.00035750

0.00078400	6.77499962	2550.97934	26554.93886
0.00081600	6.77499962	2631.97059	27638.81391
0.00084800	6.77499962	2711.14769	28722.68897
0.00088000	6.77499962	2788.51065	29806.56402
0.00091200	6.77499962	2864.05946	30890.43908
0.00094400	6.77499962	2937.79412	31974.31413
0.00097663	6.77913475	3104.07788	33039.90157
0.00100974	6.78603554	3177.05979	34091.65768
0.00104294	6.79309273	3248.12583	35140.67552
0.00107624	6.80032539	3317.26916	36186.79440
0.00110965	6.80775642	3384.48349	37229.82349
0.00114317	6.81541634	3449.76427	38269.51941
0.00117682	6.82334328	3513.10840	39305.58071
0.00121061	6.83159447	3574.51777	40337.58008
0.00124456	6.84024620	3633.99861	41364.95059
0.00127870	6.84940529	3691.56438	42386.90621
0.00131306	6.85926247	3747.25169	43402.10617
0.00134775	6.87016106	3801.13868	44408.18084
0.00138292	6.88287926	3853.42573	45399.88158
0.00141932	6.90060616	3905.01189	46356.30167
0.00145923	6.93333244	3958.65448	47210.79741
0.00149202	6.93333244	4000.39826	48271.71421
0.00151195	6.87799644	4024.69117	49705.73397
0.00153898	6.85492516	4056.48401	50933.57799
0.00156606	6.83298302	4086.91597	52160.17193
0.00159247	6.80924034	4115.23597	53406.05245
0.00161897	6.78676796	4142.29528	54649.51662
0.00164800	6.77499962	4100.97789	55819.56535
0.00168000	6.77499962	4132.98720	56903.44040
0.00170663	6.75493050	4158.00620	58143.00168
0.00171448	6.66666603	4228.56521	59927.29669
0.00174594	6.66666603	4253.16735	61026.88012
0.00177740	6.66666603	4275.86008	62126.46354
0.00180885	6.66666603	4296.64340	63226.04697
0.00184031	6.66666603	4315.51731	64325.63039
0.00187177	6.66666603	4332.48180	65425.21382
0.00193469	6.66666603	4360.68254	67624.38067
0.00199760	6.66666603	4381.24563	69823.54752
0.00203932	6.60193443	4390.65335	72637.50272
0.00208739	6.55986977	4397.35063	75267.14966
0.00213734	6.52562904	4398.96770	76531.00000
0.00219267	6.50833321	4398.14698	76531.00000

6134797.	1.669332E+10	0.00036750	0.00225215	6.50329018	4393.36205	76531.00000
6163223.	1.632642E+10	0.00037750	0.00230323	6.47628212	4398.43669	76531.00000
6191288.	1.597752E+10	0.00038750	0.00235503	6.45249748	4395.01503	76531.00000
6407351.	1.611912E+10	0.00039750	0.00239494	6.39999962	4396.09323	76531.00000
6452076.	1.583331E+10	0.00040750	0.00245519	6.39999962	4399.53707	76531.00000
6494913.	1.555668E+10	0.00041750	0.00251544	6.39999962	4395.18445	76531.00000
6535555.	1.528785E+10	0.00042750	0.00257569	6.39999962	4399.28321	76531.00000
6573529.	1.502521E+10	0.00043750	0.00263594	6.39999962	4392.51038	76531.00000
6604839.	1.475942E+10	0.00044750	0.00269619	6.39999962	4398.14227	76531.00000
6632281.	1.449679E+10	0.00045750	0.00275644	6.39999962	4396.46524	76531.00000
6658795.	1.424341E+10	0.00046750	0.00281669	6.39999962	4394.82805	76531.00000
6684975.	1.399995E+10	0.00047750	0.00287694	6.39999962	4398.94009	76531.00000
6708069.	1.376014E+10	0.00048750	0.00293719	6.39999962	4392.52047	76531.00000
6708069.	1.348356E+10	0.00049750	0.00296684	6.33848763	4389.61712	76531.00000
6708069.	1.321787E+10	0.00050750	0.00300894	6.30394554	4393.66361	76531.00000
6708069.	1.296245E+10	0.00051750	0.00305367	6.27581596	4396.93844	76531.00000
6708069.	1.271672E+10	0.00052750	0.00309962	6.25105095	4398.97818	76531.00000
6708069.	1.248013E+10	0.00053750	0.00315333	6.24166679	4395.84877	76531.00000
6708069.	1.225218E+10	0.00054750	0.00321200	6.24166679	4390.49955	76531.00000
6708069.	1.203241E+10	0.00055750	0.00326514	6.23176003	4395.46888	76531.00000
6708069.	1.182039E+10	0.00056750	0.00331290	6.21271706	4398.12089	76531.00000
6708069.	1.161570E+10	0.00057750	0.00336110	6.19509315	4399.45093	76531.00000
6779262.	1.153917E+10	0.00058750	0.00338302	6.13333321	4399.45886	76531.00000
6794358.	1.137131E+10	0.00059750	0.00344060	6.13333321	4390.15356	76531.00000
6806563.	1.120422E+10	0.00060750	0.00349819	6.13333321	4389.47255	76531.00000
6817031.	1.103973E+10	0.00061750	0.00355577	6.13333321	4395.00799	76531.00000
6827354.	1.088024E+10	0.00062750	0.00361335	6.13333321	4398.38248	76531.00000
6837530.	1.072554E+10	0.00063750	0.00367094	6.13333321	4399.59603	76531.00000
6846867.	1.057431E+10	0.00064750	0.00372852	6.13333321	4387.26073	76531.00000
6855248.	1.042623E+10	0.00065750	0.00378610	6.13333321	4387.67937	76531.00000
6855248.	1.027003E+10	0.00066750	0.00384369	6.13333321	4393.36840	76531.00000

Unfactored (Nominal) Moment Capacity at Concrete Strain of 0.003 = 6708.06898 in-kip

p-y Curve Computed by Interpolation from User-input Curves

Soil Layer Number = 1
Depth below ground surface = 0.000 in
Depth below pile head = 40.000 in

p-multiplier = 1.00000
y-multiplier = 1.00000

y, in	p, lbs/in
0.0000	0.000
0.0010	1111.111
0.1000	25000.000
0.2000	25555.556
0.3000	26111.111
0.4000	26666.667
0.5000	27222.222
0.6000	27777.778
0.7000	28333.333
0.8000	28888.889
0.9000	29444.445
1.0000	30000.000
1.1000	29968.085
1.2000	29936.170
3.2000	29297.872
6.0000	28404.255
8.0000	27765.957

p-y Curve Computed by Interpolation from User-input Curves

Soil Layer Number = 1
Depth below ground surface = 11.000 in
Depth below pile head = 51.000 in
p-multiplier = 1.00000
y-multiplier = 1.00000

y, in	p, lbs/in
0.0000	0.000
0.0010	1024.198
0.1000	23777.778
0.2000	24570.988
0.3000	25364.198
0.4000	26157.407
0.5000	26950.617
0.6000	27560.494

0.7000	28170.370
0.8000	28780.247
0.9000	29390.124
1.0000	30000.000
1.1000	29968.085
1.2000	29936.170
3.2000	29297.872
6.0000	28404.255
8.0000	27765.957

p-y Curve Computed by Interpolation from User-input Curves

Soil Layer Number = 1
Depth below ground surface = 23.000 in
Depth below pile head = 63.000 in
p-multiplier = 1.00000
y-multiplier = 1.00000

y, in	p, lbs/in
0.0000	0.000
0.0010	929.383
0.1000	22444.444
0.2000	23496.914
0.3000	24549.383
0.4000	25601.852
0.5000	26654.321
0.6000	27323.457
0.7000	27992.593
0.8000	28661.728
0.9000	29330.864
1.0000	30000.000
1.1000	29968.085
1.2000	29936.170
3.2000	29297.872
6.0000	28404.255
8.0000	27765.957

p-y Curve Computed by Interpolation from User-input Curves

Soil Layer Number = 1
Depth below ground surface = 35.000 in
Depth below pile head = 75.000 in
p-multiplier = 1.00000
y-multiplier = 1.00000

y, in	p, lbs/in
0.0000	0.000
0.0010	834.568
0.1000	21111.111
0.2000	22422.840
0.3000	23734.568
0.4000	25046.296
0.5000	26358.025
0.6000	27086.420
0.7000	27814.815
0.8000	28543.210
0.9000	29271.605
1.0000	30000.000
1.1000	29968.085
1.2000	29936.170
3.2000	29297.872
6.0000	28404.255
8.0000	27765.957

p-y Curve Computed by Interpolation from User-input Curves

Soil Layer Number = 1
Depth below ground surface = 47.000 in
Depth below pile head = 87.000 in
p-multiplier = 1.00000
y-multiplier = 1.00000

y, in	p, lbs/in
0.0000	0.000
0.0010	739.753
0.1000	19777.778
0.2000	21348.765
0.3000	22919.753

0.4000	24490.741
0.5000	26061.728
0.6000	26849.383
0.7000	27637.037
0.8000	28424.691
0.9000	29212.346
1.0000	30000.000
1.1000	29968.085
1.2000	29936.170
3.2000	29297.872
6.0000	28404.255
8.0000	27765.957

p-y Curve Computed by Interpolation from User-input Curves

Soil Layer Number = 1
Depth below ground surface = 59.000 in
Depth below pile head = 99.000 in
p-multiplier = 1.00000
y-multiplier = 1.00000

y, in	p, lbs/in
0.0000	0.000
0.0010	644.938
0.1000	18444.444
0.2000	20274.691
0.3000	22104.938
0.4000	23935.185
0.5000	25765.432
0.6000	26612.346
0.7000	27459.259
0.8000	28306.173
0.9000	29153.087
1.0000	30000.000
1.1000	29968.085
1.2000	29936.170
3.2000	29297.872
6.0000	28404.255
8.0000	27765.957

p-y Curve Computed by Interpolation from User-input Curves

Soil Layer Number = 1
Depth below ground surface = 71.000 in
Depth below pile head = 111.000 in
p-multiplier = 1.00000
y-multiplier = 1.00000

y, in	p, lbs/in
0.0000	0.000
0.0010	550.123
0.1000	17111.111
0.2000	19200.617
0.3000	21290.124
0.4000	23379.630
0.5000	25469.136
0.6000	26375.309
0.7000	27281.482
0.8000	28187.654
0.9000	29093.827
1.0000	30000.000
1.1000	29968.085
1.2000	29936.170
3.2000	29297.872
6.0000	28404.255
8.0000	27765.957

p-y Curve Computed by Interpolation from User-input Curves

Soil Layer Number = 1
Depth below ground surface = 83.000 in
Depth below pile head = 123.000 in
p-multiplier = 1.00000
y-multiplier = 1.00000

y, in	p, lbs/in
0.0000	0.000
0.0010	455.309

0.1000	15777.778
0.2000	18126.543
0.3000	20475.309
0.4000	22824.074
0.5000	25172.840
0.6000	26138.272
0.7000	27103.704
0.8000	28069.136
0.9000	29034.568
1.0000	30000.000
1.1000	29968.085
1.2000	29936.170
3.2000	29297.872
6.0000	28404.255
8.0000	27765.957

p-y Curve Computed by Interpolation from User-input Curves

Soil Layer Number	=	3
Depth below ground surface	=	95.000 in
Depth below pile head	=	135.000 in
p-multiplier	=	1.00000
y-multiplier	=	1.00000

y, in	p, lbs/in
0.0000	0.000
0.0010	1.365
0.1000	136.458
0.2000	272.917
0.3000	311.458
0.4000	350.000
0.5000	355.907
0.6000	361.815
0.7000	367.722
0.8000	373.630
0.9000	381.999
1.0000	394.059

1.1000	406.120
1.2000	418.180
3.2000	605.037
6.0000	617.980
8.0000	627.441

p-y Curve Computed by Interpolation from User-input Curves

Soil Layer Number = 3
Depth below ground surface = 107.000 in
Depth below pile head = 147.000 in
p-multiplier = 1.00000
y-multiplier = 1.00000

y, in	p, lbs/in
0.0000	0.000
0.0010	1.323
0.1000	132.292
0.2000	264.583
0.3000	307.292
0.4000	350.000
0.5000	357.798
0.6000	365.597
0.7000	373.395
0.8000	381.193
0.9000	391.243
1.0000	404.671
1.1000	418.099
1.2000	431.527
3.2000	621.630
6.0000	636.566
8.0000	648.316

p-y Curve Computed by Interpolation from User-input Curves

Soil Layer Number = 3
Depth below ground surface = 119.000 in
Depth below pile head = 159.000 in
p-multiplier = 1.00000

y-multiplier = 1.00000

y, in	p, lbs/in
0.0000	0.000
0.0010	1.281
0.1000	128.125
0.2000	256.250
0.3000	303.125
0.4000	350.000
0.5000	359.689
0.6000	369.378
0.7000	379.068
0.8000	388.757
0.9000	400.488
1.0000	415.283
1.1000	430.078
1.2000	444.873
3.2000	638.222
6.0000	655.152
8.0000	669.192

p-y Curve Computed by Interpolation from User-input Curves

Soil Layer Number = 3
Depth below ground surface = 131.000 in
Depth below pile head = 171.000 in
p-multiplier = 1.00000
y-multiplier = 1.00000

y, in	p, lbs/in
0.0000	0.000
0.0010	1.240
0.1000	123.958
0.2000	247.917
0.3000	298.958
0.4000	350.000
0.5000	361.580
0.6000	373.160
0.7000	384.740

0.8000	396.320
0.9000	409.733
1.0000	425.895
1.1000	442.057
1.2000	458.219
3.2000	654.815
6.0000	673.737
8.0000	690.067

p-y Curve Computed by Interpolation from User-input Curves

Soil Layer Number = 3
Depth below ground surface = 143.000 in
Depth below pile head = 183.000 in
p-multiplier = 1.00000
y-multiplier = 1.00000

y, in	p, lbs/in
0.0000	0.000
0.0010	1.198
0.1000	119.792
0.2000	239.583
0.3000	294.792
0.4000	350.000
0.5000	363.471
0.6000	376.942
0.7000	390.413
0.8000	403.884
0.9000	418.978
1.0000	436.507
1.1000	454.036
1.2000	471.566
3.2000	671.407
6.0000	692.323
8.0000	710.943

p-y Curve Computed by Interpolation from User-input Curves

Soil Layer Number = 3

Depth below ground surface = 155.000 in
Depth below pile head = 195.000 in
p-multiplier = 1.00000
y-multiplier = 1.00000

y, in	p, lbs/in
0.0000	0.000
0.0010	1.156
0.1000	115.625
0.2000	231.250
0.3000	290.625
0.4000	350.000
0.5000	365.362
0.6000	380.724
0.7000	396.085
0.8000	411.447
0.9000	428.223
1.0000	447.119
1.1000	466.016
1.2000	484.912
3.2000	688.000
6.0000	710.909
8.0000	731.818

p-y Curve Computed by Interpolation from User-input Curves

Soil Layer Number = 3
Depth below ground surface = 167.000 in
Depth below pile head = 207.000 in
p-multiplier = 1.00000
y-multiplier = 1.00000

y, in	p, lbs/in
0.0000	0.000
0.0010	1.115
0.1000	111.458
0.2000	222.917
0.3000	286.458
0.4000	350.000

0.5000	367.253
0.6000	384.505
0.7000	401.758
0.8000	419.010
0.9000	437.467
1.0000	457.731
1.1000	477.995
1.2000	498.258
3.2000	704.593
6.0000	729.495
8.0000	752.694

p-y Curve Computed by Interpolation from User-input Curves

Soil Layer Number	=	3
Depth below ground surface	=	179.000 in
Depth below pile head	=	219.000 in
p-multiplier	=	1.00000
y-multiplier	=	1.00000

y, in	p, lbs/in
0.0000	0.000
0.0010	1.073
0.1000	107.292
0.2000	214.583
0.3000	282.292
0.4000	350.000
0.5000	369.143
0.6000	388.287
0.7000	407.430
0.8000	426.574
0.9000	446.712
1.0000	468.343
1.1000	489.974
1.2000	511.605
3.2000	721.185
6.0000	748.081
8.0000	773.569

p-y Curve Computed by Interpolation from User-input Curves

Soil Layer Number = 3
Depth below ground surface = 196.000 in
Depth below pile head = 236.000 in
p-multiplier = 1.00000
y-multiplier = 1.00000

y, in	p, lbs/in
0.0000	0.000
0.0010	1.014
0.1000	101.389
0.2000	202.778
0.3000	276.389
0.4000	350.000
0.5000	371.822
0.6000	393.644
0.7000	415.466
0.8000	437.289
0.9000	459.809
1.0000	483.377
1.1000	506.944
1.2000	530.512
3.2000	744.691
6.0000	774.411
8.0000	803.143

p-y Curve Computed by Interpolation from User-input Curves

Soil Layer Number = 3
Depth below ground surface = 236.000 in
Depth below pile head = 276.000 in
p-multiplier = 1.00000
y-multiplier = 1.00000

y, in	p, lbs/in
0.0000	0.000
0.0010	0.875
0.1000	87.500

0.2000	175.000
0.3000	262.500
0.4000	350.000
0.5000	378.125
0.6000	406.250
0.7000	434.375
0.8000	462.500
0.9000	490.625
1.0000	518.750
1.1000	546.875
1.2000	575.000
3.2000	800.000
6.0000	836.364
8.0000	872.727

Computed Values of Load Distribution and Deflection
for Lateral Loading for Load Case Number 1

Pile-head boundary conditions are Shear and Moment (BC Type 1)
Specified shear force at pile head = 62500.000 lbs
Specified moment at pile head = 0.000 in-lbs
Specified axial load at pile head = 0.000 lbs

(Zero moment for this load indicates free-head conditions)

Depth X in	Deflect. y in	Moment M lbs-in	Shear V lbs	Slope S Rad.	Total Stress lbs/in**2	Flx. Rig. EI lbs-in**2	Soil Res. p lbs/in	Es*h F/L
0.000	0.206558	9.79E-06	62500.	-0.005095	8.13E-08	2.94E+10	0.000	0.000
1.000	0.201463	62500.	62500.	-0.005094	519.211	2.94E+10	0.000	0.000
2.000	0.196370	1.25E+05	62500.	-0.005091	1038.422	2.94E+10	0.000	0.000
3.000	0.191281	1.88E+05	62500.	-0.005085	1557.632	2.93E+10	0.000	0.000
4.000	0.186199	2.50E+05	62500.	-0.005078	2076.843	2.93E+10	0.000	0.000
5.000	0.181125	3.13E+05	62500.	-0.005068	2596.054	2.93E+10	0.000	0.000
6.000	0.176062	3.75E+05	62500.	-0.005057	3115.265	2.93E+10	0.000	0.000

				Final Analysis
7.000	0.171012	4.38E+05	62500.	-0.005043
8.000	0.165977	5.00E+05	62500.	-0.005024
9.000	0.160965	5.63E+05	62500.	-0.005000
10.000	0.155977	6.25E+05	62500.	-0.004973
11.000	0.151018	6.88E+05	62500.	-0.004944
12.000	0.146090	7.50E+05	62500.	-0.004911
13.000	0.141196	8.12E+05	62500.	-0.004876
14.000	0.136338	8.75E+05	62500.	-0.004838
15.000	0.131520	9.37E+05	62500.	-0.004797
16.000	0.126744	1.00E+06	62500.	-0.004753
17.000	0.122014	1.06E+06	62500.	-0.004707
18.000	0.117331	1.12E+06	62500.	-0.004657
19.000	0.112699	1.19E+06	62500.	-0.004605
20.000	0.108121	1.25E+06	62500.	-0.004550
21.000	0.103599	1.31E+06	62500.	-0.004492
22.000	0.099137	1.37E+06	62500.	-0.004431
23.000	0.094737	1.44E+06	62500.	-0.004367
24.000	0.090402	1.50E+06	62500.	-0.004301
25.000	0.086135	1.56E+06	62500.	-0.004231
26.000	0.081939	1.62E+06	62500.	-0.004159
27.000	0.077817	1.69E+06	62500.	-0.004084
28.000	0.073771	1.75E+06	62500.	-0.004006
29.000	0.069805	1.81E+06	62500.	-0.003925
30.000	0.065921	1.87E+06	62500.	-0.003841
31.000	0.062122	1.94E+06	62500.	-0.003755
32.000	0.058411	2.00E+06	62500.	-0.003665
33.000	0.054792	2.06E+06	62500.	-0.003571
34.000	0.051269	2.12E+06	62500.	-0.003473
35.000	0.047847	2.19E+06	62500.	-0.003371
36.000	0.044527	2.25E+06	62500.	-0.003266
37.000	0.041314	2.31E+06	62500.	-0.003159
38.000	0.038209	2.37E+06	62500.	-0.003049
39.000	0.035216	2.44E+06	62500.	-0.002935
40.000	0.032338	2.50E+06	56077.	-0.002819
41.000	0.029578	2.55E+06	43412.	-0.002700
42.000	0.026938	2.59E+06	31099.	-0.002579
43.000	0.024420	2.61E+06	19124.	-0.002457
44.000	0.022024	2.63E+06	7487.374	-0.002333
45.000	0.019753	2.63E+06	-3805.298	-0.002210
46.000	0.017605	2.62E+06	-14757.	-0.002086
47.000	0.015581	2.60E+06	-25371.	-0.001963
48.000	0.013679	2.57E+06	-35652.	-0.001841

3634.476	2.87E+10	0.000	0.000
4153.686	2.22E+10	0.000	0.000
4672.897	2.22E+10	0.000	0.000
5192.108	2.22E+10	0.000	0.000
5711.319	2.22E+10	0.000	0.000
6230.530	2.22E+10	0.000	0.000
6749.740	2.22E+10	0.000	0.000
7268.951	2.22E+10	0.000	0.000
7788.162	2.22E+10	0.000	0.000
8307.373	2.21E+10	0.000	0.000
8826.584	2.21E+10	0.000	0.000
9345.794	2.21E+10	0.000	0.000
9865.005	2.21E+10	0.000	0.000
10384.	2.21E+10	0.000	0.000
10903.	2.21E+10	0.000	0.000
11423.	2.21E+10	0.000	0.000
11942.	2.21E+10	0.000	0.000
12461.	2.21E+10	0.000	0.000
12980.	2.21E+10	0.000	0.000
13499.	2.20E+10	0.000	0.000
14019.	2.20E+10	0.000	0.000
14538.	2.20E+10	0.000	0.000
15057.	2.20E+10	0.000	0.000
15576.	2.20E+10	0.000	0.000
16096.	2.20E+10	0.000	0.000
16615.	2.20E+10	0.000	0.000
17134.	2.13E+10	0.000	0.000
17653.	2.12E+10	0.000	0.000
18172.	2.12E+10	0.000	0.000
18692.	2.12E+10	0.000	0.000
19211.	2.12E+10	0.000	0.000
19730.	2.12E+10	0.000	0.000
20249.	2.12E+10	0.000	0.000
20768.	2.12E+10	-12846.	3.97E+05
21181.	2.12E+10	-12484.	4.22E+05
21490.	2.12E+10	-12141.	4.51E+05
21698.	2.12E+10	-11809.	4.84E+05
21807.	2.12E+10	-11464.	5.21E+05
21822.	2.12E+10	-11121.	5.63E+05
21744.	2.12E+10	-10782.	6.12E+05
21577.	2.12E+10	-10446.	6.70E+05
21323.	2.12E+10	-10117.	7.40E+05

49.000	0.011898	2.53E+06	-45607.	-0.001721	20985.	2.12E+10	-9793.154	8.23E+05
50.000	0.010236	2.48E+06	-55242.	-0.001604	20565.	2.12E+10	-9476.913	9.26E+05
51.000	0.008691	2.42E+06	-64431.	-0.001489	20067.	2.12E+10	-8901.133	1.02E+06
52.000	0.007259	2.35E+06	-72570.	-0.001376	19494.	2.12E+10	-7377.468	1.02E+06
53.000	0.005938	2.27E+06	-79253.	-0.001268	18861.	2.12E+10	-5987.840	1.01E+06
54.000	0.004724	2.19E+06	-84610.	-0.001163	18178.	2.12E+10	-4726.052	1.00E+06
55.000	0.003612	2.10E+06	-88766.	-0.001062	17455.	2.12E+10	-3585.738	9.93E+05
56.000	0.002600	2.01E+06	-91839.	-0.000967	16703.	2.20E+10	-2560.436	9.85E+05
57.000	0.001679	1.92E+06	-93939.	-0.000877	15929.	2.20E+10	-1640.500	9.77E+05
58.000	0.000846	1.82E+06	-95169.	-0.000792	15142.	2.20E+10	-819.593	9.69E+05
59.000	9.52E-05	1.73E+06	-95625.	-0.000712	14348.	2.20E+10	-91.448	9.61E+05
60.000	-0.000577	1.63E+06	-95396.	-0.000635	13553.	2.20E+10	550.093	9.53E+05
61.000	-0.001175	1.54E+06	-94565.	-0.000563	12763.	2.21E+10	1111.047	9.45E+05
62.000	-0.001704	1.44E+06	-93211.	-0.000496	11982.	2.21E+10	1597.263	9.37E+05
63.000	-0.002167	1.35E+06	-91405.	-0.000433	11214.	2.21E+10	2014.396	9.29E+05
64.000	-0.002570	1.26E+06	-89214.	-0.000374	10463.	2.21E+10	2367.895	9.21E+05
65.000	-0.002915	1.17E+06	-86698.	-0.000319	9732.170	2.21E+10	2662.982	9.14E+05
66.000	-0.003207	1.09E+06	-83915.	-0.000268	9022.995	2.21E+10	2904.649	9.06E+05
67.000	-0.003450	1.00E+06	-80913.	-0.000221	8337.950	2.21E+10	3097.643	8.98E+05
68.000	-0.003648	9.24E+05	-77741.	-0.000177	7678.639	2.22E+10	3246.470	8.90E+05
69.000	-0.003804	8.48E+05	-74440.	-0.000137	7046.297	2.22E+10	3355.386	8.82E+05
70.000	-0.003922	7.75E+05	-71049.	-0.000100	6441.830	2.22E+10	3428.402	8.74E+05
71.000	-0.004005	7.06E+05	-67600.	-6.71E-05	5865.843	2.22E+10	3469.282	8.66E+05
72.000	-0.004056	6.40E+05	-64124.	-3.68E-05	5318.678	2.22E+10	3481.553	8.58E+05
73.000	-0.004079	5.78E+05	-60649.	-9.34E-06	4800.434	2.22E+10	3468.503	8.50E+05
74.000	-0.004075	5.19E+05	-57198.	1.53E-05	4311.005	2.22E+10	3433.192	8.42E+05
75.000	-0.004048	4.63E+05	-53793.	3.74E-05	3850.097	2.22E+10	3378.457	8.35E+05
76.000	-0.004000	4.11E+05	-50450.	5.49E-05	3417.255	2.92E+10	3306.924	8.27E+05
77.000	-0.003938	3.63E+05	-47184.	6.81E-05	3011.885	2.93E+10	3224.627	8.19E+05
78.000	-0.003864	3.17E+05	-44005.	7.97E-05	2633.303	2.93E+10	3133.263	8.11E+05
79.000	-0.003779	2.75E+05	-40921.	8.98E-05	2280.750	2.93E+10	3034.380	8.03E+05
80.000	-0.003684	2.35E+05	-37939.	9.85E-05	1953.404	2.93E+10	2929.393	7.95E+05
81.000	-0.003582	1.99E+05	-35065.	0.000106	1650.395	2.93E+10	2819.587	7.87E+05
82.000	-0.003473	1.65E+05	-32302.	0.000112	1370.809	2.94E+10	2706.123	7.79E+05
83.000	-0.003358	1.34E+05	-29654.	0.000117	1113.703	2.94E+10	2590.049	7.71E+05
84.000	-0.003238	1.06E+05	-27123.	0.000121	878.114	2.94E+10	2472.306	7.63E+05
85.000	-0.003115	79816.	-24710.	0.000124	663.063	2.94E+10	2353.732	7.56E+05
86.000	-0.002989	56283.	-22415.	0.000127	467.566	2.94E+10	2235.072	7.48E+05
87.000	-0.002862	34985.	-20239.	0.000128	290.636	2.94E+10	2116.984	7.40E+05
88.000	-0.002733	15804.	-18181.	0.000129	131.293	2.94E+10	2000.042	7.32E+05
89.000	-0.002603	-1376.460	-16239.	0.000129	11.435	2.94E+10	1884.749	7.24E+05
90.000	-0.002474	-16673.	-14410.	0.000129	138.506	2.94E+10	1771.534	7.16E+05

				Final Analysis
91.000	-0.002345	-30197.	-12694.	0.000128
92.000	-0.002217	-42061.	-11087.	0.000127
93.000	-0.002091	-52372.	-9587.216	0.000125
94.000	-0.001967	-61235.	-8190.363	0.000124
95.000	-0.001844	-68753.	-6893.607	0.000121
96.000	-0.001724	-75023.	-5693.512	0.000119
97.000	-0.001606	-80140.	-4586.534	0.000116
98.000	-0.001491	-84196.	-3569.061	0.000113
99.000	-0.001379	-87278.	-2637.443	0.000111
100.000	-0.001270	-89471.	-1788.017	0.000108
101.000	-0.001164	-90854.	-1017.133	0.000104
102.000	-0.001061	-91505.	-321.173	0.000101
103.000	-0.000962	-91496.	303.429	9.82E-05
104.000	-0.000865	-90898.	860.172	9.51E-05
105.000	-0.000771	-89776.	1352.475	9.21E-05
106.000	-0.000681	-88193.	1783.667	8.90E-05
107.000	-0.000593	-86209.	2156.975	8.61E-05
108.000	-0.000509	-83879.	2475.522	8.32E-05
109.000	-0.000427	-81258.	2742.317	8.04E-05
110.000	-0.000348	-78395.	2960.253	7.76E-05
111.000	-0.000272	-75337.	3132.105	7.50E-05
112.000	-0.000198	-72130.	3260.528	7.25E-05
113.000	-0.000127	-68816.	3348.059	7.01E-05
114.000	-5.78E-05	-65434.	3397.114	6.78E-05
115.000	8.96E-06	-62022.	3409.996	6.57E-05
116.000	7.36E-05	-58614.	3388.892	6.36E-05
117.000	0.000136	-55244.	3335.879	6.17E-05
118.000	0.000197	-51942.	3252.929	5.99E-05
119.000	0.000256	-48738.	3141.912	5.81E-05
120.000	0.000313	-45659.	3004.601	5.65E-05
121.000	0.000369	-42729.	2842.677	5.50E-05
122.000	0.000423	-39973.	2657.738	5.36E-05
123.000	0.000476	-37414.	2451.297	5.23E-05
124.000	0.000528	-35071.	2224.798	5.11E-05
125.000	0.000578	-32964.	1979.613	4.99E-05
126.000	0.000628	-31111.	1717.054	4.88E-05
127.000	0.000676	-29530.	1438.377	4.78E-05
128.000	0.000723	-28235.	1144.785	4.68E-05
129.000	0.000770	-27240.	837.438	4.59E-05
130.000	0.000815	-26560.	517.459	4.50E-05
131.000	0.000860	-26205.	350.881	4.41E-05
132.000	0.000903	-25858.	346.592	4.32E-05

250.859	2.94E+10	1660.765	7.08E+05
349.417	2.94E+10	1552.751	7.00E+05
435.075	2.94E+10	1447.748	6.92E+05
508.706	2.94E+10	1345.960	6.84E+05
571.156	2.94E+10	1247.551	6.77E+05
623.242	2.94E+10	1152.641	6.69E+05
665.752	2.94E+10	1061.316	6.61E+05
699.446	2.94E+10	973.630	6.53E+05
725.051	2.94E+10	889.606	6.45E+05
743.266	2.94E+10	809.245	6.37E+05
754.758	2.94E+10	732.523	6.29E+05
760.165	2.94E+10	659.397	6.21E+05
760.095	2.94E+10	589.807	6.13E+05
755.124	2.94E+10	523.679	6.05E+05
745.803	2.94E+10	460.927	5.98E+05
732.653	2.94E+10	401.456	5.90E+05
716.168	2.94E+10	345.161	5.82E+05
696.815	2.94E+10	291.933	5.74E+05
675.038	2.94E+10	241.657	5.66E+05
651.253	2.94E+10	194.215	5.58E+05
625.854	2.94E+10	149.489	5.50E+05
599.213	2.94E+10	107.358	5.42E+05
571.681	2.94E+10	67.703	5.34E+05
543.586	2.94E+10	30.408	5.26E+05
515.239	2.94E+10	-4.644	5.19E+05
486.930	2.94E+10	-37.564	5.11E+05
458.933	2.94E+10	-68.461	5.03E+05
431.505	2.94E+10	-97.438	4.95E+05
404.887	2.94E+10	-124.596	4.87E+05
379.303	2.94E+10	-150.027	4.79E+05
354.966	2.94E+10	-173.820	4.71E+05
332.073	2.94E+10	-196.060	4.63E+05
310.808	2.94E+10	-216.821	4.55E+05
291.345	2.94E+10	-236.177	4.47E+05
273.844	2.94E+10	-254.192	4.40E+05
258.454	2.94E+10	-270.925	4.32E+05
245.316	2.94E+10	-286.430	4.24E+05
234.556	2.94E+10	-300.754	4.16E+05
226.295	2.94E+10	-313.939	4.08E+05
220.642	2.94E+10	-326.020	4.00E+05
217.698	2.94E+10	-7.134	8300.000
214.812	2.94E+10	-1.445	1600.000

			Final	Analysis
133.000	0.000946	-25512.	345.220	4.23E-05
134.000	0.000988	-25168.	343.896	4.14E-05
135.000	0.001029	-24824.	342.518	4.06E-05
136.000	0.001069	-24483.	341.089	3.97E-05
137.000	0.001108	-24142.	339.609	3.89E-05
138.000	0.001147	-23803.	338.081	3.81E-05
139.000	0.001184	-23466.	336.504	3.73E-05
140.000	0.001221	-23130.	334.881	3.65E-05
141.000	0.001257	-22796.	333.214	3.57E-05
142.000	0.001293	-22464.	331.503	3.50E-05
143.000	0.001327	-22133.	329.749	3.42E-05
144.000	0.001361	-21804.	327.954	3.35E-05
145.000	0.001394	-21477.	326.120	3.27E-05
146.000	0.001427	-21152.	324.246	3.20E-05
147.000	0.001458	-20829.	322.336	3.13E-05
148.000	0.001489	-20508.	320.389	3.06E-05
149.000	0.001519	-20188.	318.406	2.99E-05
150.000	0.001549	-19871.	316.390	2.92E-05
151.000	0.001578	-19555.	314.341	2.85E-05
152.000	0.001606	-19242.	312.260	2.79E-05
153.000	0.001634	-18931.	310.148	2.72E-05
154.000	0.001660	-18622.	308.006	2.66E-05
155.000	0.001687	-18315.	305.836	2.60E-05
156.000	0.001712	-18010.	303.637	2.53E-05
157.000	0.001737	-17708.	301.412	2.47E-05
158.000	0.001762	-17407.	299.162	2.41E-05
159.000	0.001786	-17109.	296.886	2.35E-05
160.000	0.001809	-16813.	294.586	2.30E-05
161.000	0.001832	-16520.	292.264	2.24E-05
162.000	0.001854	-16229.	289.919	2.18E-05
163.000	0.001875	-15940.	287.553	2.13E-05
164.000	0.001896	-15654.	285.166	2.08E-05
165.000	0.001917	-15370.	282.760	2.02E-05
166.000	0.001937	-15088.	280.334	1.97E-05
167.000	0.001956	-14809.	277.891	1.92E-05
168.000	0.001975	-14533.	275.431	1.87E-05
169.000	0.001994	-14258.	272.954	1.82E-05
170.000	0.002012	-13987.	270.461	1.77E-05
171.000	0.002029	-13717.	267.953	1.73E-05
172.000	0.002046	-13451.	265.431	1.68E-05
173.000	0.002063	-13187.	262.895	1.63E-05
174.000	0.002079	-12925.	260.346	1.59E-05

211.939	2.94E+10	-1.297	1371.528
209.077	2.94E+10	-1.351	1368.056
206.225	2.94E+10	-1.404	1364.583
203.386	2.94E+10	-1.455	1361.111
200.558	2.94E+10	-1.505	1357.639
197.743	2.94E+10	-1.553	1354.167
194.941	2.94E+10	-1.600	1350.694
192.152	2.94E+10	-1.645	1347.222
189.377	2.94E+10	-1.690	1343.750
186.616	2.94E+10	-1.733	1340.278
183.869	2.94E+10	-1.774	1336.806
181.137	2.94E+10	-1.815	1333.333
178.421	2.94E+10	-1.854	1329.861
175.719	2.94E+10	-1.892	1326.389
173.033	2.94E+10	-1.929	1322.917
170.364	2.94E+10	-1.965	1319.444
167.710	2.94E+10	-2.000	1315.972
165.073	2.94E+10	-2.033	1312.500
162.453	2.94E+10	-2.065	1309.028
159.851	2.94E+10	-2.097	1305.556
157.265	2.94E+10	-2.127	1302.083
154.698	2.94E+10	-2.156	1298.611
152.148	2.94E+10	-2.185	1295.139
149.616	2.94E+10	-2.212	1291.667
147.103	2.94E+10	-2.238	1288.194
144.608	2.94E+10	-2.263	1284.722
142.132	2.94E+10	-2.288	1281.250
139.676	2.94E+10	-2.311	1277.778
137.238	2.94E+10	-2.334	1274.306
134.820	2.94E+10	-2.356	1270.833
132.421	2.94E+10	-2.377	1267.361
130.042	2.94E+10	-2.397	1263.889
127.683	2.94E+10	-2.416	1260.417
125.344	2.94E+10	-2.434	1256.944
123.025	2.94E+10	-2.452	1253.472
120.727	2.94E+10	-2.469	1250.000
118.449	2.94E+10	-2.485	1246.528
116.192	2.94E+10	-2.501	1243.056
113.956	2.94E+10	-2.515	1239.583
111.740	2.94E+10	-2.529	1236.111
109.546	2.94E+10	-2.543	1232.639
107.372	2.94E+10	-2.555	1229.167

			Final	Analysis
175.000	0.002094	-12666.	257.785	1.55E-05
176.000	0.002110	-12409.	255.212	1.50E-05
177.000	0.002125	-12155.	252.628	1.46E-05
178.000	0.002139	-11904.	250.033	1.42E-05
179.000	0.002153	-11655.	247.429	1.38E-05
180.000	0.002167	-11409.	244.816	1.34E-05
181.000	0.002180	-11166.	242.193	1.30E-05
182.000	0.002193	-10925.	239.563	1.27E-05
183.000	0.002205	-10687.	236.925	1.23E-05
184.000	0.002217	-10451.	234.280	1.19E-05
185.000	0.002229	-10218.	231.628	1.16E-05
186.000	0.002240	-9987.742	228.971	1.12E-05
187.000	0.002252	-9760.102	226.308	1.09E-05
188.000	0.002262	-9535.127	223.639	1.06E-05
189.000	0.002273	-9312.823	220.966	1.03E-05
190.000	0.002283	-9093.194	218.289	9.94E-06
191.000	0.002293	-8876.244	215.608	9.64E-06
192.000	0.002302	-8661.977	212.924	9.34E-06
193.000	0.002311	-8450.396	210.237	9.05E-06
194.000	0.002320	-8241.503	207.548	8.76E-06
195.000	0.002329	-8035.300	204.856	8.49E-06
196.000	0.002337	-7831.790	202.163	8.22E-06
197.000	0.002345	-7630.975	199.468	7.95E-06
198.000	0.002353	-7432.855	196.772	7.70E-06
199.000	0.002361	-7237.430	194.076	7.45E-06
200.000	0.002368	-7044.703	191.379	7.20E-06
201.000	0.002375	-6854.672	188.682	6.97E-06
202.000	0.002382	-6667.338	185.986	6.74E-06
203.000	0.002388	-6482.700	183.290	6.51E-06
204.000	0.002395	-6300.757	180.596	6.30E-06
205.000	0.002401	-6121.509	177.902	6.08E-06
206.000	0.002407	-5944.953	175.210	5.88E-06
207.000	0.002413	-5771.089	172.520	5.68E-06
208.000	0.002418	-5599.914	169.832	5.49E-06
209.000	0.002424	-5431.426	167.146	5.30E-06
210.000	0.002429	-5265.622	164.462	5.12E-06
211.000	0.002434	-5102.501	161.782	4.94E-06
212.000	0.002439	-4942.059	159.104	4.77E-06
213.000	0.002444	-4784.292	156.430	4.60E-06
214.000	0.002448	-4629.199	153.759	4.44E-06
215.000	0.002452	-4476.774	151.092	4.29E-06
216.000	0.002457	-4327.015	148.429	4.14E-06

105.220	2.94E+10	-2.567	1225.694
103.089	2.94E+10	-2.579	1222.222
100.980	2.94E+10	-2.589	1218.750
98.892	2.94E+10	-2.599	1215.278
96.825	2.94E+10	-2.609	1211.806
94.781	2.94E+10	-2.618	1208.333
92.758	2.94E+10	-2.626	1204.861
90.757	2.94E+10	-2.634	1201.389
88.778	2.94E+10	-2.642	1197.917
86.820	2.94E+10	-2.648	1194.444
84.885	2.94E+10	-2.655	1190.972
82.972	2.94E+10	-2.661	1187.500
81.081	2.94E+10	-2.666	1184.028
79.212	2.94E+10	-2.671	1180.556
77.365	2.94E+10	-2.675	1177.083
75.541	2.94E+10	-2.679	1173.611
73.738	2.94E+10	-2.683	1170.139
71.958	2.94E+10	-2.686	1166.667
70.201	2.94E+10	-2.688	1163.194
68.465	2.94E+10	-2.691	1159.722
66.752	2.94E+10	-2.693	1156.250
65.062	2.94E+10	-2.694	1152.778
63.393	2.94E+10	-2.695	1149.306
61.747	2.94E+10	-2.696	1145.833
60.124	2.94E+10	-2.697	1142.361
58.523	2.94E+10	-2.697	1138.889
56.944	2.94E+10	-2.697	1135.417
55.388	2.94E+10	-2.696	1131.944
53.854	2.94E+10	-2.695	1128.472
52.343	2.94E+10	-2.694	1125.000
50.854	2.94E+10	-2.693	1121.528
49.387	2.94E+10	-2.691	1118.056
47.943	2.94E+10	-2.689	1114.583
46.521	2.94E+10	-2.687	1111.111
45.121	2.94E+10	-2.685	1107.639
43.743	2.94E+10	-2.682	1104.167
42.388	2.94E+10	-2.679	1100.694
41.056	2.94E+10	-2.676	1097.222
39.745	2.94E+10	-2.673	1093.750
38.456	2.94E+10	-2.669	1090.278
37.190	2.94E+10	-2.665	1086.806
35.946	2.94E+10	-2.661	1083.333

			Final	Analysis
217.000	0.002461	-4179.917	145.769	4.00E-06
218.000	0.002465	-4035.476	143.114	3.86E-06
219.000	0.002468	-3893.689	140.463	3.72E-06
220.000	0.002472	-3754.549	137.817	3.59E-06
221.000	0.002476	-3618.054	135.176	3.47E-06
222.000	0.002479	-3484.197	132.540	3.34E-06
223.000	0.002482	-3352.975	129.908	3.23E-06
224.000	0.002485	-3224.381	127.282	3.12E-06
225.000	0.002489	-3098.411	124.661	3.01E-06
226.000	0.002491	-2975.059	122.046	2.91E-06
227.000	0.002494	-2854.319	119.436	2.81E-06
228.000	0.002497	-2736.187	116.832	2.71E-06
229.000	0.002500	-2620.655	114.234	2.62E-06
230.000	0.002502	-2507.719	111.641	2.53E-06
231.000	0.002505	-2397.372	109.055	2.45E-06
232.000	0.002507	-2289.609	106.475	2.37E-06
233.000	0.002510	-2184.422	103.902	2.29E-06
234.000	0.002512	-2081.805	101.334	2.22E-06
235.000	0.002514	-1981.753	98.773	2.15E-06
236.000	0.002516	-1884.259	96.219	2.09E-06
237.000	0.002518	-1789.315	93.671	2.02E-06
238.000	0.002520	-1696.916	91.130	1.96E-06
239.000	0.002522	-1607.055	88.596	1.91E-06
240.000	0.002524	-1519.725	86.068	1.85E-06
241.000	0.002526	-1434.918	83.548	1.80E-06
242.000	0.002528	-1352.629	81.034	1.76E-06
243.000	0.002529	-1272.850	78.528	1.71E-06
244.000	0.002531	-1195.573	76.028	1.67E-06
245.000	0.002533	-1120.793	73.536	1.63E-06
246.000	0.002534	-1048.501	71.051	1.59E-06
247.000	0.002536	-978.691	68.573	1.56E-06
248.000	0.002537	-911.355	66.103	1.53E-06
249.000	0.002539	-846.486	63.639	1.50E-06
250.000	0.002540	-784.077	61.183	1.47E-06
251.000	0.002542	-724.119	58.735	1.44E-06
252.000	0.002543	-666.607	56.294	1.42E-06
253.000	0.002545	-611.532	53.860	1.40E-06
254.000	0.002546	-558.886	51.434	1.38E-06
255.000	0.002547	-508.663	49.016	1.36E-06
256.000	0.002549	-460.855	46.605	1.34E-06
257.000	0.002550	-415.454	44.201	1.33E-06
258.000	0.002551	-372.453	41.805	1.32E-06

34.724	2.94E+10	-2.657	1079.861
33.524	2.94E+10	-2.653	1076.389
32.346	2.94E+10	-2.648	1072.917
31.190	2.94E+10	-2.644	1069.444
30.057	2.94E+10	-2.639	1065.972
28.945	2.94E+10	-2.634	1062.500
27.854	2.94E+10	-2.629	1059.028
26.786	2.94E+10	-2.624	1055.556
25.740	2.94E+10	-2.618	1052.083
24.715	2.94E+10	-2.613	1048.611
23.712	2.94E+10	-2.607	1045.139
22.731	2.94E+10	-2.601	1041.667
21.771	2.94E+10	-2.595	1038.194
20.833	2.94E+10	-2.589	1034.722
19.916	2.94E+10	-2.583	1031.250
19.021	2.94E+10	-2.577	1027.778
18.147	2.94E+10	-2.571	1024.306
17.294	2.94E+10	-2.564	1020.833
16.463	2.94E+10	-2.558	1017.361
15.653	2.94E+10	-2.551	1013.889
14.865	2.94E+10	-2.544	1010.417
14.097	2.94E+10	-2.538	1006.944
13.350	2.94E+10	-2.531	1003.472
12.625	2.94E+10	-2.524	1000.000
11.920	2.94E+10	-2.517	996.528
11.237	2.94E+10	-2.510	993.056
10.574	2.94E+10	-2.503	989.583
9.932	2.94E+10	-2.496	986.111
9.311	2.94E+10	-2.489	982.639
8.710	2.94E+10	-2.481	979.167
8.130	2.94E+10	-2.474	975.694
7.571	2.94E+10	-2.467	972.222
7.032	2.94E+10	-2.460	968.750
6.514	2.94E+10	-2.452	965.278
6.016	2.94E+10	-2.445	961.806
5.538	2.94E+10	-2.437	958.333
5.080	2.94E+10	-2.430	954.861
4.643	2.94E+10	-2.422	951.389
4.226	2.94E+10	-2.415	947.917
3.828	2.94E+10	-2.407	944.444
3.451	2.94E+10	-2.400	940.972
3.094	2.94E+10	-2.392	937.500

259.000	0.002553	-331.844	39.417	1.30E-06	2.757	2.94E+10	-2.384	934.028
260.000	0.002554	-293.619	37.037	1.29E-06	2.439	2.94E+10	-2.377	930.556
261.000	0.002555	-257.770	34.664	1.28E-06	2.141	2.94E+10	-2.369	927.083
262.000	0.002557	-224.291	32.299	1.28E-06	1.863	2.94E+10	-2.361	923.611
263.000	0.002558	-193.173	29.941	1.27E-06	1.605	2.94E+10	-2.354	920.139
264.000	0.002559	-164.409	27.591	1.26E-06	1.366	2.94E+10	-2.346	916.667
265.000	0.002560	-137.991	25.249	1.26E-06	1.146	2.94E+10	-2.338	913.194
266.000	0.002562	-113.911	22.915	1.25E-06	0.946299	2.94E+10	-2.330	909.722
267.000	0.002563	-92.161	20.588	1.25E-06	0.765616	2.94E+10	-2.323	906.250
268.000	0.002564	-72.734	18.270	1.25E-06	0.604229	2.94E+10	-2.315	902.778
269.000	0.002565	-55.622	15.958	1.24E-06	0.462073	2.94E+10	-2.307	899.306
270.000	0.002567	-40.817	13.655	1.24E-06	0.339083	2.94E+10	-2.299	895.833
271.000	0.002568	-28.312	11.360	1.24E-06	0.235194	2.94E+10	-2.292	892.361
272.000	0.002569	-18.097	9.072	1.24E-06	0.150342	2.94E+10	-2.284	888.889
273.000	0.002570	-10.167	6.792	1.24E-06	0.084462	2.94E+10	-2.276	885.417
274.000	0.002572	-4.513	4.520	1.24E-06	0.037488	2.94E+10	-2.268	881.944
275.000	0.002573	-1.126	2.256	1.24E-06	0.009356	2.94E+10	-2.260	878.472
276.000	0.002574	0.000	0.000	1.24E-06	0.000	2.94E+10	-2.252	437.500

Please note that because this analysis makes computations of ultimate moment capacity and pile response using nonlinear bending stiffness that the above values of total stress due to combined axial stress and bending may not be representative of actual conditions.

Output Verification:

Computed forces and moments are within specified convergence limits.

Output Summary for Load Case No. 1:

Pile-head deflection	=	0.20655782 in
Computed slope at pile head	=	-0.00509501
Maximum bending moment	=	2626828. lbs-in
Maximum shear force	=	-95624.86010 lbs
Depth of maximum bending moment	=	45.00000000 in
Depth of maximum shear force	=	59.00000000 in
Number of iterations	=	14
Number of zero deflection points	=	2

Summary of Pile Response(s)

Definition of Symbols for Pile-Head Loading Conditions:

Type 1 = Shear and Moment, y = pile-head displacment in
Type 2 = Shear and Slope, M = Pile-head Moment lbs-in
Type 3 = Shear and Rot. Stiffness, V = Pile-head Shear Force lbs
Type 4 = Deflection and Moment, S = Pile-head Slope, radians
Type 5 = Deflection and Slope, R = Rot. Stiffness of Pile-head in-lbs/rad

Load Type	Pile-Head Condition 1	Pile-Head Condition 2	Axial Load lbs	Pile-Head Deflection in	Maximum Moment in-lbs	Maximum Shear lbs
1	V= 62500.	M= 0.000	0.0000	0.2065578	2626828.	-95624.8601

Computed Pile-head Stiffness Matrix Members
K22, K23, K32, K33 for Superstructure

Top y in	Shear React. lbs	Mom. React. in-lbs	K22 lbs/in	K32 in-lbs/in
0.00362813	6250.00009	180480.08285	1722650.	49744643.
0.01164929	18814.37473	529582.16064	1615066.	45460471.
0.01956452	29820.07842	819528.47971	1524192.	41888503.
0.02601593	37628.74946	1056091.	1446373.	40594010.
0.03058057	43685.62527	1228409.	1428542.	40169595.
0.03423146	48634.45315	1368654.	1420753.	39982336.
0.03734707	52818.62750	1488162.	1414264.	39846815.
0.04011838	56443.12419	1592432.	1406914.	39693342.
0.04269221	59640.15684	1686405.	1396980.	39501467.
0.04504243	62500.00000	1770490.	1387581.	39307154.

Top Rota.	Shear React.	Mom. React.	K23	K33

rad	lbs	in-lbs	lbs/rad
5.139753E-09	0.25586613	10.00000015	49781797.
1.547220E-08	0.77023380	30.10299957	49781797.
2.452285E-08	1.22079169	47.71212547	49781797.
3.094440E-08	1.54046760	60.20599913	49781797.
3.592533E-08	1.78842750	69.89700043	49781797.
3.999505E-08	1.99102549	77.81512504	49781797.
4.343595E-08	2.16231964	84.50980400	49781797.
4.641659E-08	2.31070139	90.30899870	49781797.
4.904571E-08	2.44158337	95.42425094	49781797.
5.139753E-08	2.55866129	100.00000000	49781797.

K22 = abs(Shear Reaction/Top y)
K23 = abs(Shear Reaction/Top Rotation)
K32 = abs(Moment Reaction/Top y)
K33 = abs(Moment Reaction/Top Rotation)

This analysis ended normally.

62.5 Kips.txt
in-lbs/rad

1.945619E+09
1.945619E+09
1.945619E+09
1.945619E+09
1.945619E+09
1.945619E+09
1.945619E+09
1.945619E+09
1.945619E+09
1.945619E+09

Jan Test Campbell program.C9X

```
'CR9000X program
'Large Displacement Test
'program written by Duane Davis
'on 01-04-10

  'Load-Deflection Test: data is collected from six LMT sensors, thirty
strain gages,
  'and one 200kip load cell while the test pile is subjected to a
unidirectional, stepped
  'increasing lateral load.

  'Tabulated output includes measured and calculated values.


'---------- Declare Variables and Units ----------
Dim I

'Calibration variables for the FieldCal(..) instruction below
'FieldCal (Function, MeasureVar, Reps, MultVar, OffsetVar, Mode,
KnownVar, Index, Avg )
'  for zeroing calibrations, Function = MultVar = KnownVar = 0
Const ZReps = 1                    'value for Reps
Public ZOff(37)                    'value for OffsetVar
Public ZMode(37)                   'value for Mode
Const ZIndex = 1                   'value for Index
Const ZAvg = 100                   'value for Avg
Public ZInit(37)                   'initialize toggle for calibrations (1
or 0)
Public ZGage(37)                   'All gage measurements

Const StrGF=-2.075                 'Gage Factor for strain gages
                                   'HPI HBWF-35-125-6-50GP-SS, Gage
resistance: 350 +/- 1% Ohms
                                   'Gage Factor: 4.150 +/- 1% composite
                                   '(2.075 each active element, lot
number: 082853)

Const LMT1_mult=1/33.274128        'calibration multiplier for 30"
LMT(old), s/n: 0107-25787

Const LMT2_mult=1/66.475484        'calibration multiplier for 15"
LMT(old), s/n: 0601-16192

Const LMT3_mult=1/33.137333        'calibration multiplier for AMETEK
P-30A, s/n: DTC2038

Const LMT4_mult=1/66.421333        'calibration multiplier for AMETEK
P-15A, s/n: DTC2010

Const LMT5_mult=1/66.341333        'calibration multiplier for AMETEK
P-15A, s/n: DTC2009

Const LMT6_mult=1/66.416           'calibration multiplier for AMETEK
P-15A, s/n: DTC2008

Const LCel_mult=-200000/3.0045     'multiplier for Honeywell model 41,
s/n: 1245146,
                                   '+/- 200kip range, calibration factor:
3.0044 mV/V
```

```
                    Jan Test Campbell program.C9X
                              'LCel_mult = 200000 / 3.004

Public Load                   'Calculated Load output
Public LMT(6)                 'Calculated LMT output
Public Strain(30)             'Calculated Strain output

Public FCLoaded

'Data column headers, used here to denote physical sensors with array
values
Alias LMT(1)=LMT1
Alias LMT(2)=LMT2
Alias LMT(3)=LMT3
Alias LMT(4)=LMT4
Alias LMT(5)=LMT5
Alias LMT(6)=LMT6
Alias Strain(1)=Strain_A0
Alias Strain(2)=Strain_A1
Alias Strain(3)=Strain_A2
Alias Strain(4)=Strain_A3
Alias Strain(5)=Strain_A4
Alias Strain(6)=Strain_A5
Alias Strain(7)=Strain_A6
Alias Strain(8)=Strain_A7
Alias Strain(9)=Strain_A8
Alias Strain(10)=Strain_A9
Alias Strain(11)=Strain_A10
Alias Strain(12)=Strain_A11
Alias Strain(13)=Strain_A12
Alias Strain(14)=Strain_A13
Alias Strain(15)=Strain_A14
Alias Strain(16)=Strain_A15
Alias Strain(17)=Strain_A16
Alias Strain(18)=Strain_A17
Alias Strain(19)=Strain_A18
Alias Strain(20)=Strain_A19
Alias Strain(21)=Strain_B0
Alias Strain(22)=Strain_B2
Alias Strain(23)=Strain_B4
Alias Strain(24)=Strain_B5
Alias Strain(25)=Strain_B6
Alias Strain(26)=Strain_B7
Alias Strain(27)=Strain_B8
Alias Strain(28)=Strain_B10
Alias Strain(29)=Strain_B12
Alias Strain(30)=Strain_B15

Public StartStop As Boolean       'flag to start/stop the entire program
Public LoadDefl As Boolean        'flag to start/stop recording data
while program is running
Public ReZero As Boolean          'flag to calibrate sensor offsets
Public UnZero As Boolean          'flag to change sensor offsets to be
zero


'---------- Define Data Tables ----------

'Default calibration history table
DataTable(CalHist,NewFieldCal,100)
```

```
        CardOut(0,100)
        SampleFieldCal
EndTable

'Load Deflection Test output table
DataTable(LDef,LoadDefl,-1)
        DataInterval(0,100,mSec,0)
        CardOut(0,-1)
        Sample(1,Load,IEEE4)
        Sample(1,LMT(1),IEEE4)
        Sample(1,LMT(2),IEEE4)
        Sample(1,LMT(3),IEEE4)
        Sample(1,LMT(4),IEEE4)
        Sample(1,LMT(5),IEEE4)
        Sample(1,LMT(6),IEEE4)
        Sample(1,Strain(1),IEEE4)
        Sample(1,Strain(2),IEEE4)
        Sample(1,Strain(3),IEEE4)
        Sample(1,Strain(4),IEEE4)
        Sample(1,Strain(5),IEEE4)
        Sample(1,Strain(6),IEEE4)
        Sample(1,Strain(7),IEEE4)
        Sample(1,Strain(8),IEEE4)
        Sample(1,Strain(9),IEEE4)
        Sample(1,Strain(10),IEEE4)
        Sample(1,Strain(11),IEEE4)
        Sample(1,Strain(12),IEEE4)
        Sample(1,Strain(13),IEEE4)
        Sample(1,Strain(14),IEEE4)
        Sample(1,Strain(15),IEEE4)
        Sample(1,Strain(16),IEEE4)
        Sample(1,Strain(17),IEEE4)
        Sample(1,Strain(18),IEEE4)
        Sample(1,Strain(19),IEEE4)
        Sample(1,Strain(20),IEEE4)
        Sample(1,Strain(21),IEEE4)
        Sample(1,Strain(22),IEEE4)
        Sample(1,Strain(23),IEEE4)
        Sample(1,Strain(24),IEEE4)
        Sample(1,Strain(25),IEEE4)
        Sample(1,Strain(26),IEEE4)
        Sample(1,Strain(27),IEEE4)
        Sample(1,Strain(28),IEEE4)
        Sample(1,Strain(29),IEEE4)
        Sample(1,Strain(30),IEEE4)
EndTable

'---------- Define Subroutines ----------

'Subroutine for Load Deflection Test
Sub LDefl
  Scan(100,mSec,0,0)
    If StartStop=False Then ExitScan

    If ReZero=True
      For I = 1 To 37
        ZOff(I)=0 : ZInit(I)=0
      Next I
      ReZero=False
```

```
                    Jan Test Campbell program.C9X
    EndIf

    If UnZero=True Then
      For I = 1 To 37
        ZOff(I)=0
      Next I
      UnZero=False
    EndIf

'----- Load Cell -----


BrFull(ZGage(1),1,mV50,8,14,9,6,1,5000,True,True,50,400,LCel_mult,ZOff(1
))   'Load Cell
                        If ZInit(1)=0 Then
                                ZMode(1)=1 : ZInit(1)=1
                        EndIf
                        If ZMode(1)<=0 OR ZMode(1)=6 Then ZInit(1)=1

FieldCal(0,ZGage(1),ZReps,0,ZOff(1),ZMode(1),0,ZIndex,ZAvg)
                Load=ZGage(1)

'----- LMT sensors -----


BrFull(ZGage(2),1,mV5000,10,1,11,1,1,5000,True,True,50,400,LMT1_mult,ZOf
f(2))     'LMT1
                        If ZInit(2)=0 Then
                          ZMode(2)=1 : ZInit(2)=1
                        EndIf
                        If ZMode(2)<=0 OR ZMode(2)=6 Then ZInit(2)=1

FieldCal(0,ZGage(2),ZReps,0,ZOff(2),ZMode(2),0,ZIndex,ZAvg)
                LMT(1)=ZGage(2)


BrFull(ZGage(3),1,mV5000,10,2,11,2,1,5000,True,True,50,400,LMT2_mult,ZOf
f(3))     'LMT2
                        If ZInit(3)=0 Then
                                ZMode(3)=1 : ZInit(3)=1
                        EndIf
                        If ZMode(3)<=0 OR ZMode(3)=6 Then ZInit(3)=1

FieldCal(0,ZGage(3),ZReps,0,ZOff(3),ZMode(3),0,ZIndex,ZAvg)
                LMT(2)=ZGage(3)


BrFull(ZGage(4),1,mV5000,10,3,11,3,1,5000,True,True,50,400,LMT3_mult,ZOf
f(4))     'LMT3
                        If ZInit(4)=0 Then
                                ZMode(4)=1 : ZInit(4)=1
                        EndIf
                        If ZMode(4)<=0 OR ZMode(4)=6 Then ZInit(4)=1

FieldCal(0,ZGage(4),ZReps,0,ZOff(4),ZMode(4),0,ZIndex,ZAvg)
                LMT(3)=ZGage(4)


BrFull(ZGage(5),1,mV5000,10,4,11,4,1,5000,True,True,50,400,LMT4_mult,ZOf
```

```
                    Jan Test Campbell program.C9X
f(5))     'LMT4
                        If ZInit(5)=0 Then
                          ZMode(5)=1 : ZInit(5)=1
                        EndIf
                        If ZMode(5)<=0 OR ZMode(5)=6 Then ZInit(5)=1

FieldCal(0,ZGage(5),ZReps,0,ZOff(5),ZMode(5),0,ZIndex,ZAvg)
                LMT(4)=ZGage(5)


BrFull(ZGage(6),1,mV5000,10,5,11,5,1,5000,True,True,50,400,LMT5_mult,ZOf
f(6))     'LMT5
                        If ZInit(6)=0 Then
                          ZMode(6)=1 : ZInit(6)=1
                        EndIf
                        If ZMode(6)<=0 OR ZMode(6)=6 Then ZInit(6)=1

FieldCal(0,ZGage(6),ZReps,0,ZOff(6),ZMode(6),0,ZIndex,ZAvg)
                LMT(5)=ZGage(6)


BrFull(ZGage(7),1,mV5000,10,6,11,6,1,5000,True,True,50,400,LMT6_mult,ZOf
f(7))     'LMT6
                        If ZInit(7)=0 Then
                          ZMode(7)=1 : ZInit(7)=1
                        EndIf
                        If ZMode(7)<=0 OR ZMode(7)=6 Then ZInit(7)=1

FieldCal(0,ZGage(7),ZReps,0,ZOff(7),ZMode(7),0,ZIndex,ZAvg)
                LMT(6)=ZGage(7)

'----- Strain Gages -----
    BrFull(ZGage(8),1,mV50,4,1,6,2,1,5000,True,True,50,200,1,ZOff(8))
      'Strain Gage A0
                        If ZInit(8)=0 Then
                                ZMode(8)=1 : ZInit(8)=1
                        EndIf
                        If ZMode(8)<=0 OR ZMode(8)=6 Then ZInit(8)=1

FieldCal(0,ZGage(8),ZReps,0,ZOff(8),ZMode(8),0,ZIndex,ZAvg)
    StrainCalc(Strain(1),1,ZGage(8),0,3,StrGF,0)

    BrFull(ZGage(9),1,mV50,4,2,6,2,1,5000,True,True,50,200,1,ZOff(9))
      'Strain Gage A1
                        If ZInit(9)=0 Then
                                ZMode(9)=1 : ZInit(9)=1
                        EndIf
                        If ZMode(9)<=0 OR ZMode(9)=6 Then ZInit(9)=1

FieldCal(0,ZGage(9),ZReps,0,ZOff(9),ZMode(9),0,ZIndex,ZAvg)
    StrainCalc(Strain(2),1,ZGage(9),0,3,StrGF,0)

    BrFull(ZGage(10),1,mV50,4,3,6,2,1,5000,True,True,50,200,1,ZOff(10))
        'Strain Gage A2
                        If ZInit(10)=0 Then
                                ZMode(10)=1 : ZInit(10)=1
                        EndIf
                        If ZMode(10)<=0 OR ZMode(10)=6 Then ZInit(10)=1
```

```
                    Jan Test Campbell program.C9X
FieldCal(0,ZGage(10),ZReps,0,ZOff(10),ZMode(10),0,ZIndex,ZAvg)
    StrainCalc(Strain(3),1,ZGage(10),0,3,StrGF,0)

    BrFull(ZGage(11),1,mV50,5,1,6,1,1,5000,True,True,50,200,1,ZOff(11))
        'Strain Gage A3
                        If ZInit(11)=0 Then
                                ZMode(11)=1 : ZInit(11)=1
                        EndIf
                        If ZMode(11)<=0 OR ZMode(11)=6 Then ZInit(11)=1

FieldCal(0,ZGage(11),ZReps,0,ZOff(11),ZMode(11),0,ZIndex,ZAvg)
    StrainCalc(Strain(4),1,ZGage(11),0,3,StrGF,0)

    BrFull(ZGage(12),1,mV50,5,2,6,1,1,5000,True,True,50,200,1,ZOff(12))
      'Strain Gage A4
                        If ZInit(12)=0 Then
                                ZMode(12)=1 : ZInit(12)=1
                        EndIf
                        If ZMode(12)<=0 OR ZMode(12)=6 Then ZInit(12)=1

FieldCal(0,ZGage(12),ZReps,0,ZOff(12),ZMode(12),0,ZIndex,ZAvg)
    StrainCalc(Strain(5),1,ZGage(12),0,3,StrGF,0)

    BrFull(ZGage(13),1,mV50,5,3,6,1,1,5000,True,True,50,200,1,ZOff(13))
      'Strain Gage A5
                        If ZInit(13)=0 Then
                                ZMode(13)=1 : ZInit(13)=1
                        EndIf
                        If ZMode(13)<=0 OR ZMode(13)=6 Then ZInit(13)=1

FieldCal(0,ZGage(13),ZReps,0,ZOff(13),ZMode(13),0,ZIndex,ZAvg)
    StrainCalc(Strain(6),1,ZGage(13),0,3,StrGF,0)

    BrFull(ZGage(14),1,mV50,4,4,6,3,1,5000,True,True,50,200,1,ZOff(14))
      'Strain Gage A6
                        If ZInit(14)=0 Then
                                ZMode(14)=1 : ZInit(14)=1
                        EndIf
                        If ZMode(14)<=0 OR ZMode(14)=6 Then ZInit(14)=1

FieldCal(0,ZGage(14),ZReps,0,ZOff(14),ZMode(14),0,ZIndex,ZAvg)
    StrainCalc(Strain(7),1,ZGage(14),0,3,StrGF,0)

    BrFull(ZGage(15),1,mV50,4,5,6,3,1,5000,True,True,50,200,1,ZOff(15))
      'Strain Gage A7
                        If ZInit(15)=0 Then
                                ZMode(15)=1 : ZInit(15)=1
                        EndIf
                        If ZMode(15)<=0 OR ZMode(15)=6 Then ZInit(15)=1

FieldCal(0,ZGage(15),ZReps,0,ZOff(15),ZMode(15),0,ZIndex,ZAvg)
    StrainCalc(Strain(8),1,ZGage(15),0,3,StrGF,0)

    BrFull(ZGage(16),1,mV50,4,6,6,3,1,5000,True,True,50,200,1,ZOff(16))
      'Strain Gage A8
                        If ZInit(16)=0 Then
                                ZMode(16)=1 : ZInit(16)=1
                        EndIf
                        If ZMode(16)<=0 OR ZMode(16)=6 Then ZInit(16)=1
```

```
FieldCal(0,ZGage(16),ZReps,0,ZOff(16),ZMode(16),0,ZIndex,ZAvg)
    StrainCalc(Strain(9),1,ZGage(16),0,3,StrGF,0)

    BrFull(ZGage(17),1,mV50,5,4,6,4,1,5000,True,True,50,200,1,ZOff(17))
    'Strain Gage A9
                        If ZInit(17)=0 Then
                                ZMode(17)=1 : ZInit(17)=1
                        EndIf
                        If ZMode(17)<=0 OR ZMode(17)=6 Then ZInit(17)=1

FieldCal(0,ZGage(17),ZReps,0,ZOff(17),ZMode(17),0,ZIndex,ZAvg)
    StrainCalc(Strain(10),1,ZGage(17),0,3,StrGF,0)

    BrFull(ZGage(18),1,mV50,5,5,6,4,1,5000,True,True,50,200,1,ZOff(18))
     'Strain Gage A10
                        If ZInit(18)=0 Then
                                ZMode(18)=1 : ZInit(18)=1
                        EndIf
                        If ZMode(18)<=0 OR ZMode(18)=6 Then ZInit(18)=1

FieldCal(0,ZGage(18),ZReps,0,ZOff(18),ZMode(18),0,ZIndex,ZAvg)
    StrainCalc(Strain(11),1,ZGage(18),0,3,StrGF,0)

    BrFull(ZGage(19),1,mV50,5,6,6,4,1,5000,True,True,50,200,1,ZOff(19))
     'Strain Gage A11
                        If ZInit(19)=0 Then
                                ZMode(19)=1 : ZInit(19)=1
                        EndIf
                        If ZMode(19)<=0 OR ZMode(19)=6 Then ZInit(19)=1

FieldCal(0,ZGage(19),ZReps,0,ZOff(19),ZMode(19),0,ZIndex,ZAvg)
    StrainCalc(Strain(12),1,ZGage(19),0,3,StrGF,0)

    BrFull(ZGage(20),1,mV50,4,7,6,5,1,5000,True,True,50,200,1,ZOff(20))
     'Strain Gage A12
                        If ZInit(20)=0 Then
                                ZMode(20)=1 : ZInit(20)=1
                        EndIf
                        If ZMode(20)<=0 OR ZMode(20)=6 Then ZInit(20)=1

FieldCal(0,ZGage(20),ZReps,0,ZOff(20),ZMode(20),0,ZIndex,ZAvg)
    StrainCalc(Strain(13),1,ZGage(20),0,3,StrGF,0)

    BrFull(ZGage(21),1,mV50,5,7,6,5,1,5000,True,True,50,200,1,ZOff(21))
     'Strain Gage A13
                        If ZInit(21)=0 Then
                                ZMode(21)=1 : ZInit(21)=1
                        EndIf
                        If ZMode(21)<=0 OR ZMode(21)=6 Then ZInit(21)=1

FieldCal(0,ZGage(21),ZReps,0,ZOff(21),ZMode(21),0,ZIndex,ZAvg)
    StrainCalc(Strain(14),1,ZGage(21),0,3,StrGF,0)

    BrFull(ZGage(22),1,mV50,5,8,6,5,1,5000,True,True,50,200,1,ZOff(22))
     'Strain Gage A14
                        If ZInit(22)=0 Then
                                ZMode(22)=1 : ZInit(22)=1
                        EndIf
```

```
                    Jan Test Campbell program.C9X
                      If ZMode(22)<=0 OR ZMode(22)=6 Then ZInit(22)=1

FieldCal(0,ZGage(22),ZReps,0,ZOff(22),ZMode(22),0,ZIndex,ZAvg)
    StrainCalc(Strain(15),1,ZGage(22),0,3,StrGF,0)

    BrFull(ZGage(23),1,mV50,7,1,9,1,1,5000,True,True,50,200,1,ZOff(23))
     'Strain Gage A15
                      If ZInit(23)=0 Then
                              ZMode(23)=1 : ZInit(23)=1
                      EndIf
                      If ZMode(23)<=0 OR ZMode(23)=6 Then ZInit(23)=1

FieldCal(0,ZGage(23),ZReps,0,ZOff(23),ZMode(23),0,ZIndex,ZAvg)
    StrainCalc(Strain(16),1,ZGage(23),0,3,StrGF,0)

    BrFull(ZGage(24),1,mV50,7,2,9,1,1,5000,True,True,50,200,1,ZOff(24))
     'Strain Gage A16
                      If ZInit(24)=0 Then
                              ZMode(24)=1 : ZInit(24)=1
                      EndIf
                      If ZMode(24)<=0 OR ZMode(24)=6 Then ZInit(24)=1

FieldCal(0,ZGage(24),ZReps,0,ZOff(24),ZMode(24),0,ZIndex,ZAvg)
    StrainCalc(Strain(17),1,ZGage(24),0,3,StrGF,0)

    BrFull(ZGage(25),1,mV50,7,3,9,1,1,5000,True,True,50,200,1,ZOff(25))
     'Strain Gage A17
                      If ZInit(25)=0 Then
                              ZMode(25)=1 : ZInit(25)=1
                      EndIf
                      If ZMode(25)<=0 OR ZMode(25)=6 Then ZInit(25)=1

FieldCal(0,ZGage(25),ZReps,0,ZOff(25),ZMode(25),0,ZIndex,ZAvg)
    StrainCalc(Strain(18),1,ZGage(25),0,3,StrGF,0)

    BrFull(ZGage(26),1,mV50,8,1,9,2,1,5000,True,True,50,200,1,ZOff(26))
     'Strain Gage A18
                      If ZInit(26)=0 Then
                              ZMode(26)=1 : ZInit(26)=1
                      EndIf
                      If ZMode(26)<=0 OR ZMode(26)=6 Then ZInit(26)=1

FieldCal(0,ZGage(26),ZReps,0,ZOff(26),ZMode(26),0,ZIndex,ZAvg)
    StrainCalc(Strain(19),1,ZGage(26),0,3,StrGF,0)

    BrFull(ZGage(27),1,mV50,8,2,9,2,1,5000,True,True,50,200,1,ZOff(27))
   'Strain Gage A19
                      If ZInit(27)=0 Then
                              ZMode(27)=1 : ZInit(27)=1
                      EndIf
                      If ZMode(27)<=0 OR ZMode(27)=6 Then ZInit(27)=1

FieldCal(0,ZGage(27),ZReps,0,ZOff(27),ZMode(27),0,ZIndex,ZAvg)
    StrainCalc(Strain(20),1,ZGage(27),0,3,StrGF,0)

    BrFull(ZGage(28),1,mV50,7,7,9,5,1,5000,True,True,50,200,1,ZOff(28))
   'Strain Gage B0
                      If ZInit(28)=0 Then
                              ZMode(28)=1 : ZInit(28)=1
```

```
                    Jan Test Campbell program.C9X
                      EndIf
                      If ZMode(28)<=0 OR ZMode(28)=6 Then ZInit(28)=1

FieldCal(0,ZGage(28),ZReps,0,ZOff(28),ZMode(28),0,ZIndex,ZAvg)
    StrainCalc(Strain(21),1,ZGage(28),0,3,StrGF,0)

    BrFull(ZGage(29),1,mV50,8,7,9,5,1,5000,True,True,50,200,1,ZOff(29))
   'Strain Gage B2
                      If ZInit(29)=0 Then
                              ZMode(29)=1 : ZInit(29)=1
                      EndIf
                      If ZMode(29)<=0 OR ZMode(29)=6 Then ZInit(29)=1

FieldCal(0,ZGage(29),ZReps,0,ZOff(29),ZMode(29),0,ZIndex,ZAvg)
    StrainCalc(Strain(22),1,ZGage(29),0,3,StrGF,0)

    BrFull(ZGage(30),1,mV50,8,8,9,5,1,5000,True,True,50,200,1,ZOff(30))
   'Strain Gage B4
                      If ZInit(30)=0 Then
                              ZMode(30)=1 : ZInit(30)=1
                      EndIf
                      If ZMode(30)<=0 OR ZMode(30)=6 Then ZInit(30)=1

FieldCal(0,ZGage(30),ZReps,0,ZOff(30),ZMode(30),0,ZIndex,ZAvg)
    StrainCalc(Strain(23),1,ZGage(30),0,3,StrGF,0)

    BrFull(ZGage(31),1,mV50,8,4,9,4,1,5000,True,True,50,200,1,ZOff(31))
   'Strain Gage B5
                      If ZInit(31)=0 Then
                              ZMode(31)=1 : ZInit(31)=1
                      EndIf
                      If ZMode(31)<=0 OR ZMode(31)=6 Then ZInit(31)=1

FieldCal(0,ZGage(31),ZReps,0,ZOff(31),ZMode(31),0,ZIndex,ZAvg)
    StrainCalc(Strain(24),1,ZGage(31),0,3,StrGF,0)

    BrFull(ZGage(32),1,mV50,8,5,9,4,1,5000,True,True,50,200,1,ZOff(32))
   'Strain Gage B6
                      If ZInit(32)=0 Then
                              ZMode(32)=1 : ZInit(32)=1
                      EndIf
                      If ZMode(32)<=0 OR ZMode(32)=6 Then ZInit(32)=1

FieldCal(0,ZGage(32),ZReps,0,ZOff(32),ZMode(32),0,ZIndex,ZAvg)
    StrainCalc(Strain(25),1,ZGage(32),0,3,StrGF,0)

    BrFull(ZGage(33),1,mV50,8,6,9,4,1,5000,True,True,50,200,1,ZOff(33))
   'Strain Gage B7
                      If ZInit(33)=0 Then
                              ZMode(33)=1 : ZInit(33)=1
                      EndIf
                      If ZMode(33)<=0 OR ZMode(33)=6 Then ZInit(33)=1

FieldCal(0,ZGage(33),ZReps,0,ZOff(33),ZMode(33),0,ZIndex,ZAvg)
    StrainCalc(Strain(26),1,ZGage(33),0,3,StrGF,0)

    BrFull(ZGage(34),1,mV50,7,4,9,3,1,5000,True,True,50,200,1,ZOff(34))
   'Strain Gage B8
                      If ZInit(34)=0 Then
```

```
                    Jan Test Campbell program.C9X
                              ZMode(34)=1 : ZInit(34)=1
                        EndIf
                        If ZMode(34)<=0 OR ZMode(34)=6 Then ZInit(34)=1

FieldCal(0,ZGage(34),ZReps,0,ZOff(34),ZMode(34),0,ZIndex,ZAvg)
    StrainCalc(Strain(27),1,ZGage(34),0,3,StrGF,0)

    BrFull(ZGage(35),1,mV50,7,5,9,3,1,5000,True,True,50,200,1,ZOff(35))
   'Strain Gage B10
                        If ZInit(35)=0 Then
                              ZMode(35)=1 : ZInit(35)=1
                        EndIf
                        If ZMode(35)<=0 OR ZMode(35)=6 Then ZInit(35)=1

FieldCal(0,ZGage(35),ZReps,0,ZOff(35),ZMode(35),0,ZIndex,ZAvg)
    StrainCalc(Strain(28),1,ZGage(35),0,3,StrGF,0)

    BrFull(ZGage(36),1,mV50,7,6,9,3,1,5000,True,True,50,200,1,ZOff(36))
   'Strain Gage B12
                        If ZInit(36)=0 Then
                              ZMode(36)=1 : ZInit(36)=1
                        EndIf
                        If ZMode(36)<=0 OR ZMode(36)=6 Then ZInit(36)=1

FieldCal(0,ZGage(36),ZReps,0,ZOff(36),ZMode(36),0,ZIndex,ZAvg)
    StrainCalc(Strain(29),1,ZGage(36),0,3,StrGF,0)

    BrFull(ZGage(37),1,mV50,8,3,9,2,1,5000,True,True,50,200,1,ZOff(37))
  'Strain Gage B15
                        If ZInit(37)=0 Then
                              ZMode(37)=1 : ZInit(37)=1
                        EndIf
                        If ZMode(37)<=0 OR ZMode(37)=6 Then ZInit(37)=1

FieldCal(0,ZGage(37),ZReps,0,ZOff(37),ZMode(37),0,ZIndex,ZAvg)
    StrainCalc(Strain(30),1,ZGage(37),0,3,StrGF,0)

    CallTable LDef
    CallTable CalHist

  NextScan
  LoadDefl=false

EndSub

'----- Main Program -----
BeginProg
  For I = 1 To 37
    ZOff(I)=0 : ZMode(I)=6 : ZInit(I)=1
  Next I

  Load=0

  For I = 1 To 6 Step 1
    LMT(I)=0
  Next I

  For I = 1 To 30 Step 1
    Strain(I)=0
```

```
                    Jan Test Campbell program.C9X
  Next I
  FCLoaded=LoadFieldCal(0)

  Do
    If StartStop=True Then LDefl
  Loop

EndProg
```

Appendix C Soil Bore Logs

Bore Hole #1, Current Location of South Test Pile

Depth, m	Description (3 in. O.D. Split Spoon)	Samples		Blows (300 lb. hammer)
		Depth, m	MC, %	
0.0-0.11	Organics (grass, roots)			-
0.11-0.25	Loose, moist sandy gravel (rounded to sub-rounded, up to 3 cm) with sandy silt; content of gravel – about 60-70%			
…				
0.76-1.00	Loose, wet sandy gravel (rounded to sub-rounded, up to 3 cm) with sandy silt; content of gravel – about 60-70%			(17)
1.00-1.14	Moist, soft, grey sandy silt, slightly clayey, with gravel (less than 5%; rounded to sub-rounded, up to 2 cm)			
1.14-1.18	Dark-brown peat			
1.18-1.21	Grey sandy silt			
1.21-1.24	Dark-brown peaty sandy silt			
1.24-1.37	Moist, soft, greenish-grey sandy silt (very fine silty sand-?), uniform, with organics (rootlets)	1.32-1.37	27.9	
…				
2.44-3.20	**Shelby tube 8-10.5 ft**			
3.20-3.81	Wet (from 3.40 m – moist), soft (from 3.60 m – firm) grey sandy silt, slightly clayey, with layers of reworked dark-brown peat (at 3.53 m, 3.55-3.56 m, 3.65-3.67 m)	3.76-3.81	32.4	2-2-4-7
…				
4.58-5.34	**Shelby tube 15-17.5 ft**			
5.34-5.95	Wet (from 5.70 m – moist), soft (from 5.70 m – firm) grey sandy silt, slightly clayey, with 1-1.5 cm-thick layers of reworked dark-brown peat (at 5.70 m, 5.74 m, 5.81 m)	5.90-5.95	32.1	3-3-4-4
…				
6.10-6.86	**Shelby tube 20-22.5 ft, frozen from ~22 ft**			
6.86-7.10	Frozen, yellow-grey sandy silt, ice-rich. Cryostructure: micro-braided to micro-ataxitic, inclined	6.86-6.91	227.6	14-12-12-12 (?)
7.10-7.48	Frozen, yellow-grey sandy silt, oxidized, laminated, ice-poor. Cryostructure: latent micro-lenticular, from 7.17 – no visible ice	7.38-7.43	33.2	

Bore Hole #2, Current Location of Reaction Pile

Depth, m	Description (3 in. O.D. Split Spoon)	Samples		Blows (300 lb. hammer)
		Depth, m	MC, %	
…				
0.76-1.15	Moist, soft, brown-grey sandy silt, slightly clayey, with gravel (less than 10%; rounded to sub-rounded, up to 2.5 cm), with organics			(16)
1.15-1.23	Moist, dark-brown peat			
1.23-1.37	Moist, soft, light-grey sandy silt, uniform, with organics (rootlets)	1.30-1.35	33.3	
…				
1.45-1.55	Moist, soft, brown-grey sandy silt, with dissolved organics			4-4-6-7
1.55-1.80	Slightly moist, firm, light-grey (greenish-grey) sandy silt			
1.80-1.98	Slightly moist, firm, yellow-grey sandy silt, oxidized	1.93-1.98	28.3	
…				
2.90-2.95	Wet, dark-brown peat			3-3-4-6
2.95-3.36	Moist, soft, grey sandy silt, uniform, no inclusions; at 3.22-3.33 m – layer of dark-brown peat	3.31-3.36	37.4	
…				
4.27-4.66	Wet, soft, grey sandy silt, with undecomposed rootlets			2-3-3-5
4.66-4.74	Moist dark-brown peat (reworked)			
4.74-4.88	Moist, soft, brown-grey organics-rich sandy silt, with peat, wood inclusions	4.82-4.88	36.5	
…				
5.80-6.29	Moist, soft, grey sandy silt, with organics			3-3-5-6
6.29-6.31	Moist dark-brown peat (reworked)			
6.31-6.41	Moist, soft, grey sandy silt, with thin organics layers	6.36-6.41	33.1	
…				
6.48-6.94	Frozen, grey sandy silt, ice-rich. Cryostructure: micro-braided to micro-ataxitic, inclined (~30^0)	6.50-6.55	74.0 (?)	18-20-29-40
6.94-7.02	Frozen, yellow-grey sandy silt, oxidized, ice-poor. Cryostructure: micro-layered, sub-horizontal	6.94-7.01	55.5	

Bore Hole #3, Current Location of North Test Pile

Depth, m	Description (3 in. O.D. Split Spoon)	Samples		Blows (300 lb. hammer)
		Depth, m	MC, %	
…				
0.92-1.00	Moist, soft, grey sandy silt, slightly clayey, with gravel (less than 5%; rounded to sub-rounded, up to 2 cm)			6-12-13-15
1.00-1.09	Moist dark-brown peat			
1.09-1.53	Slightly moist, firm to stiff, light-grey sandy silt with dark-brown and black organic stains and layers	1.48-1.53	33.5	
…				
1.83-2.59	**Shelby tube 6-8.5 ft**			
…				
2.75-3.24	Wet (from 3.10 m – moist), soft grey sandy silt, with thin layers of reworked dark-brown peat			4-4-4-10
3.24-3.27	Moist dark-brown peat			
3.27-3.36	Slightly moist, soft to firm, grey sandy silt, uniform	3.29-3.36	33.7	
…				
3.51-4.27	**Shelby tube 11.5-14 ft (label – 12-14.5 ft)**			
4.27-4.63	Wet (from 4.55 m – moist), soft grey sandy silt, uniform			2-4-5-6
4.63-4.72	Moist dark-brown peat, with wood inclusions			
4.72-4.88	Moist, soft grey sandy silt, uniform, with organics	4.83-4.88	39.2	
…				
5.19-5.95	**Shelby tube 17-19.5 ft**			
5.95-6.09	Moist, soft yellow-grey sandy silt, uniform			2/6/29/43
6.09-6.15	Moist dark-brown peat			
6.15-6.29	Moist, soft yellow-grey sandy silt, with layers of dark-brown peaty silt 0.3-2.5-cm-thick	6.16-6.21	34.6	
6.29-6.56	Frozen, grey sandy silt, ice-rich. Cryostructure: micro-ataxitic, inclined, from ~6.45 – sub-horizontal	6.51-6.56	280.4	

Sieve Analysis (South Pile)

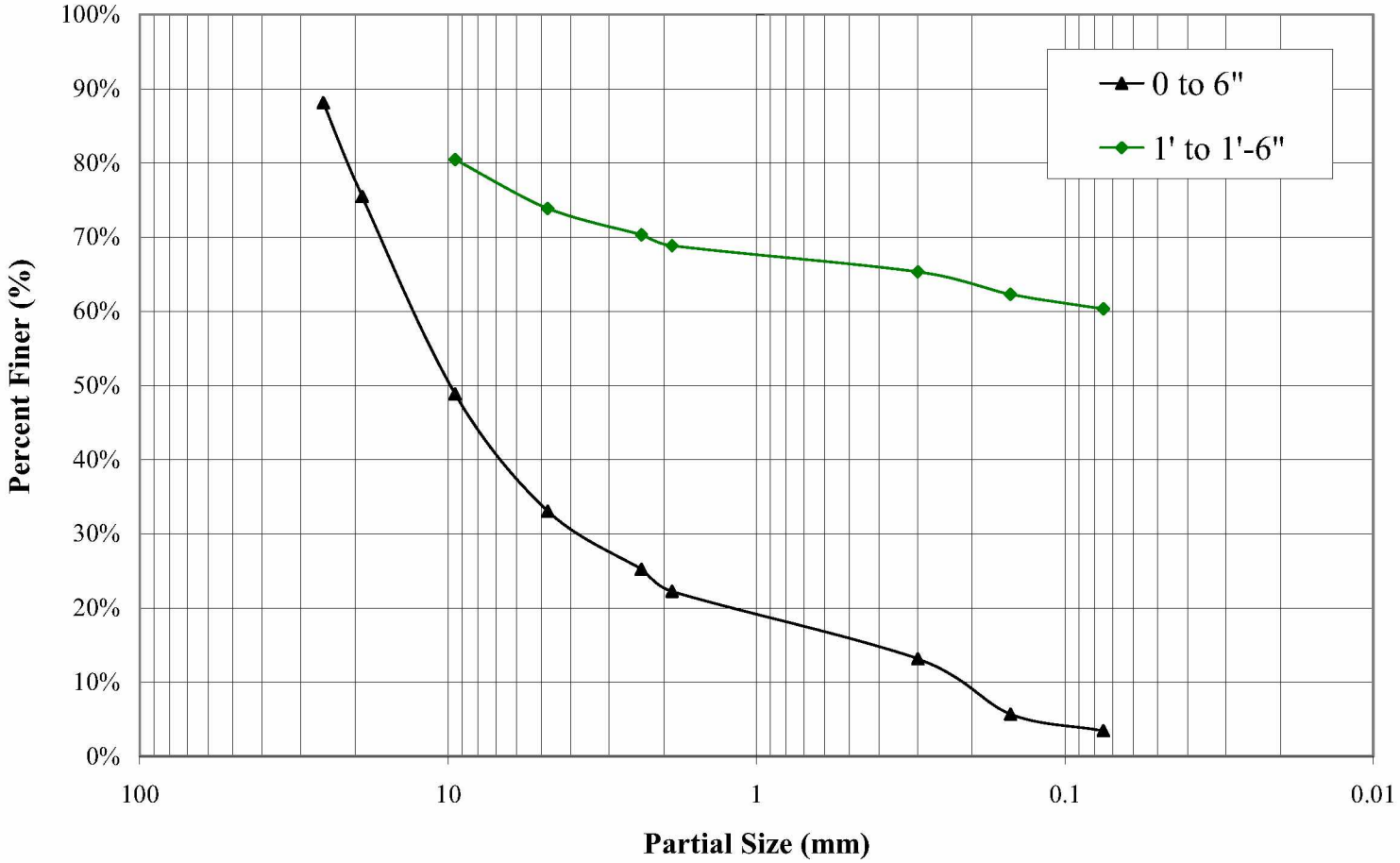

Sieve and Hydrometer Analysis North Pile

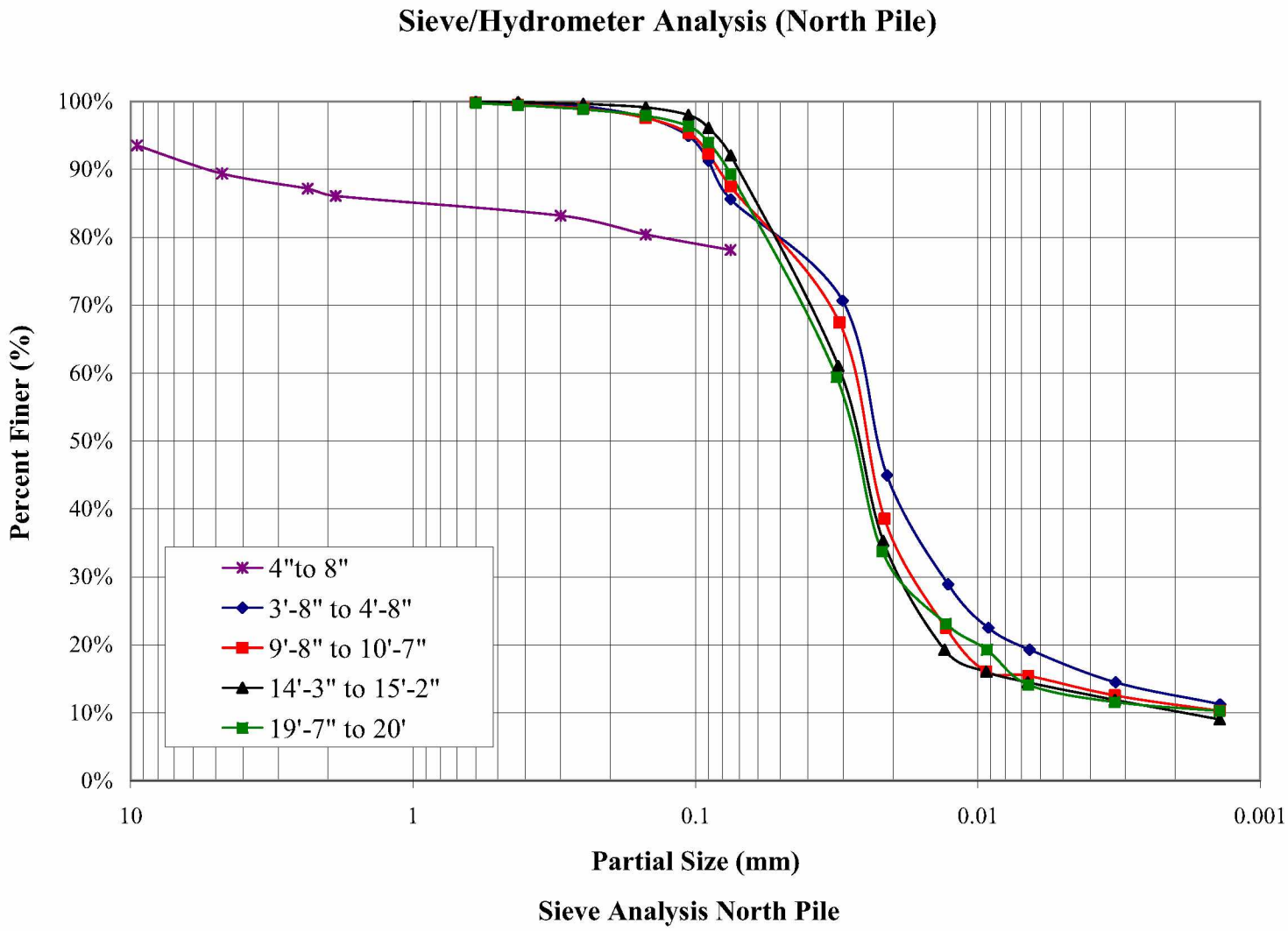
Sieve/Hydrometer Analysis (North Pile)
Percent Finer (%)
100%
90%
80%
70%
60%
50%
40%
30%
20%
10%
0%
10
1
0.1
0.01
0.001
Partial Size (mm)
4"to 8"
3'-8" to 4'-8"
9'-8" to 10'-7"
14'-3" to 15'-2"
19'-7" to 20'
Sieve Analysis North Pile

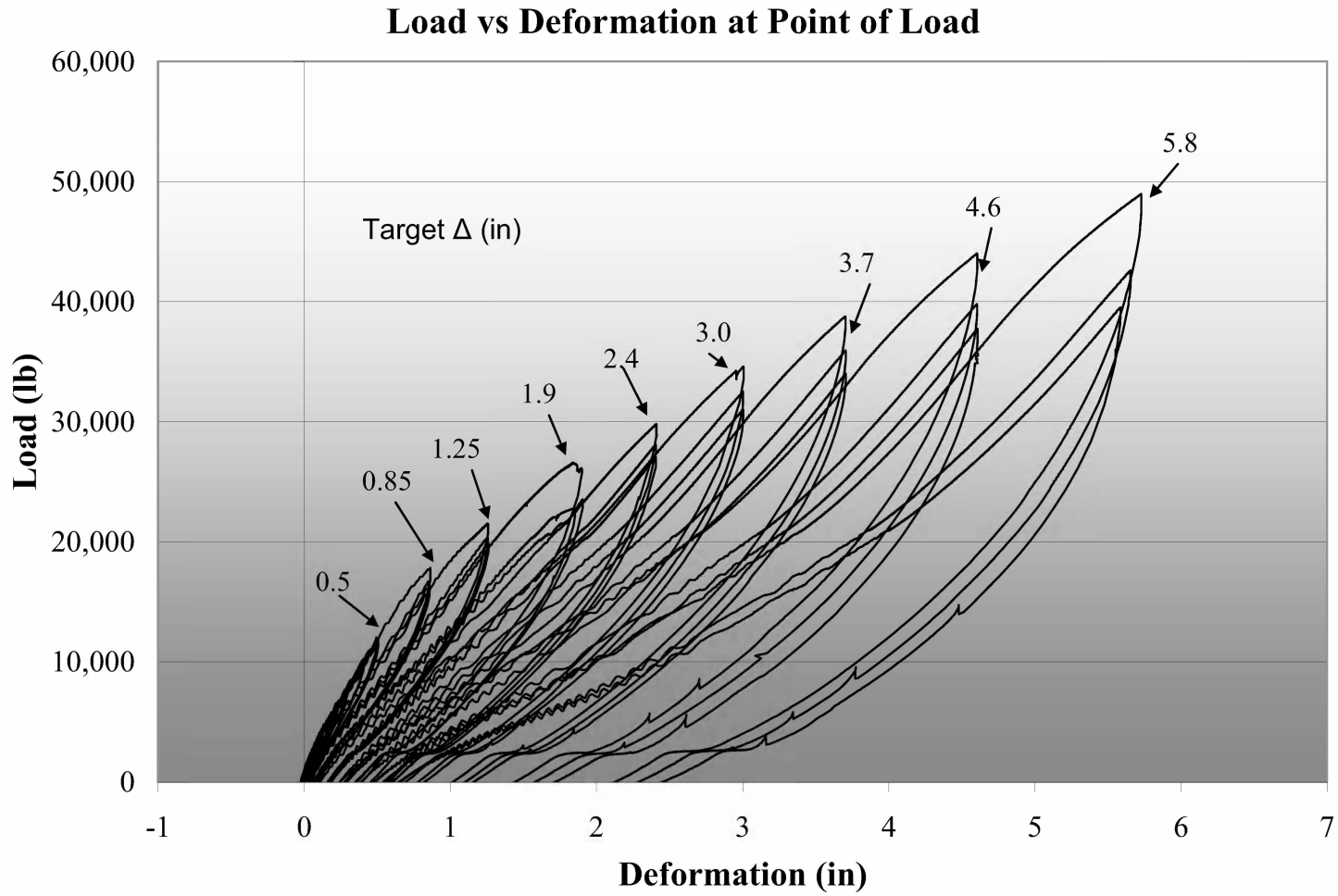

September Cyclic Load vs Deformation at Point of Load

Load vs Deformation at Point of Loading

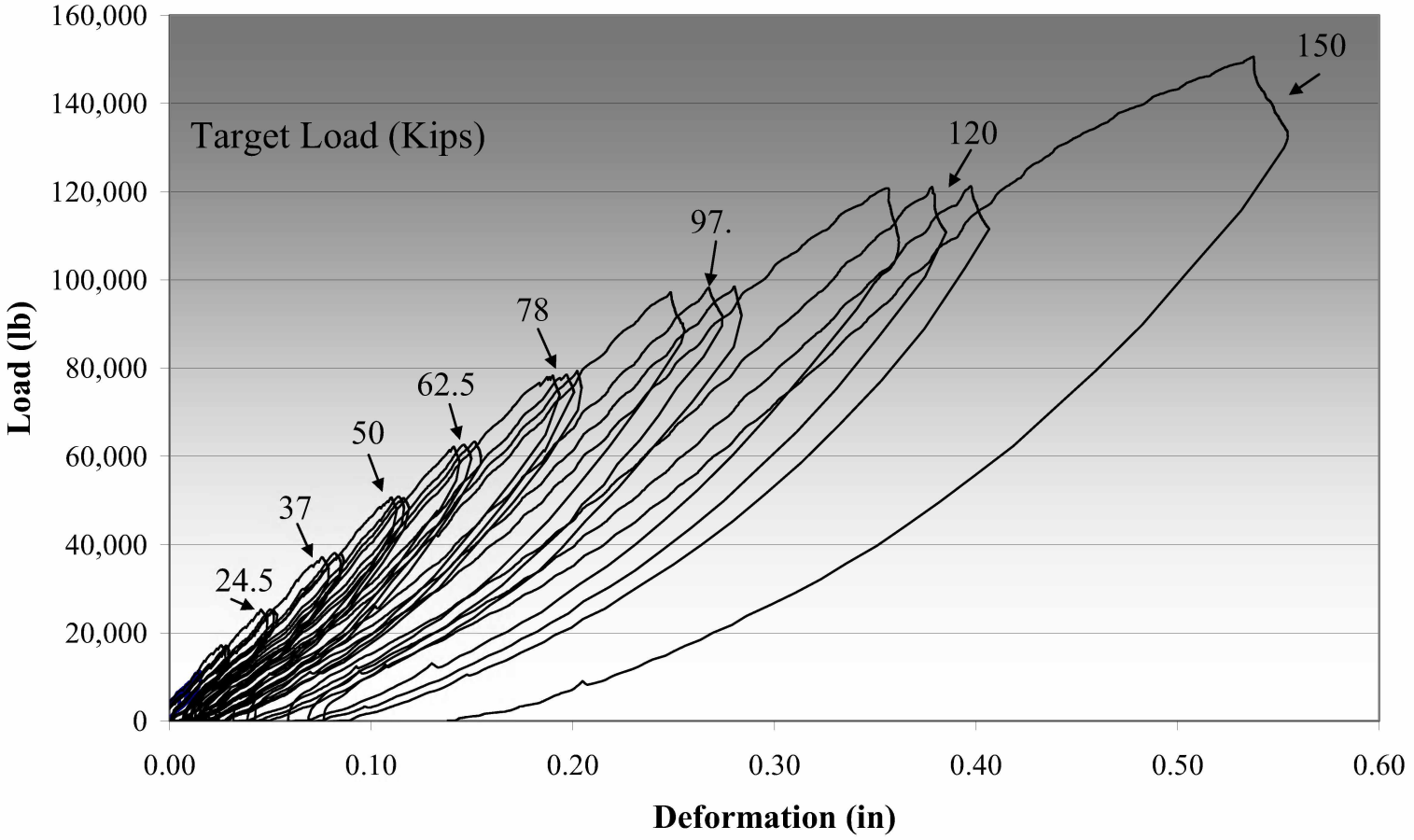

January Cyclic Load vs Deformation at Point of Load

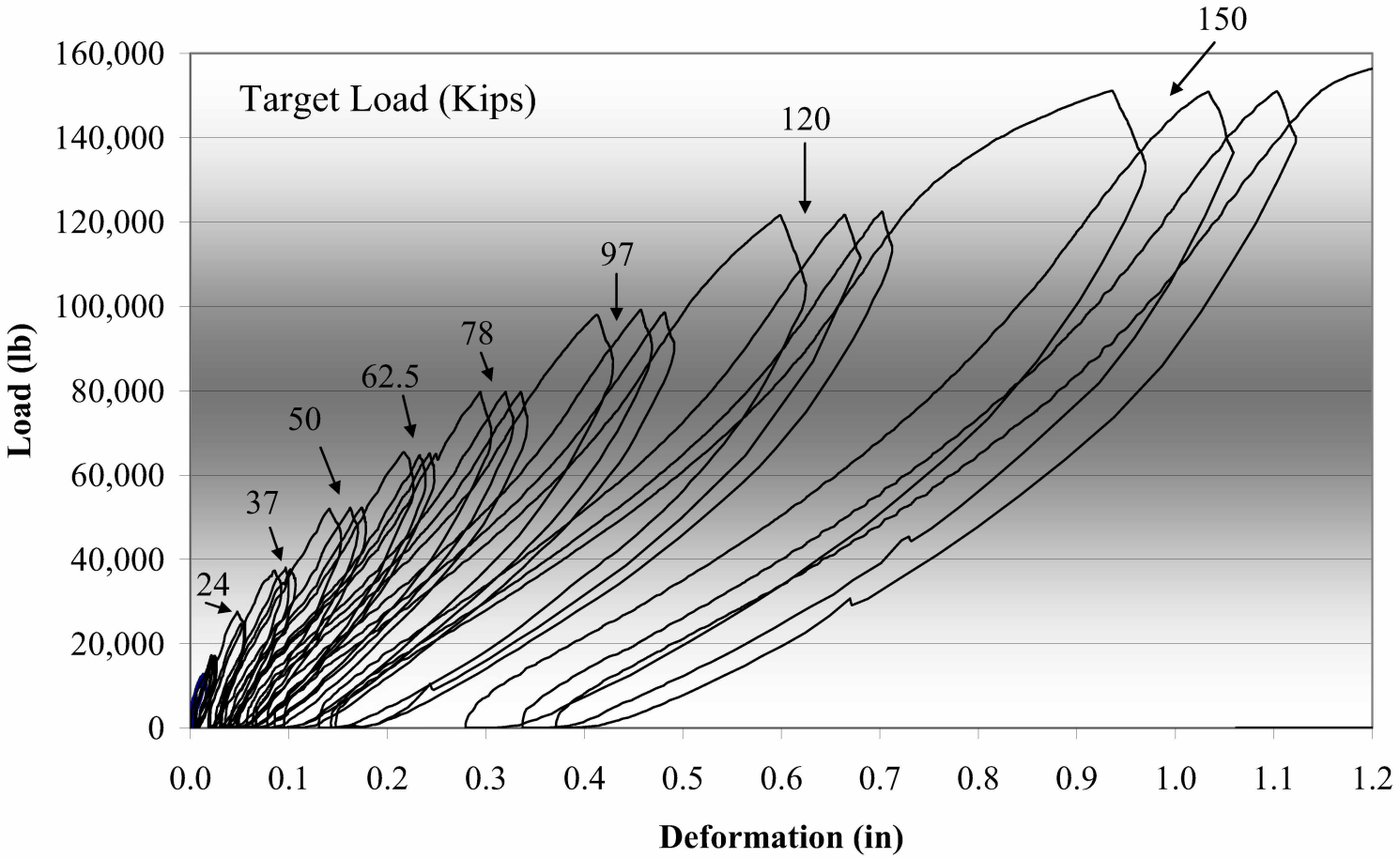

March Cyclic Load vs Deformation at Point of Load 0 to 150 Kips

Load vs Deformation at Point of Loading

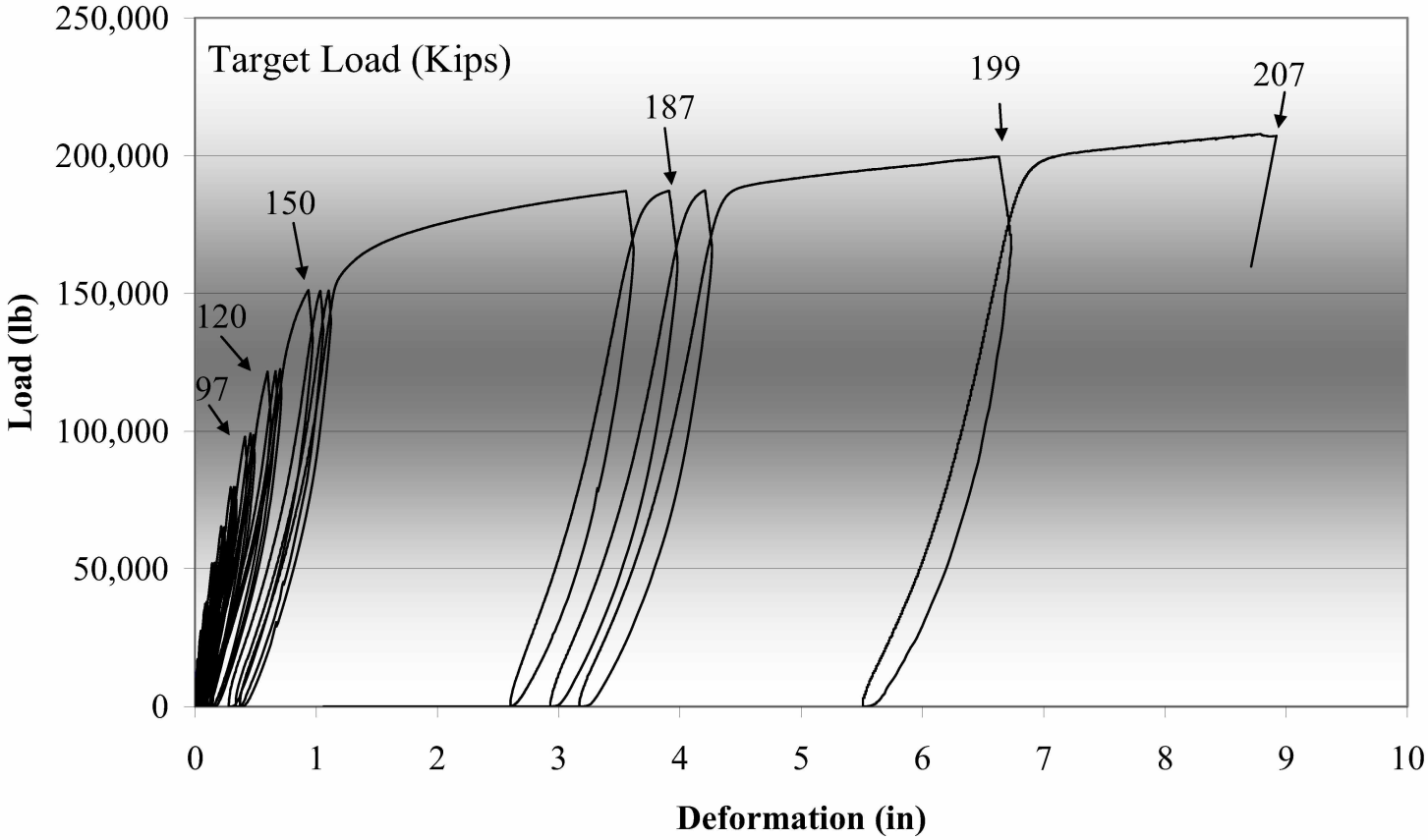

March Cyclic Load vs Deformation at Point of Load 0 to 207 Kips

Soil Springs Used Compared to Springs Computed from Modulus of Subgrade Reaction

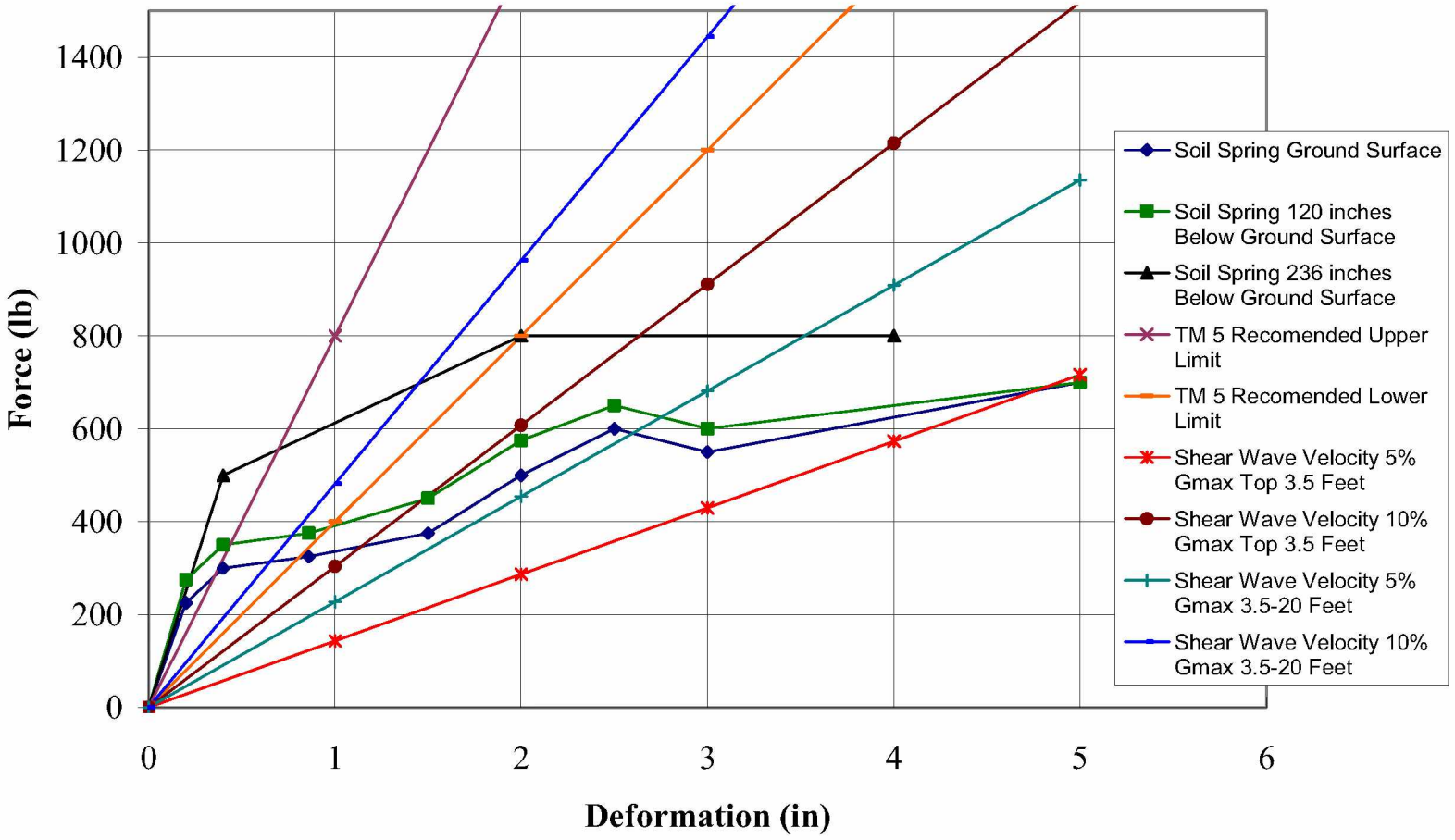

Thawed Soil Springs Used to Model September Test Compared to Soil Spring Computed from Other Methods

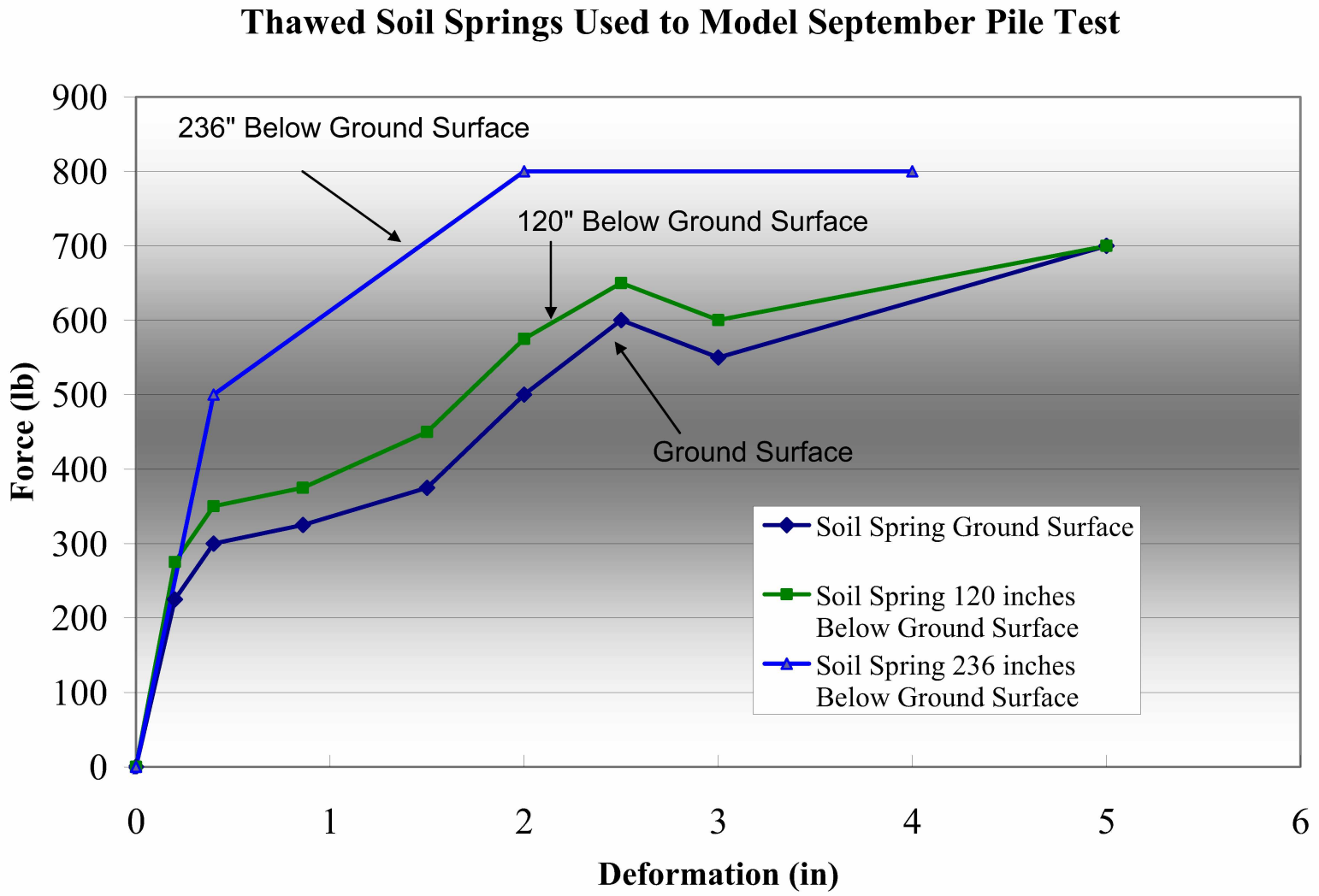

Soil Springs Used to Model September Test

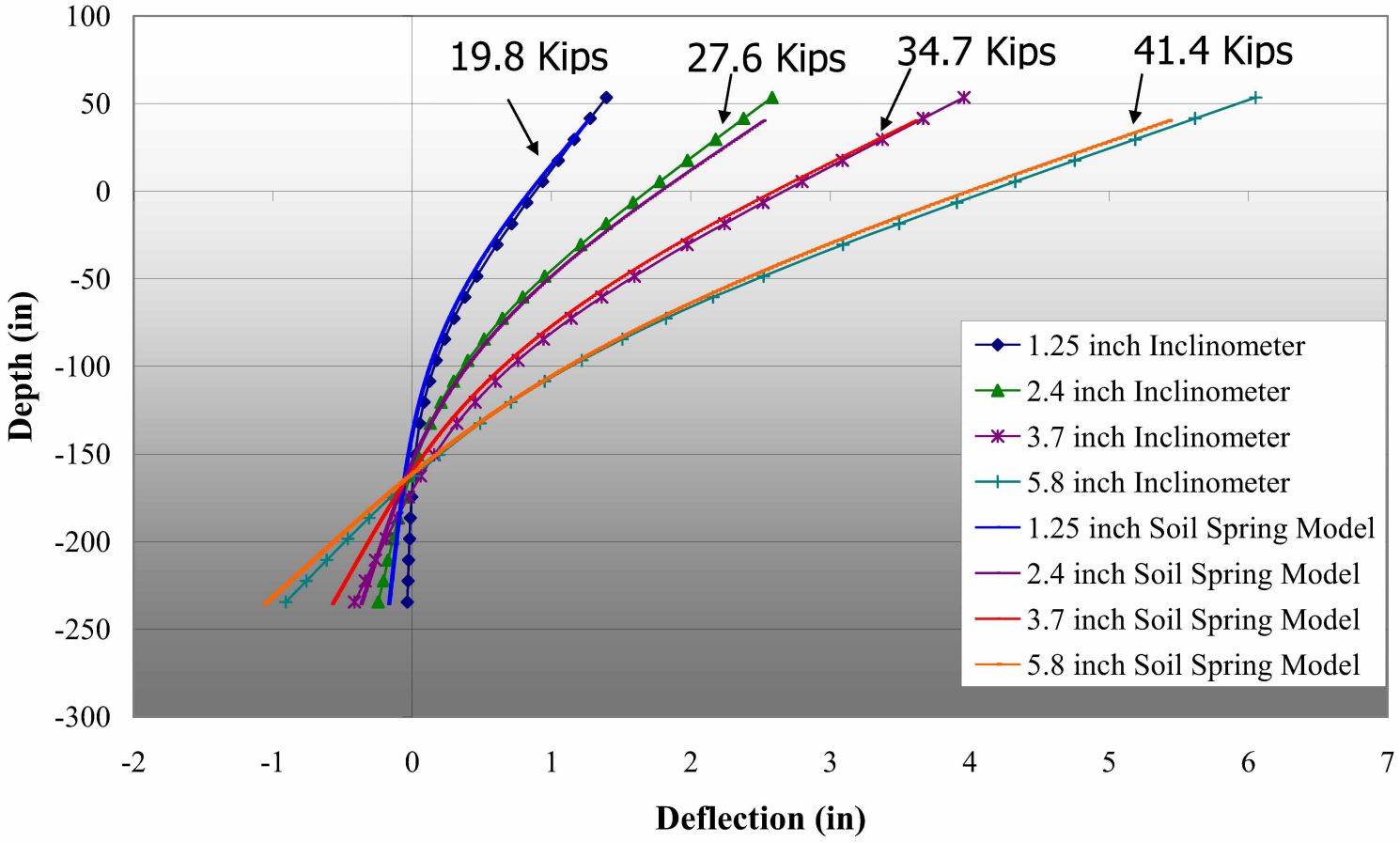

Deflected Shape Model Predicted, and Experimental

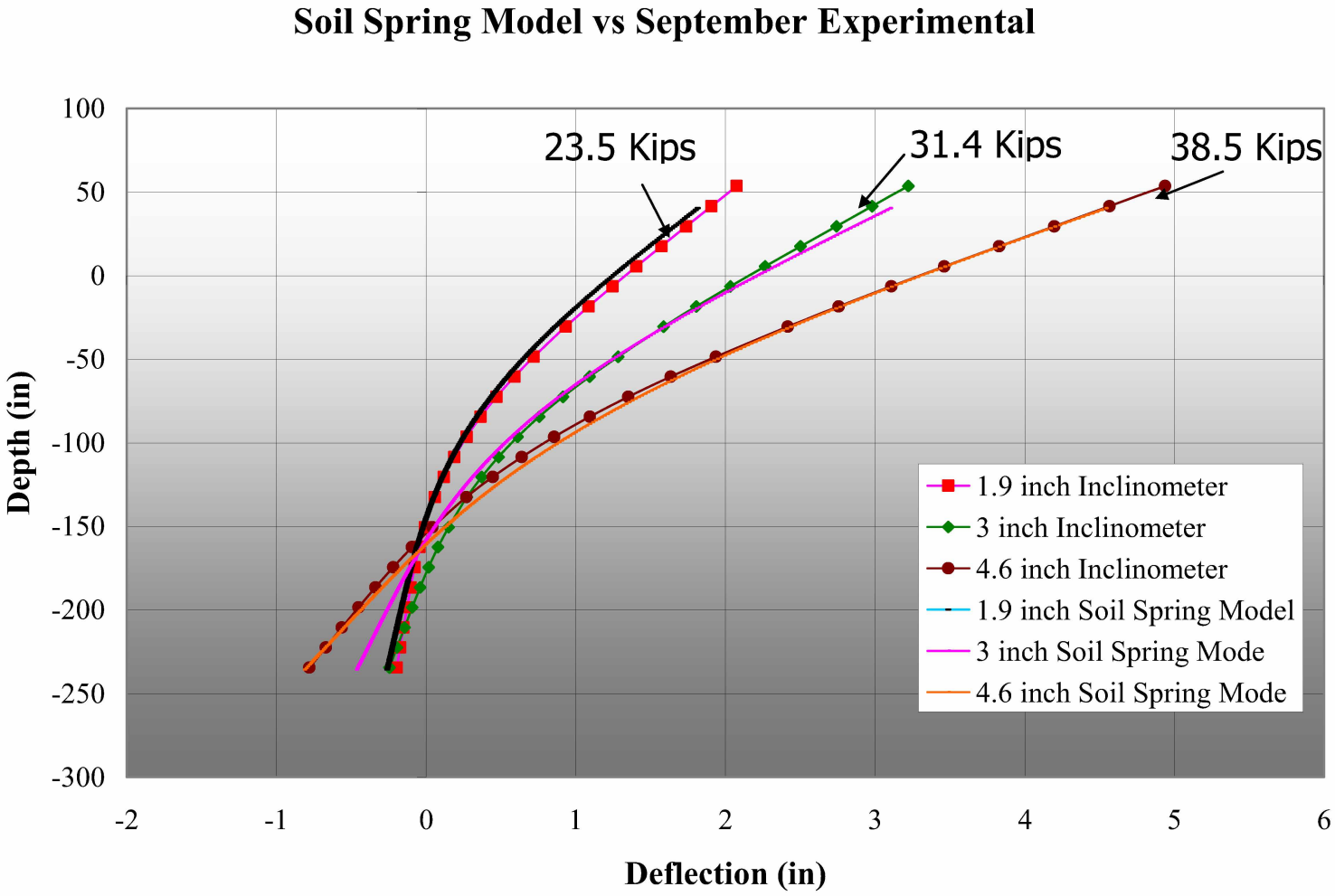

Deflected Shape Model Predicted, and Experimental

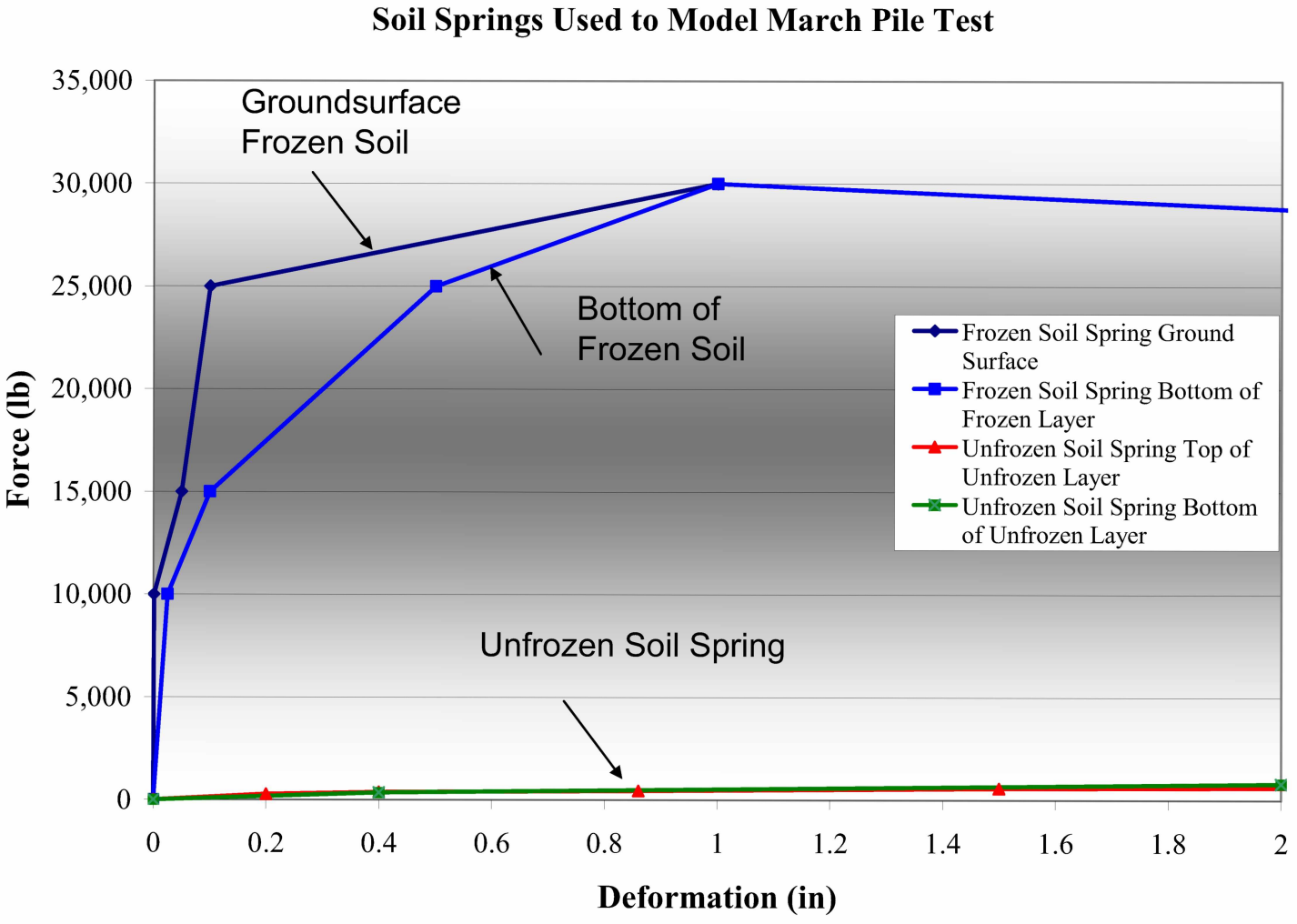

Soil Spring Used to Model March Pile Test

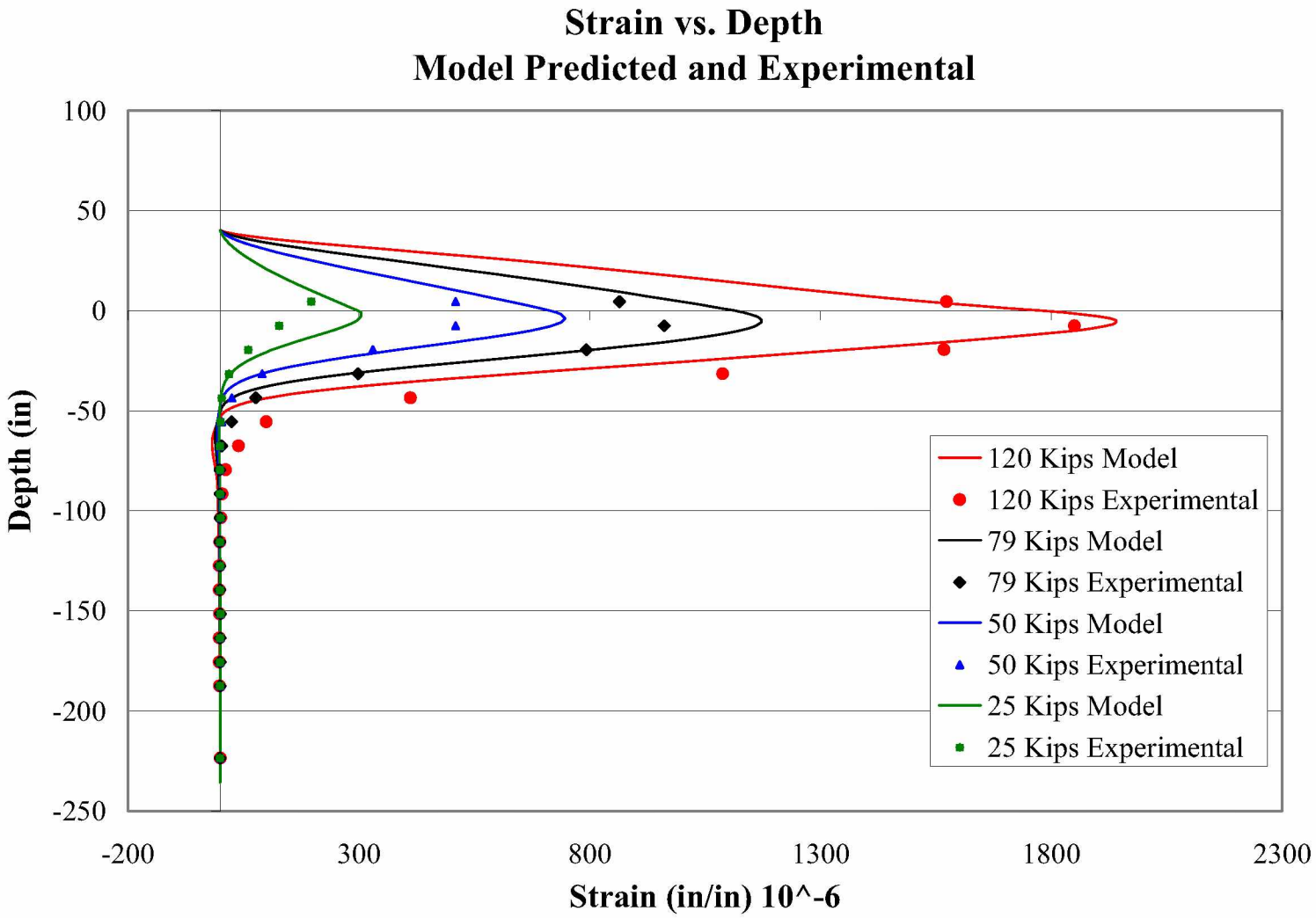

Strain, Model Predicted and Experimental March Pile Test

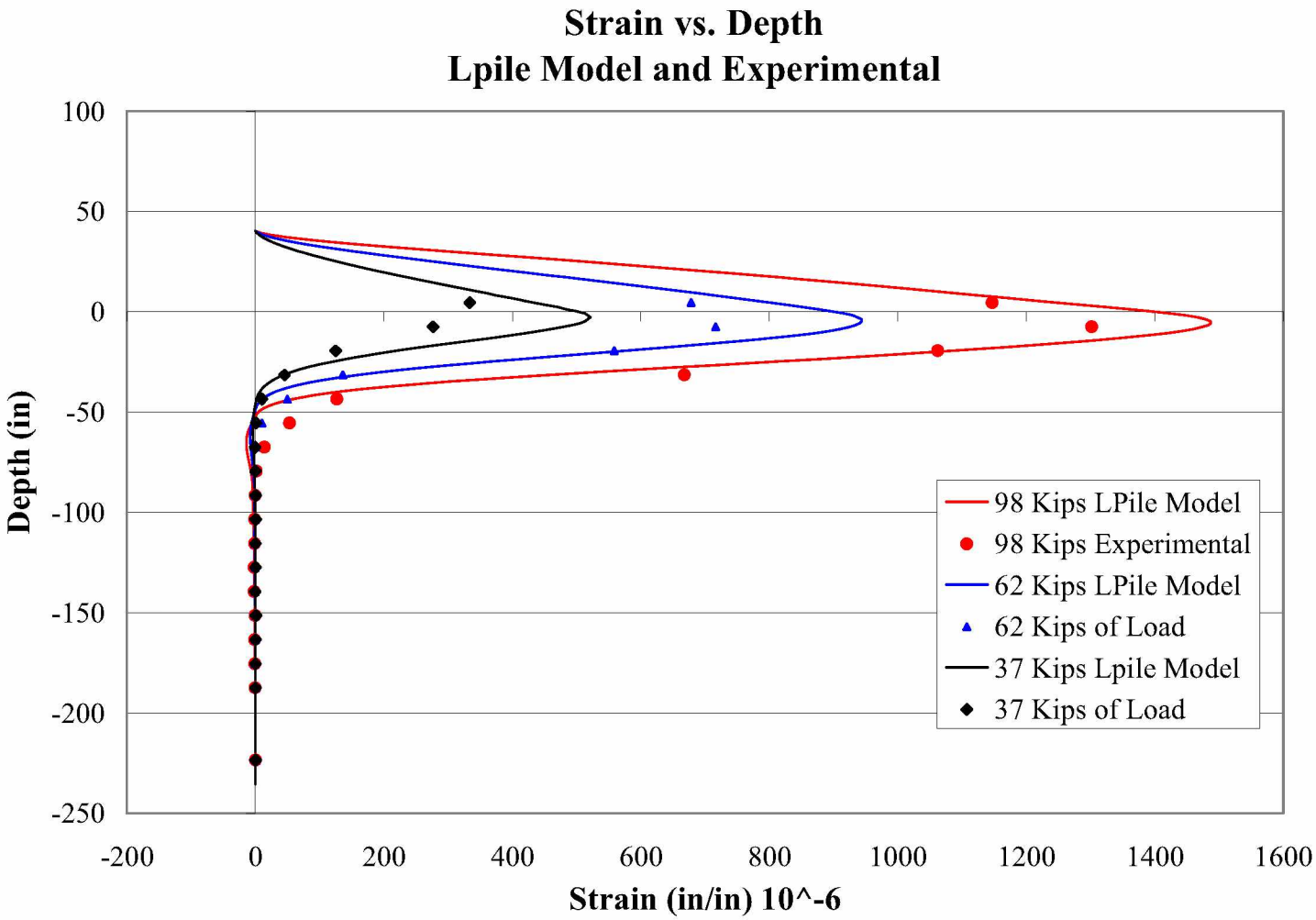

Strain, Model Predicted and Experimental March Pile Test